An Integrated Approach to Optimize Vitrification of Articular Cartilage

by

Kezhou Wu

A thesis submitted in partial fulfillment of the requirements for the degree of

Doctor of Philosophy

in

Experimental Surgery

Department of Surgery

University of Alberta

Abstract

Articular cartilage (AC) is a few-millimetres-thick hyaline cartilage tissue covering the bone end in articulating joints. AC is composed primarily of cells called “chondrocytes” and abundant surrounding cartilage matrix components. AC is a vital structure in daily joint mobility function. Thus, it is important to maintain an intact AC structure. Due to the avascular and aneural anatomical nature, AC has a poor self-repair capacity after injuries. AC defects over 1 cm^2 often progress into osteoarthritis if not properly treated. While osteochondral graft transplantation is an effective method of AC defect repair, it is limited by several factors such as donor availability and perioperative preparations, which make AC defect repair a challenging clinical issue. Cryopreservation of chondrocytes and AC for long-term storage is a promising solution that can provide clinical surgeons with a long and flexible timeframe for performing cartilage transplantation. However, this requires a well-designed tissue banking system with appropriate cryopreservation protocols to store donated AC tissues.

Cryoprotectants (CPAs) are capable of reducing ice formation within cells and tissues during the cooling–warming procedures, which plays an essential role in AC cryopreservation. However, they can exhibit undesirable effects such as osmotic or oxidative stress on chondrocytes which leads to cell dysfunction and damage. Additionally, the long CPA permeation process required for AC cryopreservation might aggravate the severity of CPA toxicity on the chondrocytes. It remains challenging to eliminate all adverse effects induced by the CPA compounds and the CPA permeation procedures. In the past decades, several promising cryopreservation approaches emerged as tools to guide the design of cryopreservation protocols for preserving AC at cryogenic temperatures. The proposed approaches include slow graded freezing (stepwise cooling), multiple

steps of cryoprotectant addition and removal, modelling of cryoprotectant transport, etc. With the emergence of vitrification, an 'ice-free' method to preserve tissue in a "glassy" solid that avoids ice crystal formation at −196 °C, more approaches have been developed including liquidus tracking of cryoprotectants, minimization of cryoprotectant toxicity by using cryoprotectant mixtures, mathematical calculation of cryoprotectant permeation and vitrifiability, etc. All of these approaches have provided information to promote the advancement of AC vitrification. Furthermore, this knowledge has been applied to intact human AC.

In this thesis, different strategies have been investigated to improve AC cryopreservation protocols from several perspectives: 1) to validate the efficiency of vitrification protocols generated *via* engineering optimization of CPA concentration, permeation temperature, duration of CPA permeation; 2) to improve heat transfer of AC during cooling and warming processes by the optimization of container size and packaging method; 3) to mitigate the toxicity of CPAs by inclusion of additives in the CPA mixtures composed of multiple types of CPAs.

The research presented in this thesis focuses on the investigation of a combination of different strategies within the continuously evolving cryopreservation protocols for porcine and human AC, and the evaluation of their protective as well as damaging mechanisms on the chondrocytes. The findings from these studies provide us better understanding and new knowledge to establish successful cryopreservation protocols for intact human AC.

Preface

This thesis is an original work by Kezhou Wu. The research project, of which this thesis is a part, received research ethics approval from the University of Alberta's Research Ethics Board. The Health Research Ethics Board-Biomedical Panel provided ethical approval for the experimental use of human tissues and cells, under study ID: Pro00001141, for the study title "Vitrification of articular cartilage". The Research Ethics Office at the University of Alberta provided ethical approval for the experimental use of animal tissues and cells, under research project ID: G522000020 and RES0036331, for the study title "Joint tissue regeneration and preservation". This work was supported by the Edmonton Orthopedic Research Committee (EORC) grants and the Edmonton Civic Employee's Charitable Assistance Fund. Kezhou Wu was supported by the Li Ka Shing Sino-Canadian Exchange Program and the Doctoral Recruitment Scholarship from the University of Alberta.

Chapter 2 has been submitted for publication in part as: Kezhou Wu, Nadia Shardt, Leila Laouar, Janet A. W. Elliott and Nadr M. Jomha. "Vitrification of particulated articular cartilage *via* engineering optimized protocols". In this chapter, K.W., L.L., N.S., J.A.W.E, and N.M.J. designed and advised on the experiments; K.W. performed the *in vitro* experiments on tissue processing, tissue vitrification and warming, the post-vitrification assessments of chondrocyte viability, metabolic activity, and matrix productivity, the data acquisition, and the data analysis; L.L. prepared the solutions for the vitrification experiments; N.S. and J.A.W.E performed the engineering modelling; K.W. wrote the draft of the manuscript except for the mathematical

modelling methods and results which were written by N.S.; the manuscript was finished with guidance from J.A.W.E. and N.M.J.; all authors reviewed and revised the final manuscript.

Chapter 3 has been published in *Cryobiology* as: Kezhou Wu, Nadia Shardt, Leila Laouar, Zhirong Chen, Vinay Prasad, Janet A. W. Elliott, and Nadr M. Jomha. "Comparison of three multi-cryoprotectant loading protocols for vitrification of porcine articular cartilage". *Cryobiology* 92 (2020): 151-160. In this chapter, K.W. designed the experiments with advice from N.M.J., J.A.W.E., and L.L.; K.W. performed the experiments including tissue processing, tissue vitrification, post-vitrification assessments, data acquisition, and data analysis; K.W., N.M.J., J.A.W.E., and V.P. were involved in the evaluation of results and statistical analysis; N.S., Z.C., and J.A.W.E. proposed the optimized protocol; L.L. prepared the solutions for the vitrification experiments; K.W. wrote the manuscript and all authors reviewed and finalized the final manuscript.

Chapter 4 has been published in *Cryobiology* as: Kezhou Wu, Leila Laouar, Rachael Dong, Janet A. W. Elliott, and Nadr M. Jomha. "Evaluation of five additives to mitigate toxicity of cryoprotective agents on porcine chondrocytes". *Cryobiology* 88 (2019): 98-105. In this chapter, K.W., N.M.J., J.A.W.E., and L.L. designed the experiments; K.W. performed the experiments including tissue processing, cryoprotective agent exposure, tissue assessments, data acquisition, and data analysis; L.L. prepared the cryoprotective agent solutions for the experiments; R. D. helped with tissue fluorescent imaging; K.W., N.M. J., and J.A.W.E. evaluated the results; K.W. wrote the manuscript and the final manuscript was reviewed and finalized by all authors.

Chapter 5 has been submitted for publication in part as: Kezhou Wu, Leila Laouar, Janet A. W. Elliott and Nadr M. Jomha. “Removing the surrounding vitrification solution is advantageous for vitrification of articular cartilage”. In this chapter, K.W. designed the experiments with suggestions from L.L., J.A.W.E., and N.M.J.; K.W. performed the experiments including tissue processing, tissue vitrification and warming, post-vitrification assessments, data acquisition, and data analysis; L.L. prepared the solutions for the vitrification experiments; K.W. wrote the manuscript with guidance from J.A.W.E. and N.M.J., and all authors reviewed and revised the final manuscript.

Dedication

This thesis is dedicated to my parents, Binghong Wu and Meiyan Wu.

Acknowledgements

I am thankful to acknowledge the following people who have helped during my journey to pursue a doctoral degree.

Firstly, I would like to express my sincerest gratitude and appreciation to my PhD supervisory committee members, Prof. Nadr M. Jomha and Prof. Janet A.W. Elliott, for their dedicated guidance, mentorship and support during my research training. Their enthusiasm, knowledge, and professionalism have always inspired me and led me to an academic career that fulfilled with critical thinking, reading and writing. Thank you for your encouragements and advices throughout my PhD study. I would like to thank Prof. Vinay Prasad, for his helpful inputs and comments on the experiments and data analysis in my research. I would like to sincerely thank Prof. Dayong Gao as the external examiner and Prof. Gregory Korbutt as the internal examiner for their time and effort in reviewing this thesis and the participation in my PhD thesis defense. Thanks to Prof. Fred Berry for being the chair of my defense committee and organizing the final oral examination. I would like to thank my graduate program administrator, Tracey Zawalusky, for her assistance in the Department of Surgery.

During the past years, I am grateful to have Dr. Leila Laouar who is a very helpful and enthusiastic lab manager and research associate to support my PhD study. Special thanks to Prof. Locksley E. McGann for the invaluable suggestions on my cryobiological research. Thanks to each of my lab members, Dr. Nadia Shardt, Rachael Dong, Mary Crisol, Johnathan Sevick, Colleen Stewart,

Kevin Duong, Ethan Candler, Zhirong Chen, Charles Bouchard, Kar Wey Yong for their tremendous contribution in many outstanding research projects.

I would like to acknowledge mentors and colleagues from the Department of Surgery, Dr. Tom Churchill, Dr. Gina Rayat, Dr. Colin Anderson, Dr. Mark Sommerfeldt, Dr. Adetola Adesida, Alex Szojka, Xiaoyi Lan, Aillette Mulet-Sierra, Melanie Kunze, Kenneth Wong, Joshua Hahn for their help during my study. I would like to thank mentors and colleagues from many external departments or universities that I have the opportunities to work with, Dr. Jason Acker, Dr. Leah Marquez-Curtis, Dr. Robert Ben, Dr. Thomas Koch, Dr. Samer Adeeb, Dr. Lindsey Westover, Jonelle Jn Baptiste, Jenny He, Nada Mohamed, Junran Sun, Ray Sun, Karan Vats, Lisa Carreiro. Thanks to Allan Muir for his assistance in tool preparation. I would like to thank Dr. James Benson, Dr. John Bischof, Dr. Greg Fahy, Dr. Yuansheng Tan, Dr. Estefania Paredes, Dr. Miao Zhang, Dr. Miaomiao Xin, Dr. Jiaji Pan, Fazil Panhwar, Zonghu Han, Nicole Evans, Amelia Hanson for the wonderful time and discussions during the Society for Cryobiology annual meetings and Extreme Cryo symposiums. I would like to thank Woo Jung Cho, Greg Plummer, Steve Ogg from the Cell Imaging Centre for technical assistances in microscopy.

I would like to thank the Li Ka Shing Foundation and the Edmonton Orthopaedic Research Committee for funding support in this work. Thanks to the Society for Cryobiology, Canadian Institutes of Health Research, Faculty of Graduate Studies and Research, Graduate Student Association, the Department of Surgery, the Department of Laboratory Medicine and Pathology

for providing numerous travel awards that allows me to present my work at the world-class meetings.

I am lucky to have many friends who are always supportive during my study in Edmonton. Thanks to Jilei Zhang, Yan Liang, Wenlong Huang, Xiaohua Huang, Junqiang Ma, Yixiong Wang, Qi Wang, Muhao Hsu, Tingting Wang, Cameron Lindsay, Jinwen Zheng, Xia Xu, Yue Zhao, Jiaxin Lin, Haopeng Lin, Xiao Qi, Yang Mei, Lei Zhang, Yongneng Zhang, Xueyi Chen, Yongzhe Hong, for the great time we spent together.

Lastly, I would like to deeply thank my dear families for their continued love and support to me throughout these years of study in medicine.

Table of Contents

List of Figures

List of Tables

List of Abbreviations

AA: ascorbic acid

AC: articular cartilage

ACI: autogenous chondrocyte implantation

CPA: cryoprotectant, or cryoprotective agent

CS: chondroitin sulphate

DMEM: Dulbecco's modified eagle medium

DMSO: dimethyl sulfoxide

ECM: extracellular matrix

EG: ethylene glycol

Fm: formamide

FRIR: Fourier transform infrared spectroscopy

GAG: glycosaminoglycan

GlcN: glucosamine

Gly: glycerol

HBV: hepatitis B virus

HEPES: 4-(2-hydroxyethyl)-1-piperazineethanesulfonic acid

HIV: human immunodeficiency virus

HLA: human leukocyte antigen

M: molar

OA: osteoarthritis

PBS: phosphate buffered saline

PF-68: Pluronic F-68

PG: propylene glycol

TGF: transforming growth factor

TMP: 2,3,5,6-tetramethylpyrazine

Chapter One: Introduction

1.1 Thesis overview

Articular cartilage (AC) is a thin connective tissue covering the bone ends of articulating joints. Defects of AC result in painful joint movements and reduction of normal activities. Large AC defects often develop into osteoarthritis without proper treatments. Resurfacing of AC using cartilage allografts is an accepted procedure used by orthopaedic surgeons to treat AC defects. However, due to the relatively short storage period currently available for fresh AC allografts, the process of allograft resurfacing is limited to the availability of donated AC allografts in a very restricted number of tissue banks. Preservation of AC grafts with extended storage time is a way to alleviate the shortage issue in current orthopaedic practice. Cryopreservation *via* vitrification is a promising approach to store viable and functional AC to repair AC defects. Cryopreservation of AC has been developed over the past decades with significant progresses even though this technology requires optimization for clinical translation. This thesis aims to study the current obstacles and possible resolutions to successfully cryopreserve AC *via* vitrification for long-term storage at cryogenic temperatures.

Chapter One introduces the anatomic structure of AC, the current situation of AC defect repair, and strategies that have been developed and main challenges that remain in order to successfully cryopreserve AC. Based on the clinical settings, Chapter Two to Chapter Five of this thesis present potential vitrification protocols to cryopreserve three scales of AC grafts for different surgical repair purposes. Chapter Two validated two engineering optimized vitrification protocols for small particulated cartilage cubes with a size of 1 mm^3. Chapter Three compared three vitrification

protocols for medium osteochondral grafts with two sizes of 6.9 mm diameter and 10 mm diameter. In addition to the validating the effectiveness of an engineering model, Chapter Three investigated the relationship between the vitrification outcomes and tissue sizes and container sizes. Chapter Four evaluated five potential additives for their protective effects on chondrocytes that have been exposed to high concentrations of multiple cryoprotectant mixtures. Chapter Five incorporated the best approaches obtained from the previous chapters for the vitrification of large femoral condyle grafts with a size of approximately 50×30×20 mm^3. Chapter Five provided a new perspective for vitrification and storage of large AC tissue at cryogenic temperatures. From these experiments, this thesis demonstrated a practical pathway to optimize vitrification of AC with encouraging results. The knowledge presented from these studies will further promote the development of AC vitrification to address the clinical shortage of AC grafts.

1.2 Articular cartilage anatomy

Articular cartilage (AC) is a few-millimeter-thick hyaline cartilage tissue that covers articulating joint surfaces. The main function of AC is to produce near frictionless motion between two joint surfaces for daily joint movement and weight-bearing. Grossly, AC is a semi-transparent connective tissue with a smooth, firm surface that relies on synovial fluid for nutrient exchange and waste transportation[76,184]. Unlike other tissue, it does not contain blood vessels or lymphatic systems and is not innervated[219], and thus the ability of the AC to regenerate or adapt to mechanical changes is very limited. AC has a varied thickness depending on its location with a mean thickness of 2.4 mm in adult knee AC of medial femoral condyles[101]. AC is composed of an extracellular matrix (ECM) structure with a highly specialized cell type called chondrocyte. Chondrocytes play

an important role in the development, maintenance, and repair of the ECM. The chondrocytes present in AC account for only up to 10% of the total cartilage volume[33] with a density of approximately 10,000 chondrocytes per mm^3 of AC tissue, and the mean diameter of chondrocytes is 13 μm under microscopic analysis[101]. From the AC lamina splendens to the tidemark that connects subchondral bone, AC is divided into four zones with varied amounts of chondrocytes and ECM: the superficial zone, the middle zone, the deep zone, and the calcified zone[76,100,184]. In recent years, some literatures reported a very few stem cell like progenitor cells in the presence of the superficial zone in AC[18,57,94,107], which may play a role in the cartilage healing process after mild injury.

Within the AC, the amount of chondrocytes in relation to the amount of ECM is relatively small. The semi-transparent structure surrounding the chondrocytes, the ECM (see Table 1.1), is mostly composed of water, collagen, and proteoglycans, with other non-collagenous proteins and glycoproteins present in lesser amounts[219]. The water content in AC ranges from 80% in the superficial zone to 65% in the deep zone. The major collagen synthesized by chondrocytes in AC is collagen type II, which accounts for 90~95%, while the other minor collagens are type V, VI, IX, X and XI[95]. These collagens are uniquely orientated in different AC zones to provide AC a strong tensile property. Proteoglycans are secreted by chondrocytes into the ECM and they contribute 10~15% of the wet weight of AC. The proteoglycan is a large molecule with a protein core covalently bound with a glycosaminoglycan (GAG) side chain, and numerous proteoglycans linked to a long hyaluronic acid chain *via* the link proteins will turn into a complex structure called a proteoglycan aggregate[184]. There are three major types of disaccharide units on a GAG side chain, including chondroitin sulfate (CS), keratin sulfate, and dermatan sulfate. These disaccharide units

hold a negative charge that further interacts with positively charged ions such as Ca^{2+} and Na^{+}, which can cause interstitial water movement within the ECM. The fixed negative charge of aggrecan plays a key role in the osmotic swelling and shrinking resulting from the interstitial water movement, giving an elastic nature to support AC compressive strain during weight loading and relaxing phases[219].

Table 1.1 Composition List of Articular Cartilage[76]

Components	**Amount by wet weight (%)**
Chondrocytes	5~10%
Water	65~80%
Collagen (type II)	10~20%
Proteoglycans	10~15%
Collagen (type V, VI, IX, X, XI)	<5%
Aggrecan	<5%
Hyaluronate	<5%
Lipids	<5%

1.3 Articular cartilage defects

As a highly complicated structure, AC plays an important role in providing normal joint motility. AC defects do not heal spontaneously after injury because the avascular and aneural structure of AC provide limited self-repair capacity[34,76]. Once AC is injured, its repair has been an extremely challenging problem. According to the Outerbridge classification for AC defects (see Table 1.2)[179],

the development of injured AC into osteoarthritis is divided into five grades based on the morphological changes of the AC surface and subchondral bone base. Large cartilage defects over 1 cm^2 often progress into osteoarthritis if not properly treated[33]. An animal study by Schinhan *et al.*[206] documented that focal AC defects of 1.4 cm diameter on the ovine medial femoral condyles developed into severe osteoarthritis with significant degeneration of meniscus after 3 months. Osteoarthritis (OA) is a worldwide leading cause of work disability which results in a massive socioeconomic burden both to the individual and general society, with an affected population of 3.6 million in Canada and over 30 million in the USA[210]. Early intervention to prevent the development of OA in joints will improve patients' quality of life and reduce the medical cost for the treatment of OA disease.

Table 1.2 Outerbridge Classification: Grade of Articular Cartilage Defects[179]

Grade level	Description of articular cartilage defect morphology
Grade 0	Intact articular cartilage with normal, smooth surface
Grade 1	Intact joint surface with cartilage softening and swelling, focal color change
Grade 2	Fissuring appearance in superficial layer of articular cartilage
Grade 3	Formation of fissures and fragments extended to deep articular cartilage matrix
Grade 4	Development of erosions affecting subchondral bone and bone eburnation

1.4 Resurfacing technique for articular cartilage defects

Over the past decades, orthopedic surgeons have developed different approaches to repair AC defects and helped patients to return to work and recreational activities with a better quality of life.

There are several surgical procedures proposed to treat AC defects, e.g., microfracture[217,221,254], drilling[91], autogenous chondrocyte implantation[19,117,133,164], osteochondral autograft transplantation[104,160] and osteochondral allograft transplantation[37,83,87,118,173]. In addition, stem cell and cartilage tissue engineering are also being investigated and reported as potential resurfacing techniques in both animal and clinical studies[109,131,154,201,231].

1.4.1 Microfracture

With a small cartilage defect after joint injury, microfracture is one of the quickest interventions[217,221,254]. The basic concept in microfracture is to stimulate new AC growth by providing a blood supply near the AC defect. After removing the damaged AC, multiple holes are generated *via* a sharp awl into the subchondral bone beneath the AC defect site. This procedure leads to migration of bone marrow derived cells into the AC defect, which enables a fibrocartilaginous healing process. This procedure is convenient, inexpensive and can be done under arthroscopy with one visit[254]. However, this technique is limited to small AC defects[217], usually in young patients with a single chondral lesion.

1.4.2 Drilling

AC repair by drilling is another procedure in an orthopedic surgery[41,79,214]. In this procedure, several holes are made through the AC matrix and the subchondral bone in the AC defect area using a surgical drill. The drilling will penetrate the subchondral bone and provide small channels to allow cell migration and stimulate the new growth of healthy AC. Drilling is similar to microfracture and it can be performed under arthroscopy.

1.4.3 Autogenous chondrocyte implantation

Autogenous chondrocyte implantation (ACI)[19,47,164,172,174], is a stepwise technique which involves laboratory assistance. In this procedure, at the first stage, healthy articular cartilage from the non-weightbearing area of the donor joint is harvested, and chondrocytes are isolated and cultured to increase the cell number for the following 3−6 weeks. At the second stage, these chondrocytes after cell culture will be transplanted to cover the AC defect area for AC regeneration[19,164,189]. In short, this technique applies new grown healthy chondrocytes to repair the AC defect using the donor chondrocytes from the patient themselves. This procedure is advantageous because of less immune rejection after transplantation and it is more common in younger patients with a single defect with a size > 2 cm diameter. However, this AC repair approach is expensive and time-consuming, and requires more operations in hospital.

1.4.4 Cartilage tissue engineering

Tissue engineering involves a wide range of research using stem cells, platelet-rich plasma, and growth factors for the regeneration of AC for cartilage repair[123,201,231]. Stem cells isolated from bone marrow have been differentiated and cultured to produce cartilage grafts targeting AC repair[7,109,131,231]. Platelet-rich plasma is a therapy using concentrated platelets with autologous blood growth factors, and it has been used in clinical trials to evaluate its potential in AC regeneration[132,214]. Chondrocytes cultured with growth factors, such as transforming growth factor beta 1 (TFG β1), have been shown to successfully induce cartilage regeneration for repairing AC defects[175]. Animal studies on rats, rabbits, and goats have documented the encouraging

effectiveness of regenerated cartilage tissues[7,175]. However, the engineered cartilage tissues were mostly under laboratory investigations and have not been used in human clinical transplantation.

1.4.5 Osteochondral autograft transplantation

Osteochondral autograft transplantation is another technique for focal AC repair. The main concept of this procedure is to harvest and transplant healthy AC grafts from the non-weightbearing area to repair AC defects in the same patients using their own cartilage tissues. The AC defect size indication for osteochondral autograft transplantation is 1 to 4 cm^2 full thickness lesion[104,160]. This procedure is a one-stage operation for repair of small AC defects, which is performed by using a single osteochondral autograft or multiple osteochondral autografts (mosaicplasty[91,160]). One of the major drawbacks of this technique is that it will induce AC defects on the joints that may lead to development of OA in the non-weightbearing area[160]. In addition, the osteochondral autografting will depend on the available healthy AC in the patient joints because the grafts can only be taken in limited areas of the joints; therefore, this procedure is not practical for large AC defects.

1.4.6 Osteochondral allograft transplantation

Osteochondral allograft transplantation is a joint resurfacing procedure to transplant healthy AC donated by a deceased donor to a patient who has AC defects[173,244]. The use of osteochondral allografts is a vital option in the treatment of a variety of osteochondral lesions in the knee, ankle, or elbow joints[23]. This resurfacing technique can restore an intact joint surface by filling the AC defect with a healthy osteochondral allograft on a bone base regardless of the size of AC

defects[227,244,250]. The allograft is harvested after the donor death and stored in a tissue bank under sterile conditions. The allograft is measured for graft size matching and tested for any infectious diseases before shipping to the orthopedic surgeons who make a request. Upon sample arrival in the operating room, the osteochondral allograft is prepared into a matched size graft and implanted into the patient joints that have large AC defects. This resurfacing technique is a one-time procedure and has shown satisfying outcomes according to clinical follow ups; however, it is limited by the available cartilage allograft donors[37,83,227,244].

1.5 Fresh osteochondral allografts

Using fresh osteochondral allografts for cartilage transplantation is a popular treatment for resurfacing AC defects in orthopedic clinics. Hypothermic preservation of fresh osteochondral allografts at 4 °C has been established in most tissue banks around the world to provide healthy human cartilage grafts for the repair procedure[242,246]. However, the major limitation of hypothermic preservation is its short timeframe for storage of cartilage grafts. The standard shelf time of fresh human osteochondral allografts stored at 4 °C in a Ringer's lactate solution is usually 28 days in the tissue banks[86,242]. Although some studies reported using fresh donated AC that had been kept in the tissue bank for up to 6 weeks (42 days) before clinical transplantation[31,145], evidence has shown that chondrocytes in AC start declining after 1 week of storage at 4 °C[243,246]. This finding is consistant with an early investigation of osteochondral autografts stored in tissue culture medium using hypothermic preservation that showed chondrocyte decline after 10 days[151]. More importantly, fresh osteochondral allografts are required to be screened for transmissible diseases, e.g., hepatitis B virus (HBV), human immunodeficiency virus (HIV), or syphilis, for a

minimum of 14 days to finish the reglulatory process, according to the standards of the American Association of Tissue Banks and the Food & Drug Adminstration regulations[86,141]. Thus, the tight timeframe of fresh stored cartilage grafts at 4 °C makes it challenging for the surgeon to transplant these cartilage grafts in time, and the avaliability of fresh osteochondral allografts limits the clinical practice of using this resurfacing technique.

1.6 The need for articular cartilage preservation

Fresh osteochondral allograft transplantation has been proven to be an effective surgical procedure[87] for large cartilage defects over 1 cm^2 , but it is limited by the availability of fresh joint donors, and by the long duration for the essential medical testing before the transplant procedure[36]. Preservation of fresh AC in tissue banks has been a routine procedure to aid AC repair in clinical practice. Currently, the shelf life of fresh AC is limited according to the protocols in standard tissue banks. Fresh osteochondral allografts are currently stored for a minimum of 2 weeks to undergo reglulatory clearance, e.g. microbiological testing, and a study by Laparde *et al.* showed an average age of 20 days for the stored grafts to be implanted into the patients[138]. When the shelf life of cartilage allograft expires, the stored allografts have to be discarded. The lack of suitable preservation protocols for human AC has resulted in a large amount of cartilage graft waste every year, according to reports of tissue banks located in the US[23,83].

The storage of either isolated chondrocytes or osteochondral grafts requires a well-designed tissue banking system with appropriate preservation protocols. Successfully cryopreserved cartilage allografts should allow storage for months or years, and provide surgeons with the practical

flexibility to handle medical issues such as graft size matching, infectious disease testing, blood and human leukocyte antigen (HLA) typing, and graft transportation to the operating room[191].

In short, preservation of AC for the long term is a challenging issue in tissue banks. Successful cryopreservation of AC should extend the availability of the tissue and allow long-term banking of AC. This would enable cartilage defect repair, and would ease the difficult situation of fresh AC allograft shortage. Therefore, modern tissue banks with well-performing standard protocols for preserving donated AC tissues would enable future clinical transplantation to repair AC defects.

1.7 Approach for cryopreserving articular cartilage

1.7.1 Cryopreservation

Cryopreservation, also known as “cryogenic preservation”, is a widely used approach for long-term storage of biological products in a tissue bank. Cryopreservation is a process that uses cryoprotective agents to preserve biological constructs such as organelles, cells, tissues, extracellular matrix, or organs at cryogenic temperatures that mitigate any cell decline caused by unregulated chemical kinetics, typically stored at −80 °C in a deep freezer or at −196 °C in liquid nitrogen[105]. There are two typical approaches in cryopreservation, slow programmable freezing and ice-free vitrification that are two basic methods of cryopreservation[156,198]. The discovery of cryoprotective agents greatly promoted the development of cryopreservation; see Fig 1.1 for the timeline of discovery for several commonly used cryoprotective agents.

1.7.1.1 Cryoprotective agents

A cryoprotective agent, also called a "cryoprotectant" (CPA), is a solute that can be used in a medium to reduce freezing injury during the cryopreservation cycle (freeze–thaw) for improving cell recovery[124]. In 1940, Luyet[149] found that ice crystals account for cell death during cooling to subzero temperatures; he concluded that mitigating ice formation would benefit preserving cells at low temperatures. Later, the discoveries that certain molecules could function as CPAs led to the finding that ice formation can be inhibited by adding CPAs[124,147,148,190]. Since then, CPAs have become popular and are widely used to protect cells from cryoinjury when cooled to cryogenic temperatures. There are two major classifications of CPAs: penetrating CPAs and non-penetrating CPAs, based on their ability to permeate into cells (penetrating CPAs form one group of CPAs which can penetrate across cell membranes while non-penetrating CPAs cannot penetrate cell membranes) during CPA loading (a step usually required before cooling to low temperature)[186]. Glycerol (Gly), dimethyl sulfoxide (DMSO), ethylene glycol (EG), and propylene glycol (PG) were discovered to be cryoprotective in the 1960s (see Fig. 1.1), and are four permeating CPAs commonly used in many cryopreservation protocols[163]. Sucrose, trehalose, lactose, and mannitol are four typical non-permeating CPAs used in combination with permeating CPAs in some established protocols as reviewed by Karow[124].

1.7.1.2 Protective effects of cryoprotective agents

In addition to inhibiting ice crystal formation during cell freezing at low temperatures, the other cryoprotective mechanisms of CPAs have been studied by numerous researchers. As defined by Karow[124], CPAs are divided into two classes based on their molecular weight, small molecular weight (penetrating) CPAs and high molecular weight (non-penetrating) CPAs, and the major

properties of both penetrating and non-penetrating CPAs include freezing point depression, ice formation inhibition, and ion concentration reduction during cooling to super low temperatures. Theories have been proposed to explain the mechanisms of CPA protection for cryogenic storage. Nash[171] was one of the first who studied erythrocyte cryopreservation and he proposed that CPA protection was associated with hydrogen bonding ability with water. Doebbler[55] reviewed the ability of CPAs to hydrogen bond with water, and he concluded that this property was strongly correlated with the protective effects of different CPAs. Doebbler and his colleagues[56] also investigated the physical properties of aqueous solutions including different CPAs, and pointed out that the viscosity of these aqueous solutions would increase as the temperature decreased, which would affect the ice nucleation kinetics and ice crystal growth. Another opinion was reported by Arakawa et al[13], where the toxicity level of CPAs was temperature-dependent; they concluded that CPAs could stabilize proteins on cell membranes during freezing at low temperature and destabilize them at elevated temperature.

It is instructive to name a few representative CPAs and their cryoprotective capacities. Glycerol was the first cryoprotective compound and it was discovered by Polge and Smith[190] in 1949. Glycerol was used previously as an agent to immobilize sperm for microscopic examination. Glycerol interacts with polar head groups of phospholipids on the cell membrane lipid bilayers[10], thereby providing stabilization of the cell membrane. It has since been proven to be cryoprotective in sperm of various species[12,90] and in many other cell types[146,162,186]. DMSO is the most commonly used penetrating CPA. An early study by Odink *et al.*[176] reported the influence of DMSO and cooling conditions on the cryopreservation of human platelets. It was reported to be a membrane protein stabilizing compound, according to Baxter and Lathe[22], that demonstrated protein

stabilizing or destabilizing tendency after addition and removal of DMSO. As reported by Wolker *et al.*[220], DMSO can decrease the cell membrane disturbance at low temperature (−40 °C) and also delay protein denaturation during rewarming to physiologic temperature (37 °C) of cryopreserved human pulmonary endothelial cells. EG is another typical penetrating CPA that been applied in many cryopreservation protocols, such as human erythrocytes[56], mouse blastocysts[262], human oocytes[42] etc. The protective mechanism of EG involves two aspects in reducing osmotic effects and membrane disturbance by specific interactions with membrane phospholipids. Trehalose is a typical non-penetrating cryoprotectant commonly used in sperm cryopreservation, which is known to preserve the membrane structure of sperm from oxidative and cold shock damage[6]. It can induce a hypertonic environment in media which further leads to cellular osmotic dehydration before freezing, and in return decreases cell injury due to ice crystal formation[224].

1.7.1.3 Adverse effects of cryoprotective agents

As a new class of drug, CPAs have been investigated for their adverse effects in both cryobiological and non-cryobiological applications[124]. CPAs are usually non-toxic at lower concentration[26]; they only become toxic to cells when used at a high concentration (e.g. 2M DMSO is non-toxic to chondrocytes while 6M DMSO is toxic at room temperature (22 °C) after 15 min exposure[63]). These high concentrations (usually up to several molar) of CPAs are often required for achieving "vitrification"[70]. A recent study by Fahmy *et al.* investigated CPA injury to human chondrocytes using different doses of CPAs[65]. They concluded that CPA toxicity was concentration-dependent and demonstrated that glycerol and PG were more toxic compared to DMSO and EG. Some strategies such as a combining several CPAs as a mixture have been used to lower the adverse effects of high CPA concentrations in chondrocytes and AC vitrification[113],

as well as other cells such as mouse blastocysts[103] and animal and human embryos[125] with moderate success.

According to Arakawa *et al.*[13], DMSO, PG, and EG were usually excluded from the hydration shell of proteins at low temperatures; however, at higher temperatures these solvents could interact hydrophobically with proteins and act as protein destabilizers. They presented important evidence that CPAs (e.g. DMSO) were effective in cryoprotection but that they can be toxic to cells at higher temperatures, which may be due to the temperature-dependent capacity of these molecules to interact with cell membrane proteins. CPA cytotoxicity can depend on the target cells. For instance, EG was reported to be metabolized by alcohol dehydrogenase to glycoaldehyde and then by aldehyde dehydrogenase to produce glycolic acid in the liver and caused metabolic acidosis in cells[81,96]. PG has less toxic effects in certain conditions as evidenced by the fact that it has been safely used in many food products at low concentration, while it often exhibits high toxicity when used as a CPA in high concentrations[51]. PG can increase serum hyperosmolality and anion gap metabolic acidosis[259]. A study by Aye *et al.*[15] evaluated genotoxicity of three CPAs including DMSO, EG, and PG when used for human oocyte vitrification and they showed that EG was significantly genotoxic in the presence of an external cytochrome-based P450 oxidation system while DMSO was not, and that both EG and PG were clastogenic and could induce *in vitro* chromosomal loss in eukaryotic cells. In summary, the diversities of adverse effects reported for these compounds make it more challenging when designing an appropriate cryopreservation protocol for a specific cell type, and even more complicated for larger tissues that include several cell types.

1.7.1.4 Application of cryoprotective agents in chondrocytes

Cryopreservation of chondrocytes has been investigated by numerous researchers since the 1950s, and promising successes have been achieved in modern studies[39,52], outlining the possibility of storing chondrocytes for clinical transplantation. The first report of chondrocyte cryopreservation was in 1956 by Curran and Gibson[49]; however, the unsuccessful experiment of cartilage slice preservation by their group led to the development of cryopreservation of isolated chondrocytes. Later, Heyner[97] reported promising results on cryopreserved chondrocytes isolated from rabbits, dogs, monkeys, and followed by Smith[215] in adult mammals, see Fig 1.1. Cetinkay and Arat[39] conducted a study using slow freezing for preservation of isolated bovine knee chondrocyte cell suspensions with positive results for cell viability, membrane integrity, and metabolic functionality after post-thaw procedures. However, isolated chondrocytes have limited regenerative potential without extracellular matrix (ECM) for healing large size cartilage defects[212].

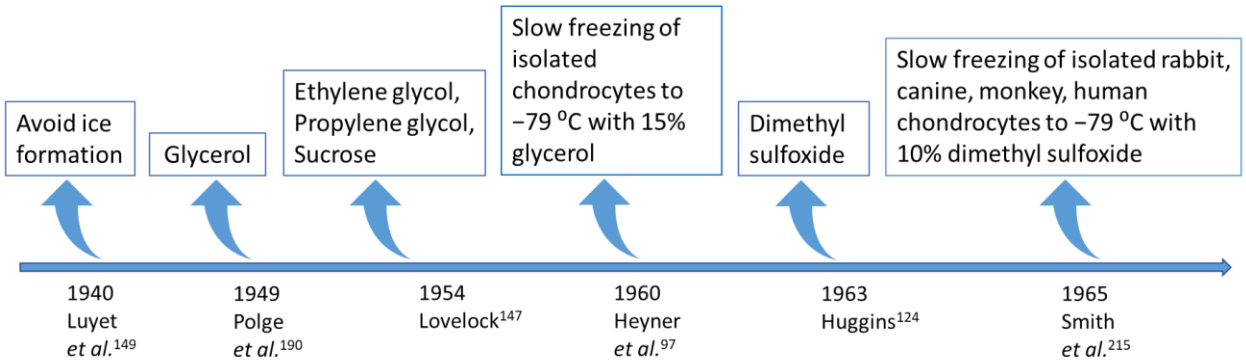

Figure 1.1 The discovery of cryoprotective agents and their first application in chondrocytes

1.7.2 Slow freezing and two-stage cooling

Slow freezing is an approach to use CPAs to prevent ice formation in cells when being cooled to cryogenic temperatures. The basic principle of preserving cells *via* freezing is to reduce or stop cell metabolism at super-low temperatures, therefore maintaining the cell structure and functionality[186]. Slow freezing has been used widely to cryopreserve numerous cell lines. However, slow freezing can be harmful to cells because the process allows ice crystal formation outside the cells[156]. Early in the 1940s, Luyet[149] documented that avoidance of ice formation in the cells was critical for keeping the cell intact and functional after freezing. Intracellular ice formation during the slow freezing process can result in rupture of cell membranes and cell death. Two-stage cooling is a more complex approach aimed at controlling the cooling rates to minimize the effects of freezing injury incorporating the two factor theory, i.e., to avoid the solute effects caused by cooling too slowly and the intracellular ice formation caused by cooling too rapidly[74].

1.7.3 From slow freezing to vitrification

Vitrification is an "ice-free" technique developed for cell and tissue preservation without ice crystal formation. Vitrification is one of most popular methods in many biological disciplines and is regarded as the ideal technology for long-term preservation of intact tissue in a "glass" state at extremely low temperatures (e.g., −196 °C)[230]. Physically, vitrification is a process whereby a liquid being cooled below the glass transition temperature becomes an amorphous solid without crystalline formation[245]. Theoretically, this "glassy" solid will last sufficiently long if stored appropriately at a low enough temperature (e.g., −196 °C).

Ice formation within the AC matrix is an important factor that alters the mechanical properties of cryopreserved AC. The high proportion of water content (65~80% of wet weights) within the chondrocytes and AC matrix make it challenging to cryopreserve AC without ice crystal formation. Eliminating ice crystal formation during cooling and warming processes is a key to achieve successful cryopreservation of AC. Both the slow freezing and two-stage cooling of AC induced ice crystal formation in the cartilage matrix, and this practice has been shown to alter the mechanical properties of AC[169,204], and this was demonstrated by the AC having a shorter graft life after allograft transplantation in a sheep model[169]. Jomha *et al.*[114] also showed unsatisfactory results for cryopreserved intact human AC using the slow freezing approach. This previous knowledge indicated that an advanced method was required to solve the ice problem in AC cryopreservation. Fig. 1.2 shows the path of AC cryopreservation from slow freezing to vitrification. The potential of vitrification has resulted in it being the most used approach in attempts to preserve AC at cryogenic temperatures over the last two decades, including work by Song *et al.*[218], Pegg *et al.*[185], Brockbank *et al.*[30], and Jomha *et al.*[113], each expending great effort on vitrifying animal and human AC such as small osteochondral dowels.

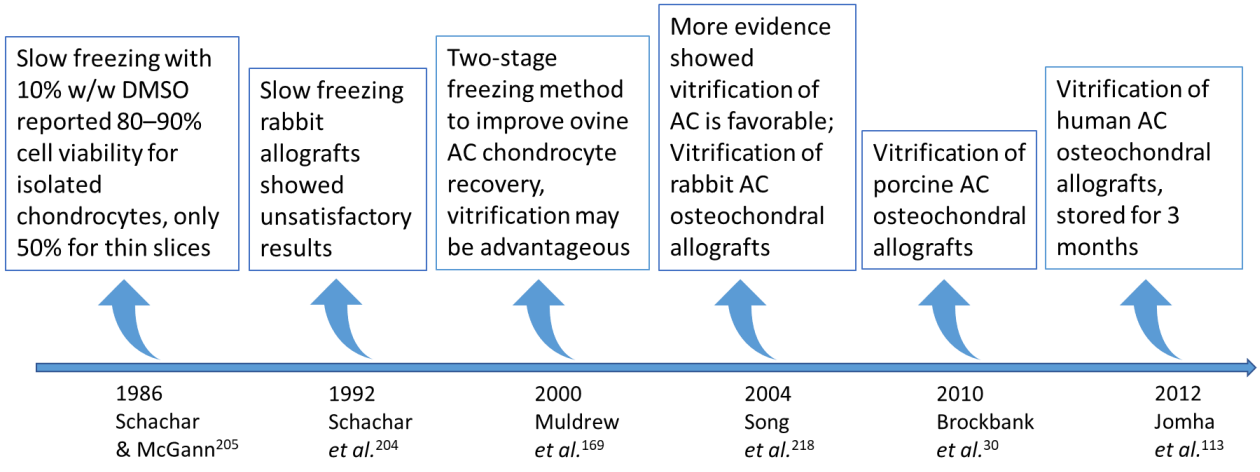

Figure 1.2 From slow freezing to vitrification: the path of articular cartilage cryopreservation

1.7.4 Vitrification of articular cartilage

Cryopreservation by vitrification of articular cartilage has emerged as one promising pathway to aid in clinical repair of articular cartilage defects[3,113]. A variety of studies have been conducted to develop successful vitrification protocols for osteochondral dowels with a bone base, which resulted in numerous techniques that have been introduced into this field[52,113,187,249]. Pegg and his colleagues have done many studies on chondrocytes and AC cryopreservation, and used the "liquidus-tracking method"[185,237] to design a preservation protocol for AC. Brockbank *et al.*[30] conducted a study on vitrification of porcine AC and reported vitrification was superior to conventional cryopreservation, and suggested an advanced technology that focused on vitrification of AC be developed for long-term storage. Jomha *et al.*[113] reported successful vitrification of 10-mm osteochondral dowels and large fragments of human knee AC with promising chondrocyte cell recovery, cellular metabolic function, and extracellular matrix generation potential. See Table 1.3 for a summary of the current vitrification protocols for animal and human AC grafts. Although some progress has been achieved in AC cryopreservation, successful cryopreservation on large portions of knee joints (e.g. full condyles) remains unsolved and an extremely difficult challenge in the field of tissue banking.

Table 1.3 Summary of vitrification protocols for articular cartilage grafts

Group	Year	Approach	Sample	Cryoprotectant	Cooling protocol	Storage	Warming protocol	Cryoprotectant removal	Chondrocyte assement	Clinical relavance
Song *et al.* [218]	2004	Vitrification	Rabbit; osteochondral graft (4 mm diameter)	Multiple CPAs (DMSO, Fm, PG)	43 °C/min from 4 °C to −100 °C, slow cool 3 °C/min to −135 °C/min	Stored at −135 °C for 24 h	Slow warming (30 °C/min) to −100 °C followed by rapidly warming (225 °C/min)	Sequential CPA removal	HE staining	Animal model
Pegg *et al.* [185]	2006	Vitrification	Lamb; 6 mm diameter discs	DMSO	Liquidus-tracking with step changes	Stored at −80 °C for 18 h	Stepwise accelerated warming	Stepwise CPA removal	35S uptake	Animal model
Brockbank *et al.* [30]	2010	Vitrification	Porcine; osteochondral graft (6 mm diameter)	Multiple CPAs (DMSO, Fm, PG)	43 °C/min from 4 °C to −100 °C, slow cool 3 °C/min to −135 °C/min	Stored at −135 °C for 24 h	Slow warming (30 °C/min) to −100 °C followed by rapidly warming (225 °C/min)	Sequential CPA removal	alamarBlue™ assay	Animal model
Jomha *et al.* [113]	2012	Vitrification	Human; osteochondral graft (10 mm diameter) and 12.5 cm^2 large piece	Multiple CPAs (DMSO, Gly, PG, EG)	Liquidus-tracking with stepwise CPA loading with fixed temp at each step	Stored at −196 °C up to 3 months	Rapidly warming to 37 °C	Passive CPA removal	Cell membrane intergrity assay; alamarBlue™ assay; Histology	Human articular cartilage
Onari *et al.* [178]	2012	Vitrification	Rabbit; osteochondral graft (2.7 mm diameter)	Two CPAs (EG, Surcose)	Two step CPA loading	Stored at −196 °C for 20 min	Rapid warming to 22 °C	Two step in PBS + Sucrose	Cell membrane integrity assay; HE staining; Transmission electron microscopy	Animal model
Wu *et al.* [248] (Chapter Three)	2020	Vitrification	Porcine; osteochondral graft (6.9 mm and 10 mm diameter)	Multiple CPAs (DMSO, Gly, PG, EG)	Liquidus-tracking with stepwise CPA loading with fixed temp at each step	Stored at −196 °C for 1~7 days	Rapidly warming to 37 °C	Passive CPA removal	Cell membrane intergrity; alamarBlue™ assay	Animal model

DMSO: dimethyl sulfoxide; EG: ethylene glycol; Fm: formamide; Gly: glycerol; PBS: phosphate buffered saline; PG: propylene glycol

1.8 Current obstacles to articular cartilage cryopreservation

The mechanisms of cryoinjury were detailed in a comprehensive review by Gao and Critser[21,78]. Cryopreservation was widely used to preserve living cells and diminishing their metabolic activity at low temperatures[162]. However, the process of cryopreservation can be harmful to the cells that is called cryoinjury[155,157,158], such as solute effects, intracellular ice formation, recrystallization, etc. Successful cryopreservation of AC has been limited due to several factors including CPA permeation, CPA toxicity, osmotic stress, heat transfer, and tissue storage[3,85,186](see Fig. 1.3). The main obstacles in AC cryopreservation included questions such as: 1) how to achieve sufficient CPA permeation within a practical time frame; 2) how to achieve rapid cooling and warming while resulting in less thermal-mechanical stress to the AC; 3) what kind of appropriate storage can be used for AC vitrification at cryogenic temperatures; 4) how to reduce toxicity of CPAs to an acceptable level, etc. These questions will be discussed in the following sections.

Cryopreservation by vitrification is a preserving method based on vitrifying an aqueous solution into a glassy state using high concentrations of CPAs and a sufficiently rapid cooling rate. However, the application of vitrifiable concentrations of CPAs brings both high toxic effects[65] and osmotic stress[60] to the chondrocytes. Many investigations on using different CPAs[26] or a combination of CPAs[9,116] to reduce the toxic effects have proven to be promising. In addition to CPA toxicity, another problem in AC cryopreservation is the CPA permeation into the AC[105], which is a basic component of cryopreservation. CPA permeation is a process that describes the permeation of CPA into chondrocytes and AC matrix in order to have sufficient amounts everywhere to inhibit ice formation when AC is cooled to low temperatures. Because of the dense AC matrix and the AC

thickness, it is difficult to permeate CPA within a short time period. For example, for 2-mm thick AC, it will take 7 h to 9.5 h to achieve a vitrifiable concentration of CPAs in the AC[113,208]. The long duration of CPA permeation makes the process impractical to be completed in a reasonable amount of time in a tissue bank and requires shortening and optimization.

Osmotic stress is one type of cell injury induced by exposure to the CPAs[60]. Osmotic stress that results in membrane disturbance is induced by the high concentration of solutes and the resultant water movement, which are unavoidable in many cryopreservation protocols[10]. According to Rowe[202], the cell membrane is one of the major targets of freezing injury to cells. This theory was further supported by Crowe's group[48] who focused on the cell membrane stability and used Fourier Transform Infrared spectroscopy (FTIR) to target the hydrophobic interactions among membrane bilayers, amino acids, and sugars. Osmotic rupture of chondrocyte membrane caused by freezing injury has been investigated by Muldrew *et al.*[166,168] and further used to guide the design of cryopreservation protocols for AC[1,62,194].

Convective heat transfer is the method commonly used in many cryopreservation protocols based on heat transfer from a surrounding fluid that has fluid motion[17]. Cryopreservation by vitrification is easier for small size samples and isolated cells, because they can be cooled and warmed more quickly in their entirety and therefore require lesser concentrations of CPAs to be vitirified[69,186]. According to Manuchehrabadi *et al.*, convective cooling can be used to achieve vitrification in large volumes; however, only fast convective warming of $\leq$ 3 ml in a vial is predicted to be successful without failure[152]. Due to the underlying principles of heat transfer, there is a size limit

in the case of surface heating beyond which crystallization cannot be prevented at the center of the specimen.

Tissue storage is now a popular topic in the cryopreservation field. Although it is possible to physically vitrify large tissues up to 80 ml[152] , the technology of tissue storage and the following rewarming approach is limited and difficult to translate into other cryopreservation protocols such as for AC grafts to reproducibly rewarm AC grafts at sufficiently fast and uniform rates to avoid failure by devitrification and cracking[187,260]. Therefore, it remains impractical to vitrify large sized tissues such as whole femoral condyles with present knowledge, and new technologies such as nanowarming[27,216] or new methods by temperature control are required to solve this problem.

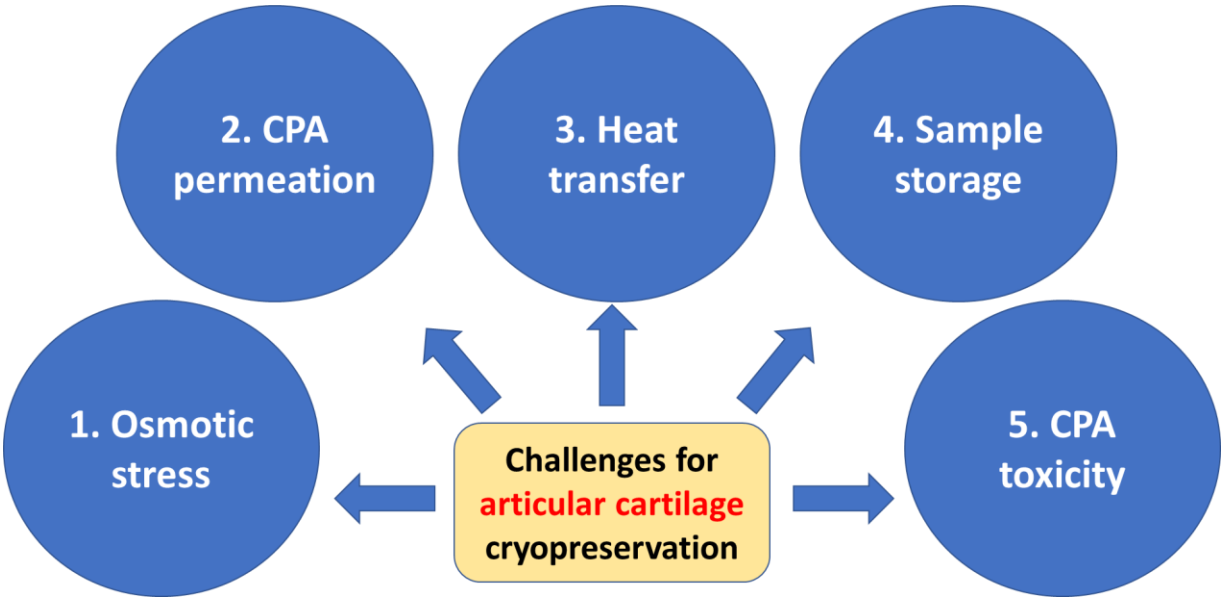

Figure 1.3 The current challenges to improve outcomes of articular cartilage cryopreservation

1.9 The mainstream strategies for articular cartilage cryopreservation

1.9.1 Strategies to reduce osmotic stress on chondrocytes

Osmotic stress is physiological dysfunction in cells that have been exposed to a rapid change in a high solute concentration extracellularly that results in extensive movement of water across the cell membrane[177]. Water movement across chondrocyte membranes may cause cell rupture and cell death, a reason that osmotic stress needs to be avoided or mitigated during cryopreservation. Fig 1.4 demonstrated the development of strategies to reduce osmotic stress on chondrocytes for the cryopreservation of AC. Osmotic stress on chondrocytes has been shown to affect the chondrocyte GAG production in human AC[207], and it can further activate the chondrocyte apoptotic pathway that leads to chondrocyte apoptosis[197].

McGann *et al.*[161] investigated the osmotic water movement in isolated chondrocytes and explored its potential application to AC cryopreservation. They measured the cell response based on the kinetic volume change of chondrocytes in a hypertonic solution at different temperatures, determining the hydraulic conductivity of chondrocyte plasma membrane and the Arrhenius activation energy that describes its temperature dependence. And they concluded that the least damaging cooling rate for chondrocytes in suspension without the presence of CPA solutes is 10 °C/min. In addition, they found that the isolated chondrocytes contained a higher percentage of osmotically bound water than other cell types, which provided information about the osmotic water permeability characteristics of chondrocytes for development of new cryopreservation protocols for chondrocytes and AC tissue. The osmotic resistance in chondrocytes was also confirmed by Pegg *et al.*[187] in the later practice of AC cryopreservation.

Muldrew *et al.*[168] studied the osmotic rupture of cells under the osmotic driving force from water movement and they proposed a hypothesis that the cell membrane could fail if the pressure exceeded the tensile strength of the cell plasma membrane. Muldrew[166,167] demonstrated that intracellular ice formation during rapid cooling was harmful to the chondrocytes in AC and other mammalian tissues, and this finding supported the design of two-stage cooling protocols for AC cryopreservation.

As mentioned earlier in the AC anatomy, the fixed charge of aggrecan throughout the AC matrix plays a vital function in AC deformation, e.g. AC swelling, and this knowledge was developed into a biphasic theory that included the fluid and solid phases. Lai *et al.*[137] incorporated the biphasic theory with an ion phase that became a triphasic theory. In their work, they pointed out that this triphasic model can be applied to both equilibrium and non-equilibrium swelling of AC, and this knowledge aided in the explanation of compressive stiffness of AC, and volume change of AC that can occur and may be relevant to osmotic effects experience by the chondrocytes. The triphasic approach was further expanded into a biomechanical model by Abazari *et al.*[1] that incorporated thermodynamically non-ideal solutions and fit to experimental data to determine the transport parameters (e.g., water permeability, solute permeability, diffusion coefficient of solute) of the transport equation when AC was exposed to a CPA solution. Based on this model, they were able to predict the increase of CPA solute in the AC matrix, which provided valuable direction for designing successful AC cryopreservation protocols (Fig. 1.4).

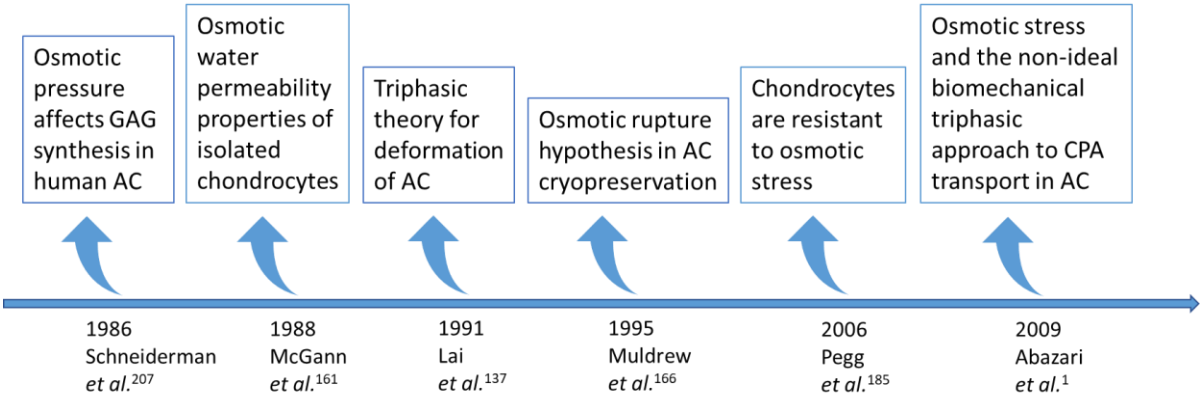

Figure 1.4 Developing strategies to reduce osmotic stress on articular cartilage

1.9.2 Strategies to improve cryoprotective agent permeation

CPA permeation is an essential component of a cryopreservation protocol. Fig 1.5 describes the brief history of development in CPA permeation strategies that have promoted the cryopreservation of intact AC. Achieving an efficient CPA permeation will determine the success of AC cryopreservation. CPA permeation into AC depends on the CPA diffusion kinetics into the cartilage matrix and the thickness of the AC, and this procedure is also partially limited by the CPA toxicity, practical processing time etc[3]. Kawabe and Yoshinao[127] investigated the viability and function of chondrocytes in rabbit cartilage slices after CPA exposure to a combination of different CPA concentrations, times of exposures, and temperatures followed by cooling to −80 °C. This study provided information indicating CPA kinetics were closly associated with the cryopreservation outcomes for AC slices. Muldrew *et al.*[170] determined the permeation kinetics of DMSO in AC, and following that, more CPA kinetics have been measured in porcine AC[115,211], e.g. for PG, EG, and Gly. The kinetic parameters obtained from these studies were helpful for modelling CPA transport in AC[165,209].

In 1965, Farrant[73] evaluated the mechanism of cell injury during the freezing and thawing cycle and he realized that by staying above the freezing point ice crystals in the cells being cooled can be eliminated or avoided, which was regard as the origin of "liquidus-tracking theory". This theory has greatly promoted the development and advances of cryopreservation of AC. Pegg *et al.*[185] applied the liquidus-tracking approach to improve CPA permeation of DMSO gradually to achieve a high enough concentration in the AC matrix that is required for ice-free cryopreservation of AC.

CPA permeation optimized by engineering modelling is a new advanced approach to efficiently generate protocols for improving cryopreservation of AC. Based on Fick's law of CPA diffusion kinetics, Shardt *et al.*[208] combined calculation of spatial, temporal transport of CPA with vitrifiability scoring[239], to make predictions of CPA concentration, freezing point, and vitrifiability of the AC tissue using available CPA molarity, CPA permeation duration and temperature. Using this approach, they were able to shorten an AC CPA permeation protocol while maintaining a similar vitrifiability for a given thickness of cartilage[208].

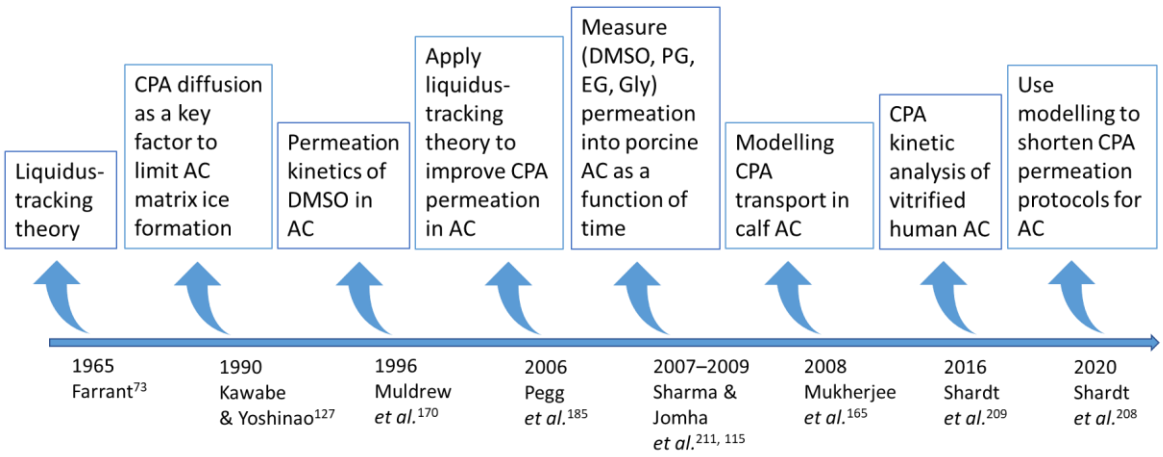

Figure 1.5 Developing strategies to improve cryoprotective agent permeation into articular cartilage

In the current thesis, I validated several new CPA permeation protocols that were generated from the engineering model developed by Shardt *et al.*[208] for the vitrification of both porcine and human AC. In Chapter 2, I applied two 2-step CPA permeation protocols for the vitrification of 1 mm^3 particulated porcine and human AC. In Chapter 3, I compared three CPA permeation protocols for their effectiveness in the vitrification of 6.9-mm and 10-mm diameter porcine osteochondral dowels. And in Chapter 5, I used the optimized 7-hr protocol developed by Shardt *et al.*[208] for the vitrification of full porcine femoral condyles. The findings from this thesis provide important experimental evidence to support the accuracy of the engineering model developed by Shardt *et al.*[208].

1.9.3 Strategies to improve heat transfer during cryopreservation of articular cartilage

Heat transfer is a critical factor that affects the outcome of cryopreservation of AC. Scientists have been working on heat transfer for decades and have developed automatic machines to cool and warm isolated cells at superfast speeds[126], but the practice of cooling and warming a large sample at a superfast speed remains very challenging[236]. The traditional approach in most current protocols to achieve fast cooling and warming rates is the use of convection heat transfer whereby the specimen is exposed to a temperature-controlled environment[59].

Fig 1.6 illustrates the investigations of cooling and warming (heat transfer) for cryopreservation of chondrocytes and AC over the last four decades. In 1986, Schachar and MaGann[205] identified an optimal cooling rate of 1.3 °C per min for slow-cooling of isolated bovine chondrocytes and documented that it would provide a chondrocyte survival of 53.6% after cryopreservation and storage in a deep freezer at −70 °C. Muldrew *et al.*[167,169] showed that a two-stage cooling approach can reduce the osmotic stress due to intracellular ice formation on ovine chondrocytes by the avoidance of cooling too rapidly. Pegg *et al.*[185] applied a multi-step cooling-loading method using DMSO as a CPA to cryopreserve lamb cartilage disk with 6 mm diameter. Brockbank *et al.*[30] investigated a controlled cooling approach to vitrify porcine osteochondral plugs with a diameter of 2 mm and 4 mm. Jomha *et al.*[113] first documented the possibility of vitrification of intact human AC tissue (10 mm diameter osteochondral dowels and 12.5 cm^2 osteochondral fragments) using a multi-step, multi-temperature and multi-CPA permeation approach followed by plunge in liquid nitrogen in a Falcon tube filled with 5 ml CPA solution at a cooling rate of approximately 60 K/min according to Weiss *et al.*[239].

Gao *et al.*[181] investigated the technique of electromagnetic resonance heating using magnetic nanoparticles and documented a promising fast warming rate of 200 °C per min for the 10 ml bulk CPA solutions. Nanowarming is a new emerging technology for uniform, rapid warming with the combination of radio-frequency heating and the use of nanoparticles, e.g. iron oxide[27]. The application of nanowarming technology in AC cryopreservation has not been investigated. Preliminary assessments such as permeability of nanoparticles into AC or rewarming with the radio-frequency heating approach may be valuable for improving AC cryopreservation.

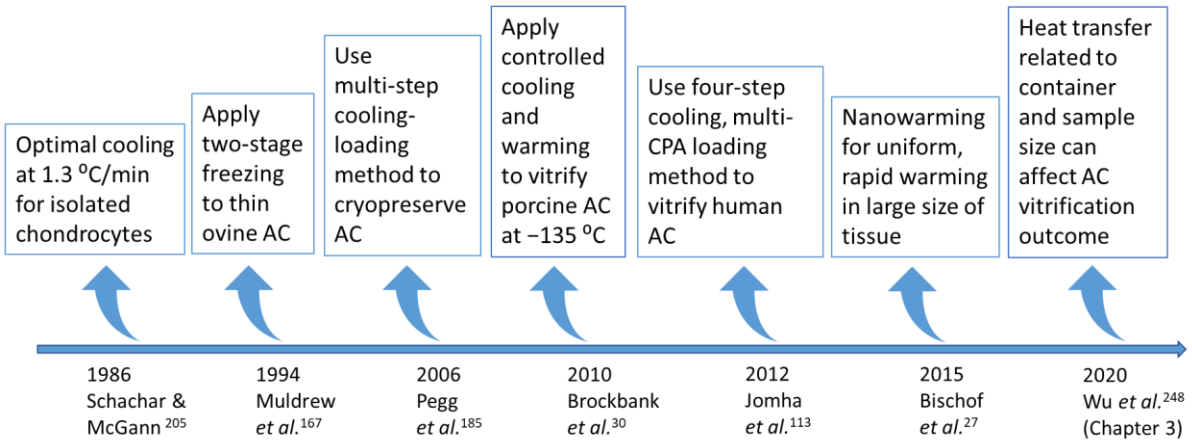

Figure 1.6 Developing strategies to improve heat transfer for cryopreservation of articular cartilage

In this thesis, I evaluated the role of heat transfer by comparing the responses of two container sizes (15 ml and 50 ml Falcon tube for tissue storage) for the vitrification of porcine osteochondral grafts (see Chapter 3). When AC tissue is stored with a large container, the heat transfer from the surroundings to the AC tissue is slowed and further results in injuries to the chondrocytes such as those caused by devitrification, therefore showing a low chondrocyte survival after vitrification.

Conversely, AC tissue stored in a small but sufficient container has faster cooling and warming rates and the AC undergoes vitrification and rewarming procedures with a high chondrocyte survival. The findings from this thesis provided data reinforcing that smaller container sizes for the storage of osteochondral grafts increase the ease of obtaining successful vitrification outcomes for AC, and this provided direct information for the design of AC vitrification protocols (see Chapter 5).

1.9.4 Strategies to avoid tissue cracking during cryopreservation of articular cartilage

The thermo-mechanical stress that develops during the cooling and warming of a solid from the outside can result in the solid cracking, which is a big challenge for tissue vitrification. Fig 1.7 highlights the developments of strategies to minimize the cracking effects during cryopreservation of AC. Kroener and Luyet[134] reported observation of crack formation in a glycerol solution during cooling below the glass transition temperature for vitrification. Rall and Meyer[199] investigated the fracture damage of cryopreserved mammalian embryos. They concluded that solution fracturing was induced by rapid temperature changes and this phenomenon was blamed for further zona pellucida damage in the embryos. Rubinsky *et al.*[203] found that glass cracks during the liquid–solid phase change due to the development of aggressive thermal stress in the liquid–solid mixture.

Solution cracks are harmful to biological tissue and result in tissue fractures. Williams[241] pointed out that solution fracturing could initiate an interface for ice nucleation and result in the

development of tissue devitrification. Pegg *et al.*[188] studied the fracture of cryopreserved arteries and showed that solution cracks could be limited by the controlling of cooling and warming rates of the cryopreservation solution near the glass transition temperatures. Rabin *et al.*[196] investigated the thermal stress of freezing biological samples, and they demonstrated that the thermal expansion of biological structures can be predicted and calculated. However, the calculation of thermo-mechanical stress is complicated for AC grafts. Thermal expansion of AC during cryopreservation has been investigated by Xu *et al.*[252] and they found that inhomogeneous thermal expansion in cryopreserved AC was the main reason for cryopreservation failure. In addition, they showed that a higher concentration of CPA (e.g. 60% DMSO) used for cryopreservation can contribute to a smaller thermal strain change when AC was cooled close to the glass transition temperature. Eisenberg *et al.*[59] investigated a new approach by combining the technology of nanowarming with thermo-mechanical stress modelling, and they found that volumetric heating during the rewarming phase could alleviate the size limit of the VS55 cocktail solution (a mixture of 3.1 M DMSO, 2.2 M PG and 3.1 M formamide (Fm)[198]); however, the strong mechanical stress in a large volume still resulted in structural fracture in the vitrified solution.

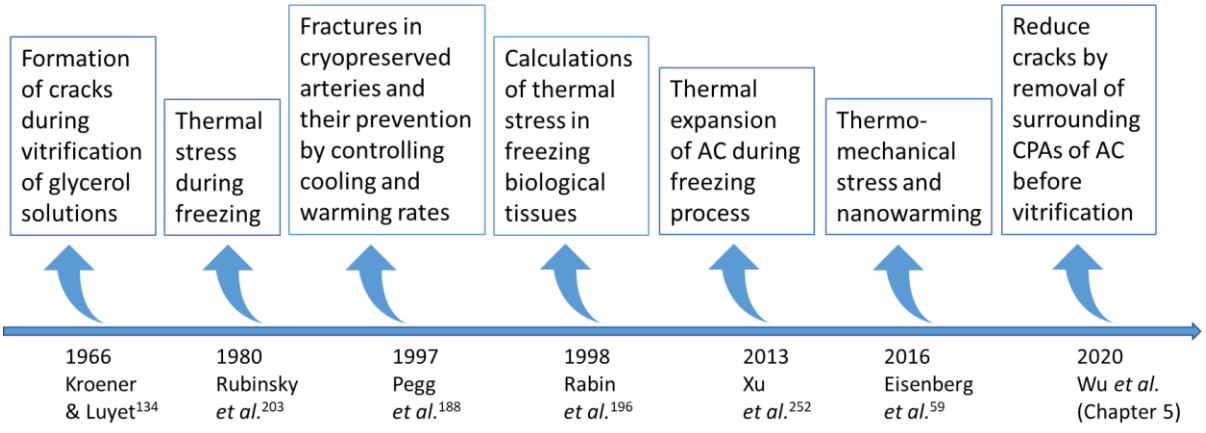

Figure 1.7 Developing strategies to avoid tissue cracking during cryopreservation of articular cartilage

In this thesis, I evaluated a novel method for storing vitrified AC at cryogenic temperature (see Chapter 5). Since CPA permeation was already completed to provide a sufficient amount of CPA into the chondrocytes and AC matrix, the vitrification could occur without the presence of the surrounding CPA solutions. After CPA permeation with the 7-hr optimized protocol[208], I removed the surrounding CPA solution and vitrified porcine AC grafts (both 10 mm diameter osteochondral dowels and full femoral condyles) in vacuumed storage bags. The findings in this chapter documented a new approach to store intact AC for vitrification. This new approach may change the current vitrification practice of solid tissues.

1.9.5 Strategies to reduce cryoprotective agent toxicity

CPA toxicity is a major limitation in the development of cryopreservation protocols. Many investigations have been done to minimize the toxicity of CPA on cells and tissues being cryopreserved. Fig 1.8 shows the development of strategies to reduce or neutralize CPA toxicity on chondrocytes for AC cryopreservation. Tomford *et al.*[232] measured the toxicity limits of DMSO and glycerol on bovine chondrocytes, and they pointed out that a high concentration of CPA was associated with high toxicity to chondrocytes during the CPA permeation processes. Fahy *et al.*[198] proposed the use of a CPA mixture including DMSO, PG, and formamide for the successful vitrification of mouse embryos, and, later, they demonstrated that a single CPA at a higher concentration was more lethal to the cells than a mixture of multiple CPAs using lower concentrations of each individual CPA[68]. Elmoazzen *et al.*[63] determined the DMSO toxicity on 70-μm thick porcine AC slices; they provided information to systematically analyze the toxicity to

chondrocytes *in situ* and the evaluation was further extended to other CPAs, e.g. PG, EG and formamide[115,116]. Brockbank *et al.*[30] applied a CPA mixture solution containing DMSO, PG, and formamide for the vitrification of porcine AC. When using the same total molarity concentration, Almansoori *et al.*[9] confirmed that multi-CPA solutions were less toxic than a single-CPA solution on isolated human chondrocytes with the best chondrocyte survival after exposure to a 6 M DMSO-EG-Gly-Fm solution for 30 min at 0 °C. Fahmy *et al.*[65] further explored the dose relationship of multi-CPA toxicity on human AC slices. Cell injury caused by different CPAs plays an important role in AC cryopreservation, indicating the choice of CPAs needs to be optimized or their oxidative effects need to be mitigated when developing a protocol.

In addition to careful selection of CPA types and concentrations, another approach to reduce CPA toxicity is to include additives into the CPA cocktail solution. Additives, such as antioxidants, have been shown to provide protective effects on cells after cryopreservation[20,32]. Cryopreservation has been proven to induce oxidative stress on the target cells being preserved both intracellularly and extracellularly during the freeze–thaw procedures[24,225,226]. Oxidative stress is one factor that may aggravate cell sensitivity to high concentrations of CPA. The oxidative reaction between cells and CPAs is an important side effect during CPA loading, and may lead to severe cell injury during CPA loading and cooling to super low temperature in the presence of CPA. Additives, for instance chondroitin sulphate, have been included in AC cryopreservation[30,113]. Hahn *et al.*[89] conducted a study to compare the protective effects of several potential additives on human AC during CPA exposure to glycerol, and they found the inclusion of additives in the glycerol solution was beneficial to reduce the damage induced by glycerol and to improve chondrocyte survival.

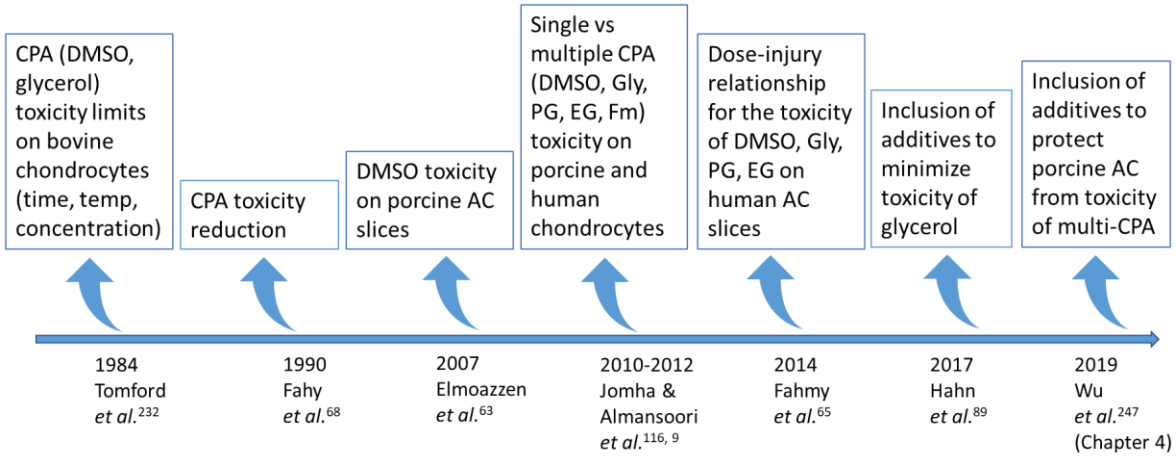

Figure 1.8 Developing strategies to reduce cryoprotective agent toxicity on articular cartilage

In this thesis, in addition to using the stepwise CPA addition strategy to minimize CPA toxicity on chondrocytes (see Chapter 3), I evaluated the efficiency of different additives (e.g. chondroitin sulphate (CS), glucosamine (GlcN), ascorbic acid (AA), and tetramethylpyrazine (TMP)) for their protective effects on porcine chondrocytes in a CPA loading protocol *via* exposure to several high concentration of multi-CPA cocktail solutions including DMSO, EG, and PG (see Chapter 4). I further compared the effects between chondroitin sulphate (CS) and ascorbic acid (AA) on vitrification of porcine AC (see Chapter 5). The findings from this thesis provide information to guide the usage of additives in the cryopreservation of AC and to aid in the development of protocols for the long-term storage of AC tissue

Chapter Two: Vitrification of particulated articular cartilage *via* engineering optimized protocols

Authors: Kezhou Wu[a,b], Nadia Shardt[c], Leila Laouar[a], Janet A. W. Elliott[c,d]*, Nadr M. Jomha[a]*

Affiliations:

[a]Department of Surgery, University of Alberta, Edmonton, Alberta, Canada

[b]Department of Orthopedic Surgery, First affiliated hospital, Shantou University Medical College, Shantou, Guangdong, China

[c]Department of Chemical and Materials Engineering, University of Alberta, Edmonton, Alberta, Canada

[d]Department of Laboratory Medicine and Pathology, University of Alberta, Edmonton, Alberta, Canada

Contact information:

*Co-Corresponding Author. Address: Department of Chemical and Materials Engineering, University of Alberta, Edmonton, Alberta, Canada T6G 1H9, Fax: +17804922881. Email address: janet.elliott@ualberta.ca (Janet A. W. Elliott)

*Co-Corresponding author. Address: 2D2.32 WMC Department of Surgery, University of Alberta Hospital, Edmonton, Alberta, Canada T6G 2B7, Fax: +17804072819. Email address: njomha@ualberta.ca (Nadr M. Jomha)

2.1 Abstract

Preserving viable articular cartilage is a promising approach to address the shortage of graft tissue and enable the clinical repair of articular cartilage defects in articulating joints, such as the knee, ankle and hip. In this study, we developed two 2-step, dual-temperature, multi-cryoprotectant loading protocols to cryopreserve particulated articular cartilage (cubes approximately 1 mm^3 in size) using an engineering approach, and we experimentally measured chondrocyte viability, metabolic activity, cell migration, and matrix productivity after implementing the designed loading protocols, vitrification, and warming. We demonstrated that porcine and human articular cartilage cubes can be successfully vitrified, and rewarmed, maintaining high cell viability and excellent cellular function. This is the first report of vitrified articular cartilage stored for a period of six months with no significant deterioration in chondrocyte viability and functionality. Our approach enables high-quality long-term storage of viable articular cartilage that can alleviate the shortage of grafts for use in clinically repairing articular cartilage defects.

2.2 Introduction

Articular cartilage defects are difficult to self-repair due to the avascular and aneural structure of articular cartilage[100]. Particulated articular cartilage transplantation can provide viable chondrocytes *in situ* for articular cartilage repair, and it is regarded as a reliable treatment for articular cartilage defects in the early stage, especially for focal chondral lesions[159,200,233]. Since 2007, approximately 8,700 particulated articular cartilage transplantations have been performed and significant improvement was reported in the clinical outcomes of patients with articular

cartilage defects[201]. However, this procedure is limited by the availability of donated articular cartilage. Fresh articular cartilage is most commonly stored for up to 28 days at 4 °C in a tissue bank, and chondrocyte viability starts to decline after 14 days of storage at this temperature[84,242]. This short window of time for viable articular cartilage makes successful cartilage transplantation challenging in the clinical scenario, because it takes approximately 2 weeks to obtain regulatory clearance for disease screening and make clinical preparations such as patient matching, disease checking, operation scheduling and sample delivery[83,84]. The lack of appropriate preservation protocols for storage results in large amounts of articular cartilage waste every year around the world[83]. If viable articular cartilage could be stored for extended periods of time beyond 28 days, the shortage of articular cartilage tissue in clinics would be eased, and more widespread clinical use of articular cartilage grafts (e.g., particulated articular cartilage) for cartilage defect repair would be possible.

Preservation of articular cartilage has been a challenge for decades, especially for large specimens (e.g., osteochondral grafts, hemicondyles) containing live cells that are very sensitive to osmotic stress, chemical toxicity, and ice growth during the cooling and warming processes[3,168,169], and this sensitivity compromises cell survival and function. Cryopreservation by vitrification is an ice-free storage method that can be achieved by superfast cooling or in the presence of high concentrations of cryoprotectants to inhibit ice crystallization inside the tissue[69]. Porcine articular cartilage has been used as a successful animal model for articular cartilage research due to its biological similarity to human articular cartilage, especially related to its thickness in the hind stifle joint relative to the human knee joint[3,113]. Past work in the vitrification of articular cartilage tissue has investigated the use of single or multi-cryoprotectant solutions at one or several progressively

decreasing temperatures: Pegg *et al.*[185] permeated dimethyl sulfoxide into thin lamb articular cartilage slices at progressively lower temperatures that traced the liquidus line of the solid–liquid phase diagram to a sufficiently high concentration of cryoprotectants inside the cartilage before storage at −80 °C; Brockbank and co-workers loaded multiple cryoprotectants (dimethyl sulfoxide, formamide, propylene glycol) into porcine articular cartilage plugs (6 mm diameter osteochondral plugs) gradually from low to high concentrations at 4 °C before rapid cooling to −135 °C[30,218]; our group developed a stepwise multi-cryoprotectant loading method that permeates multiple cryoprotectants (dimethyl sulfoxide, ethylene glycol, propylene glycol, glycerol) at progressively lower temperatures from 0 °C down to −20 °C to reach a high concentration of cryoprotectants within human articular cartilage dowels (10 mm diameter osteochondral plugs and 12.5 cm^2 large fragments) before plunging into liquid nitrogen at −196 °C for vitrification[113].

Given the practically inaccessible range of potential cryoprotectant combinations, temperatures, and times of exposure, engineering modelling provides a systematic framework for screening and identifying successful cryoprotectant loading protocols. Such models can make simultaneous calculations of pertinent properties—cryoprotectant concentration, cytotoxicity, solution freezing point, vitrifiability, and/or temperature—as a function of location in the cartilage and time of exposure. For example, cryoprotectant concentration has been calculated using biomechanical models[1,2,5] and Fick's law[139,165,209]; a mathematical toxicity cost function was introduced by Benson *et al.* to quantify the cumulative toxicity experienced by cells over the course of cryoprotectant loading[25]; and vitrifiability[208,239] and freezing point[61,208,263] have been accurately modeled. These engineering models usually require parameterizations extracted from

experimental data that can depend on tissue type and size, cryoprotectant type and concentration, and temperature.

To implement engineering models for articular cartilage preservation, the kinetic diffusion parameters in porcine articular cartilage, osmotic virial coefficients, and contributions to multi-cryoprotectant solution vitrifiability of three common cryoprotectants—dimethyl sulfoxide (DMSO, also known as Me_2SO), ethylene glycol (EG), and propylene glycol (PG)—have previously been obtained by our group: Abazari *et al.*[4] determined parameters for the temperature-dependent diffusion kinetics of these cryoprotectants in porcine articular cartilage *via* fitting Fick's law of diffusion to experimental measurements (using these empirically-fitted diffusion coefficients for kinetic predictions of cryoprotectant diffusion has been shown to agree reasonably with predictions obtained using the non-ideal triphasic biomechanical model that considers water transport[2] and with experimental measurements of efflux from human cartilage[209]); Zielinski *et al.* determined osmotic virial coefficients for common cryoprotectants by fitting the multi-solute osmotic virial equation proposed by Elliott *et al.*[61,193,194,263] to experimental data of freezing point; and Weiss *et al.*[239] quantified the vitrifiability of multi-cryoprotectant saline solutions using a statistical model fit to experimental observations obtained for 5-ml solutions cooled at a rate of approximately 60 K/min. Our group's first successful vitrification protocol[113] was developed for osteochondral dowels (articular cartilage with underlying bone), where each of four cryoprotectants was loaded sequentially in a separate loading step to attain a specified minimum concentration of each cryoprotectant at the cartilage–bone junction over a total loading time of 9.5 hr. Then, our group investigated the diffusion dynamics of this 2012 protocol, proposing a hypothetical 3-step loading procedure totaling 7 hr in duration that still attained the targeted

minimum concentration of each cryoprotectant[209]. In Shardt *et al.*[208], we further modified the 2012 protocol by (i) reducing all cryoprotectant loading solution concentrations, (ii) removing glycerol as a cryoprotectant, and (iii) introducing an equilibration step. In addition, Nadia Shardt calculated the spatial and temporal distribution of vitrifiability, and based on this calculation, our group designated potential loading protocols as having sufficient cryoprotectant permeation once the minimum vitrifiability exceeded the threshold determined by Weiss *et al.*[239] arriving at a more optimal 7-h protocol[208] for osteochondral dowels shown experimentally to be successful at preserving chondrocyte viability and metabolism in porcine articular cartilage[248 Chapter 3]. The vitrification of particulated articular cartilage (whether human or from an animal model) has not yet been reported in the literature. Herein, we present two 2-step, dual-temperature, multi-cryoprotectant protocols for vitrifying particulated articular cartilage (cubes approximately 1 mm^3 in size) for extended periods of time (6 months) at cryogenic temperatures while maintaining high cell viability and function for use in a clinical setting. Nadia Shardt used engineering modelling to determine optimal cryoprotectant exposure times and temperatures (*via* calculations of spatially- and temporally-resolved cryoprotectant concentration, solution freezing point, and vitrifiability, while qualitatively minimizing cytotoxicity with an appropriate selection of cryoprotectant type and concentration in the loading solution and not unnecessarily exceeding required loading times. We prove the success of these protocols by experimentally measuring chondrocyte viability, metabolic activity, cell migration, and matrix productivity after cryoprotectant loading, vitrification, and rewarming of both porcine and human particulated articular cartilage. Pigs are considered the best animal model for articular cartilage cryopreservation[150]; thus we include porcine samples to show the best case scientific results when tissue is harvested immediately post

mortem from young individuals compared with the more clinically applicable results for human where tissue is harvested from deceased older donors some hours after death.

2.3 Materials and Methods

2.3.1 Computational Methods

To design our loading protocols, Nadia Shardt calculated the spatial and temporal distribution of cryoprotectant concentration, solution freezing point, and vitrifiability, bringing together the work of Abazari *et al.*[4,115] on diffusion coefficients; Prickett *et al.*[194], Elliott *et al.*[61], and Zielinski *et al.*[263] on the multi-solute osmotic virial equation[61,193,194,263] for predicting freezing point; and Weiss *et al.*[239] on solution vitrifiability. We first presented this three-part engineering model in a previous paper where we proposed an optimal protocol for preserving articular cartilage dowels[208] that was shown to yield high cell viability when implemented experimentally (see Chapter 3)[248]. Herein, Nadia Shardt used our group's three-part model to develop protocols for articular cartilage cubes.

The first step of developing a vitrification protocol is to choose the cryoprotectant types and concentrations. Protocol E–D–P is based on our previous work on articular cartilage dowels[208], and as we did there, here we select EG, DMSO, and PG to load at progressively lower temperatures. In the first loading step at a temperature of 0 °C, we select EG and DMSO because these permeate the quickest and depress the freezing point quickly for the subsequent loading step to take place. In the second loading step, propylene glycol is added. In both steps, the concentrations of EG and DMSO are 3 M (the same concentration as we used previously for cartilage dowels[208] based on experimental evidence that 3 M solutions of these cryoprotectants are associated with low

toxicity[116]), while the concentration of PG is 2 M (a concentration selected to permit the attainment of a vitrifiable concentration at the end of the loading protocol within a reasonable time period).

Protocol E–D is designed to avoid the use of PG, which has been identified as more toxic than EG and DMSO. For this protocol, we select a loading solution of 3 M EG in the first loading step at a temperature of 0 °C. In the second loading step, we select a solution with DMSO and EG both at 4 M (a concentration selected to expedite the diffusion into the cartilage for the protocol to take a similar amount of time as Protocol E–D–P).

Given the above defined concentrations for the loading solutions of each protocol, the only remaining variables to be defined are the times of each loading step and the temperature of the second loading step. From the practical perspective, we note that a single loading step cannot be less than 10 min long because of the time taken for the experimental procedure. Therefore, Nadia Shardt varied the time of each loading step between 10 min and 40 min in intervals of 5 min. For the initial iteration of protocol development, Nadia Shardt set the temperature of the second step to be 0 °C and calculated the expected spatial and temporal distributions of cryoprotectant concentration, solution freezing point, and solution vitrifiability for each combination of loading step times. Of all the possible protocols, Nadia Shardt selected the shortest protocol that predicts a vitrifiability score at all spatial points in the cartilage to exceed the minimum vitrifiability score. Based on the predicted maximum freezing point at the end of this protocol's first step, Nadia Shardt chose a temperature for the second loading step that is greater than this freezing point. Finally, Nadia Shardt confirmed that this new temperature also ensures that all spatial points in the cartilage remain vitrifiable.

2.3.1.1 Cryoprotectant Concentration

Fick's law of diffusion is used in one dimension to calculate the spatial and temporal evolution of cryoprotectant permeation:

$$\frac{\partial C}{\partial t} = D\frac{\partial^2 C}{\partial x^2} \quad (1)$$

where C is cryoprotectant concentration (mol/L), t is time (s), D is the diffusion coefficient (m^2/s), and x is position in the cartilage. The diffusion coefficient is calculated as a function of absolute temperature (T) using the Arrhenius expression:

$$D = A\exp\left(-\frac{E_a}{RT}\right) \quad (2)$$

where A is the pre-exponential factor (m^2/s) and E_a is the activation energy (kcal/mol), as listed in Table 2.1 for each cryoprotectant; R is the ideal gas constant.

Table 2.1. Coefficients for use in calculating the diffusion coefficient of each cryoprotectant in porcine cartilage (Equation (2)) [4].

	A (m^2/s)	E_a (kcal/mol)
DMSO	2.9895×10^{-7}	3.9 ± 1.6
PG	1.6971×10^{-5}	6.63 ± 0.04

EG	1.833×10^{-7}	3.8 ± 0.7

Experimentally, condyles are minced into cubes with side lengths of 1 mm. Based on this geometry, Nadia Shardt selected a one-dimensional line from the centre of one cube face to the centre of the cube (length of 0.5 mm) for her calculations, as illustrated in Fig. 2.1A. Nadia Shardt selected this dimension for her diffusion calculations because 0.5 mm is the shortest distance from the cartilage–solution boundary to the center of the cube. Using this geometry, the calculated concentration at the center is a lower bound on the expected concentration, given that diffusion also occurs from each side of the exposed cube.

The following boundary and initial conditions are used to solve Equation (1) for calculating the spatial and temporal distribution of cryoprotectant concentration during loading. First, the concentration of each cryoprotectant at the outer surface of the cube is equal to the concentration in the solution:

$$C(x = 0.5\ \text{mm}, t) = C_{\text{solution}} \tag{3}$$

At the center of the cube, there is no flow of cryoprotectant:

$$\frac{\partial C}{\partial x}(x = 0\ \text{mm}, t) = 0 \tag{4}$$

Finally, the initial condition at the beginning of the first loading step is:

$$C(0 < x < 0.5\ \text{mm}, t = 0) = 0 \tag{5}$$

The concentration profile of each cryoprotectant at the end of the first loading step is used as the initial condition for the second loading step.

2.3.1.2 Vitrifiability

Given the distribution of cryoprotectant concentration calculated using Equation (1), the corresponding spatial distribution of vitrifiability can be determined for the volume and cooling rate expected during the vitrification of cartilage cubes. For our predictions, Nadia Shardt used the statistical model of vitrifiability developed by Weiss *et al.*[239], where 5 mL solutions containing between 6 M and 9 M of cryoprotectants were placed in 10 mL polypropylene tubes and plunged into liquid nitrogen (a ~60 K/min cooling rate[112,239]) for 30 min. The solutions were then immersed in a 37 °C water bath until they liquified completely, for which an ordinal score was assigned based on visual inspection (on a scale from 0 to 4 outlined in Table 2.). The following statistical model was developed with proportional-odds logistic regression based on the experimental scores of ordinal vitrifiability for 164 cryoprotectant solutions[239]:

$$\sum_{i=1}^{p}\left[\beta_i C_i + \sum_{j=1}^{i}\beta_{ij} C_i C_j\right] \geq |\alpha_n| \qquad (6)$$

where β_i and β_{ij} are single and interaction terms (including self-interactions) for each cryoprotectant i and cryoprotectant pair ij, respectively, as listed in Table 2.[239], and C_i is the molar concentration (mol/L). If the summation calculated over the p cryoprotectants exceeds a threshold value of α_n, the solution will reach a vitrifiability score of at least n (Table 2.). The coefficients listed in Table 2. are only valid for predicting vitrifiability under the same or more favorable conditions as the experiments in Weiss *et al.*[239], i.e., for 5 mL solutions in 10 mL polypropylene

tubes cooled at ~60 K/min and thawed in a 37 °C water bath. Herein, cartilage cubes are placed into a 1.8 mL Cryovial tube for vitrification and warming, which is a smaller volume than that used by Weiss *et al.*[239]. A smaller volume increases the rate of cooling and warming and improves the vitrifiability of the cryoprotectant solution within the cartilage matrix. Thus, any protocol that satisfies the vitrifiability criterion determined by Weiss *et al.*[239] is also expected to be vitrifiable under the experimental conditions used herein.

Table 2.2. Ordinal scores for the ordinal model of vitrifiability[239]

Ordinal Score	Description
0	No vitrification
1	Complete devitrification
2	Partial devitrification
3	Devitrification at edges
4	No devitrification

Table 2.3. Numerical thresholds (α) and coefficients (β) for the ordinal model of vitrifiability[239]

Parameter	Estimate
$\boldsymbol{\alpha_1}$	167.6 ± 29.2
$\boldsymbol{\alpha_2}$	184.0 ± 31.5
$\boldsymbol{\alpha_3}$	186.8 ± 31.8
$\boldsymbol{\alpha_4}$	190.5 ± 32.0
$\boldsymbol{\beta_{PG}}$	57.1 ± 10.6

$\boldsymbol{\beta_{EG}}$	39.9 ± 8.0
$\boldsymbol{\beta_{DMSO}}$	36.4 ± 6.7
$\boldsymbol{\beta_{PG\_EG}}$	−5.9 ± 1.3
$\boldsymbol{\beta_{DMSO\_PG}}$	−5.9 ± 1.2
$\boldsymbol{\beta_{PG\_PG}}$	−4.1 ± 0.9
$\boldsymbol{\beta_{DMSO\_EG}}$	−3.7 ± 0.9
$\boldsymbol{\beta_{EG\_EG}}$	−2.3 ± 0.6
$\boldsymbol{\beta_{DMSO\_DMSO}}$	−1.4 ± 0.4

2.3.1.3 Freezing Point

The distribution of freezing point as a function of position in the cartilage is calculated using[61,194,263]

$$T_{\mathrm{FP}}^{0} - T_{\mathrm{FP}} = \frac{\left[W_1 / \left(\overline{s_1^{0\mathrm{L}}} - \overline{s_1^{0\mathrm{S}}}\right)\right] R T_{\mathrm{FP}}^{0} \pi}{1 + \left[W_1 / \left(\overline{s_1^{0\mathrm{L}}} - \overline{s_1^{0\mathrm{S}}}\right)\right] R \pi} \tag{7}$$

where T_{FP}^{0} is the freezing point of pure water (273.15 K), T_{FP} is the freezing point of the cryoprotectant mixture, π is the osmolality (osmol/kg solvent), W_1 is the molar mass of pure water, and $\overline{s_1^{0\mathrm{L}}} - \overline{s_1^{0\mathrm{S}}} = 22.00$ J/mol K is the change in molar entropy between pure liquid and pure solid water at T_{FP}^{0}.

The multi-solute osmotic virial equation[61,193,194,263] is used to calculate solution osmolality with the fitting coefficients determined by Zielinski *et al.*[263]. Only the second-order virial coefficients

(B) are needed to accurately describe cryoprotectant solutions containing DMSO, PG, and EG with an isotonic amount of NaCl:

$$\pi = \sum_{i=2}^{r} k_i m_i + \sum_{i=2}^{r} \sum_{j=2}^{r} \frac{B_i + B_j}{2} k_i m_i k_j m_j \tag{8}$$

where k is the dissociation constant and m is the molality, which is calculated with:

$$m_i = \frac{\left(1000 \frac{\mathrm{L}}{\mathrm{m}^3}\right) C_i}{\rho_1 \left[1 - \sum_{i=2}^{r-1} C_i V_{m,i}\right]} \tag{9}$$

where ρ_1 is the density of pure water (998 kg/m^3 at 22 °C[140]) and V_m is the molar volume (L/mol) at 22 °C[54]. Dissociation constants, osmotic virial coefficients, and molar volumes are listed in Table 2. for each cryoprotectant. The volume of mixing and the volumes of NaCl (and other minute additives) are assumed negligible in Equation (9).

Table 2.4. Dissociation constants and virial coefficients for Equation (8)[263] and the molar volume[54] of each cryoprotectant for Equation (9).

	k	B (molal^{-1})	V_m (L/mol)
DMSO	1	0.108 ± 0.005	0.0709
PG	1	0.039 ± 0.001	0.0735
EG	1	0.020 ± 0.001	0.0559
NaCl	1.678	0.044 ± 0.002	–

2.3.1.4 Code and Data Availability

MATLAB code is available upon request, and all pertinent calculations are listed in the supplementary information.

2.3.2 Experimental Methods

2.3.2.1 Porcine articular cartilage cube preparation

Hind legs with joints (N = 23 porcine hind legs) from sexually mature pigs aged over 54 weeks were obtained from a meat-processing plant slaughter house in Wetaskiwin, Alberta, Canada. No animals were specifically euthanized for this research. Porcine joints were harvested and immersed in phosphate buffered saline (PBS) immediately then transported to the research laboratory within 4 hours. After joint dissection, articular cartilage was shaved from the condyles, minced into cubes approximately 1 mm^3 in size using a sterile scalpel blade and cleaned with 50 ml sterile PBS (Ca^{2+}/Mg^{2+} free) plus antibiotics [100 units/ml penicillin, 100 µg/ml streptomycin, and 0.25 µg/ml amphotericin B (Gibco)] for 15 minutes under a biological safety cabinet (NuAire, MN, USA).

2.3.2.2 Human articular cartilage cube preparation

Healthy knee joints (N = 3 donors) from deceased donors aged 48, 50, and 59 years (Mean ± SD: 52.3 ± 5.8 years) were obtained from the Comprehensive Tissue Center in Edmonton, Alberta, Canada with consent from patients' families to use donated cartilage for research. Human research ethics approval was obtained from the University of Alberta Research Ethics Office. After tissue harvesting, knee joints were stored in 500 ml X-VIVO 10 (Lonza, California, USA, a serum-free medium has been approved for clinical use) and transported to the research laboratory within 24 hours. Healthy articular cartilage was shaved from the condyles, minced into cubes approximately

1 mm^3 in size using a sterile scalpel blade, and immediately immersed in PBS, then cleaned with 50 ml sterile PBS (Ca^{2+}/Mg^{2+} free) plus antibiotics [100 units/ml penicillin, 100 µg/ml streptomycin (Gibco)] for 15 minutes under a biological safety cabinet.

2.3.2.3 Cryoprotectant cocktail solution preparation and stepwise cryoprotectant loading protocol

Multi-cryoprotectant cocktail solutions were made from three cryoprotectants: ethylene glycol (EG) (Fisher), dimethyl sulfoxide (DMSO) (Fisher) and propylene glycol (PG) (Fisher). Fresh cryoprotectant cocktail solutions were prepared in 50 ml final volumes with Dulbecco's Modified Eagle Medium F12 (DMEM) (Gibco) for porcine cartilage or with X-VIVO 10 serum-free medium for human cartilage on the same day of the experiment, using the following concentrations of cryoprotectants (M = molar): Protocol E–D–P: Solution One [3 M EG + 3 M DMSO] and Solution Two [3 M EG + 3 M DMSO + 2 M PG]; and Protocol E–D: Solution One [3 M EG], and Solution Two [4 M EG + 4 M DMSO]. After weighing, cartilage cubes were transferred into the prepared 50 ml cryoprotectant cocktail solutions for cryoprotectant permeation at specific temperatures and times: Protocol E–D–P: Solution One at 0 °C for 10 min, followed by Solution Two at −10 °C for 20 min; Protocol E–D: Solution One at 0 °C for 20 min, followed by Solution Two at −5 °C for 15 min. After the cryoprotectant loading into the cartilage, the particulated cartilage cubes were quickly removed from the Falcon tubes with a mesh strainer, and transferred into a sterile 1.8 mL Cryovial tube using a chemical spoon. After closing the vial lid, the Cryovial tube was placed onto a Cryovial cane and quickly plunged into liquid nitrogen for vitrification.

2.3.2.4 Cryoprotectant removal from articular cartilage cubes

The Cryovial tube containing vitrified cartilage cubes was quickly removed from the liquid nitrogen and warmed in a 37 °C water bath until the glass was melted. The cartilage cubes were extracted with a sterile spatula and washed three times in 25 ml DMEM (for porcine cartilage) or 25 ml X-VIVO 10 serum-free medium (for human cartilage) for 30 min each wash to remove the permeated cryoprotectants from the cartilage cubes.

2.3.2.5 Assessment of chondrocytes in situ

2.3.2.5.1 Chondrocyte viability by cell membrane integrity stain

Chondrocyte viability was assessed by a cell membrane integrity stain [6.25 µM Syto 13 and 9.0 µM propidium iodide mixed in PBS] using a membrane-permeant nucleic acid stain (Syto 13; Molecular Probes) which fluoresced green, and a membrane-impermeant stain (propidium iodide; Sigma) that penetrates only into cells with disrupted cell membranes, fluorescing red. After incubation of cartilage cubes in the dyes for 20 min, cartilage cubes were rinsed in PBS (Ca^{2+}/Mg^{2+} free) and imaged using a laser scanning confocal fluorescent microscope (model: TCS SP5; Leica). The dual filters used to image all the cartilage cubes in this study had the following spectra peak maxima wavelengths: excitation/emission: 488 nm/503 nm and 535 nm/617 nm. Three replicate cartilage cubes from one Cryovial were imaged at each time point. Cartilage cubes were imaged at three time points, t_1 = positive control before cryoprotectant loading (fresh cartilage cubes after mincing), t_2 = after vitrification in LN_2 (< 24 hours, Day 0) and tissue warming followed by cryoprotectant removal in medium, t_3 = after vitrification for 180 days (Day 180) and tissue warming followed by cryoprotectant removal in medium. A positive control (fresh cartilage cubes after mincing) and a negative control group (freeze/thaw in liquid nitrogen (LN_2) without

cryoprotectants) from the same condyle were used to screen sample viability. A minimum 80% absolute chondrocyte viability in the positive (fresh) controls before cryoprotectant exposure (chondrocyte viability at t_1) was used to screen out unhealthy cartilage donors.

2.3.2.5.2 Chondrocyte metabolic activity by alamarBlue

Chondrocyte metabolic activity was assessed by an alamarBlue assay (Invitrogen, Burlington). Rewarmed articular cartilage cubes (approximately 0.2 g wet weight) after cryoprotectant removal were washed in 5 ml sterile PBS (Ca^{2+}/Mg^{2+} free) plus antibiotics for 15 minutes in a biological safety cabinet. Cartilage cubes were incubated with the alamarBlue assay solution [5 ml X-VIVO 10 medium supplemented with 0.1 mM ascorbic acid, 10 nM dexamesasone, 10 ng/ml transforming growth factor (TGF) beta 1 and mixed with 500 µl alamarBlue] at 37 °C for 48 hr. Images of the fluorescence color change of alamarBlue assay solutions of the culture plates were taken at 0 hr, 24 hr and 48 hr using a digital camera (Canon PowerShot ELPH 180). The average of two replicate readings of the blank samples (alamarBlue assay solution without cartilage sample) was subtracted from the average of the experimental samples to yield a value in relative fluorescent units (RFU) divided by gram weight. The RFU were determined by the CytoFluor II software with emission wavelengths of 580/50 nm, excitation wavelengths of 485/20 nm and a fluorescent intensity gain set to 45.

2.3.2.6 Assessments of isolated chondrocytes

2.3.2.6.1 Articular cartilage digestion for chondrocyte isolation

After cryoprotectant removal, 0.2 g of porcine cartilage cubes or 0.5 g of human cartilage cubes were weighed and cleaned with 5 ml sterile PBS (Ca^{2+}/Mg^{2+} free) plus antibiotics [100 units/ml

penicillin, 100 µg/ml streptomycin (Gibco)] for 15 minutes under a biological safety cabinet. The cartilage cubes were then transferred to an empty 50 ml Falcon tube and 5 ml of 0.15% collagenase solution was added under sterile conditions [for 10.5 ml of collagenase solution, prepare: 10 ml DMEM supplemented with antibiotics (PS), 15 mg of 300 units type II collagenase (Filtered, Worthington), and 0.5 ml FBS]. The Falcon tubes containing cartilage cubes were placed in an orbital shaker (250 rpm) at 37 °C for cartilage digestion for 22 hours. Once the cartilage digestion was finished, a sterile 100 µm cell strainer was used to filter the digested chondrocytes. The collagenase was neutralized by adding 10 ml of DMEM supplemented with 10% fetal bovine serum (FBS). The chondrocytes were collected by centrifugation for 10 min at 433 g at 22 °C, followed by two washes in 10 ml sterile PBS (Ca^{2+}/Mg^{2+} free), then resuspended in 12 ml of DMEM complete for chondrocyte recovery.

2.3.2.6.2 Chondrocyte recovery and chondrocyte collection

After chondrocyte recovery in an appropriate tissue culture flask (BD, Falcon) in a humidified incubator with 20% O_2 and 5% CO_2 at 37 °C for 72 hr, the chondrocyte monolayer was washed with 5 ml sterile PBS (Ca^{2+}/Mg^{2+} free) twice. 2 ml 1×0.02% trypsin-EDTA solution (Gibco) was added to the tissue culture flask to disassociate chondrocytes for 5 min at 37 °C, then neutralized with 5 ml of DMEM complete supplemented with 10% FBS. Chondrocytes were collected for cell counting *via* centrifugation for 10 min at 433 g at 22 °C.

2.3.2.6.3 Chondrocyte counting by Trypan blue

After chondrocytes were resuspended in DMEM complete media, 15 µl cell suspension and 15 µl Trypan blue were mixed by pipetting. Then 10 µl of this mixture was gently placed in a

hematocytometer using a pipette for chondrocyte counting, where the cell count was determined by adding the counted cells in four equally-sized areas, dividing by 4, and then multiplying by a dilution factor of 10,000 and the total volume of chondrocyte suspension solution. Trypan blue is a vital stain used to selectively color dead cells with a blue color, and live cells with intact cell membranes remain unstained. Since live chondrocytes are excluded from staining, this staining method can be used as a dye exclusion method to identify the number of living chondrocytes.

2.3.2.6.4 Scratch wound healing assay and chondrocyte migration quantification

After chondrocyte recovery for 72 hr, chondrocytes were counted with Trypan blue and seeded onto a 24-well tissue culture plate (Aaka Scientific Inc.) with a density of 10^5 per well and cultured in a humidified incubator with 20% O_2 and 5% CO_2 at 37 °C for 168 hours. Chondrocytes were grown until they reached over 90% confluence as a monolayer in the culture plate in 2 ml DMEM complete supplemented with 10% FBS with the medium changed twice a week. For the scratch wound healing assay, a sterile 200 µl pipette tip was used to slowly scratch the confluent monolayer (90% or higher) from left to right across the center of the well and introduce a 1 mm wide empty gap in the wells[43]. The wells were refilled with 2 ml fresh DMEM complete and images of the well were taken at 0 hr, 24 hr, and 48 hr to monitor the migration of chondrocytes. Image J software was used to calculate chondrocyte migration percentage every 24 hr. Chondrocyte migration was normalized to the initial empty gap width at 0 hr and plotted to show the chondrocyte migration speed based on the 24 hr and 48 hr timepoints.

2.3.2.6.5 Chondrocyte aggregate by pellet culture for 21 days

After isolated chondrocytes were plated for 72 hr for cell recovery, chondrocytes were washed with sterile PBS (Ca^{2+}/Mg^{2+} free) twice. Then chondrocytes were trypsinized for 5 min at 37 °C and centrifuged at 433 g for 5 min to collect chondrocytes for making pellets following the procedure below[142]. After a cell wash and cell counting with Trypan blue, 5×10^5 chondrocytes were resuspended in 500 µl defined serum-free medium [SFM: high glucose DMEM, HEPES (10 mM), human serum albumin (125 mg/ml), ascorbic acid 2-phosphate (365 lg/ml), dexamethasone (100 nM), and L-proline (40 lg/ml) (Sigma-Aldrich), ITS + 1 premix (5 µl, 100x) (Corning, Discovery Labware, Inc.), 100 units/ml penicillin, 100 µg/ml streptomycin, TGF-b3 (10 ng/ml; ProSpec, NJ, USA,] in a 1.5 ml sterile conical microtube (Bio Basic Inc, Ontario, Canada). Then, chondrocytes were centrifuged at 433 g and 22 °C for 5 min to form a pellet at the bottom of the microtube using an Allegra X-22R centrifuge (Beckman Coulter, US). The pellets were cultured in the SFM under 3% O_2 and 5% CO_2 at 37 °C in a humidified incubator for 21 days, with SFM changes twice a week.

2.3.2.6.5 Assessment of pellets after a 21-day culture

2.3.2.6.5a Wet weight and histology of pellets

After a 21-day culture, pellets were rinsed with sterile PBS (Ca^{2+}/Mg^{2+} free) and wet weights were measured using an electric balance (Mettler Toledo; Switzerland). Pellets were imaged with a Zeiss camera (AxioCam ERc 5s) for gross morphology and fixed with 10% formalin for 24 hr before paraffin embedding. A microtome (Leica) was used to prepare pellet sections with thicknesses of 5 µm, followed by section drying at 37 °C overnight in a dry incubator. Pellet sections were then processed with Safranin O staining to quantify and identify proteoglycan content in the pellets. Stained sections were imaged with a Nikon digital camera (model: DS-Fi2)

equipped on a Nikon inverted microscope (model: ECLIPSE Ti-5): exposure time for 100× magnification = 8 ms; exposure time for 200× magnification = 40 ms; gain = 0.

2.3.2.6.5b GAG/DNA measurement

Glycosaminoglycan (GAG) content of pellets was quantified by a dimethylmethylene blue (DMMB) assay. Pellets were weighed and rinsed with PBS and stored in a −80 °C freezer before use. After warming, pellets were digested in 250 µl of 1 mg/ml proteinase K overnight at 56 °C using a dry block heater (Thermo Fisher Scientific). PBE/cysteine buffer (100 mM Na_2HPO_4, 10 mM Na_2EDTA, pH = 6.5, 1.75 mg/mL cysteine, Sigma) and ~0–100 µg/mL chondroitin sulphate A sodium salt (CS, Sigma-Aldrich) were used as controls for a standard curve. The standard curve was prepared in 8 Eppendorf tubes with a total volume of 100 µL and an increasing concentration of CS. After protein digestion, a 5 µL digested sample was pipetted into an ultra-clear 96 well plate in triplicate (NUNC, Thermo Fisher Scientific). The digested sample in each well was mixed with 5 µL PBE/cysteine buffer and diluted by 1:50 in concentration by adding 250 µL DMMB dye (Sigma-Aldrich). Each plate was read at 525 nm and data was normalized to the blank reading of H_2O (260 µL, without DMMB) and the CS standard controls. DNA content was quantified by using the CyQUANT™ proliferation assay kit for cells in culture (Invitrogen, ON, Canada). After cartilage digestion with 1 mg/mL Proteinase K, a 5-µL sample was pipetted into a 96-well plate in triplicate. In each well, 195 µL working buffer was added to make the total volume equal to 200 µL. DNA solutions and working buffer were prepared using an assay kit[142]. For 20 mL working buffer, 50 µL CyQUANT® GR dye, 1 mL Cell-lysis buffer were mixed with 19 mL Milli-Q water. The spectra peak maxima for excitation of 450/50 nm and emission of 530/25 nm were used to read the plates, and the supplied λDNA of bacteriophage was used as standard reference.

2.3.2.7 Statistical analysis

The numerical data are presented as means ± standard deviation (SD). Based on the Mauchly's test of sphericity or the Levene's test of equality, the analysis of variance (ANOVA) with post hoc test (Tukey's multiple comparison) was performed on the experimental groups, otherwise, the nonparametric test (Kruskal–Wallis with pairwise comparison) was performed to compare experimental variables in multiple groups. Sample size and the p values are reported in the figure legends. All data were analyzed using SPSS 20.0 software for statistical significance and figures were plotted using GraphPad Prism 8 software.

2.4 Results

2.4.1 Computational generation of cryoprotectant loading protocols for particulated articular cartilage

Optimized protocols are developed based on a combined consideration of the spatial and temporal distribution of cryoprotectant concentration, solution freezing point, and cryoprotectant vitrifiability, an approach that our group used for the development of successful protocols for preserving articular cartilage dowels[113,208,248]. Based on the toxicity studies of Almansoori *et al.*[9] and Jomha *et al.*[116] that ranked the relative toxicity of commonly-used cryoprotectants for human and porcine chondrocytes, we selected the least toxic compounds for our protocols: EG, DMSO, and PG. Our first protocol loaded all three cryoprotectants (named Protocol E–D–P), and the second protocol loaded only two cryoprotectants (EG and DMSO; named Protocol E–D) because, of the three cryoprotectants, PG is associated with the most cytotoxicity[65].

To predict spatial and temporal distributions of concentration, Nadia Shardt used Fick's law of diffusion over a one-dimensional line through a cube of cartilage (see Fig. 2.1A) with effective diffusion coefficients previously obtained by fitting to experiments that measured the uptake of cryoprotectant in porcine cartilage as a function of time and temperature[4,115]. It has been previously noted that Fick's law underestimates cryoprotectant diffusion when compared to experimental measurements and to our group's nonideal triphasic model, but it is within an average of 15% from experimental measurements of cryoprotectant efflux from human cartilage dowels (using Fick's law in 2-dimensions with diffusion coefficients from porcine cartilage as an approximation of those in human)[1,2,5]. Thus, Nadia Shardt used Fick's law in one-dimension to ensure that we developed conservative protocols that will be robust to small variations in, for example, cube size, diffusion coefficients (inhomogeneities in the cartilage matrix may cause deviations), and heat transfer rates during vitrification (in our experiments, we achieve a cooling rate of approximately 140 K/min, where 0.5 g of articular cartilage cubes after cryoprotectant permeation are placed in a dry 1.8 mL cryovial and plunged in liquid nitrogen, reaching −150 °C from −10 °C in ~60 s based on 5 independent measurements).

To predict spatial and temporal distributions of freezing point accounting for the nonideal behavior of highly-concentrated cryoprotectant solutions, Nadia Shardt used the multi-solute osmotic virial equation[61,193,194,263] with the osmotic virial coefficients determined by Zielinski *et al.*[263] combined with the Gibbs–Duhem equation[61,193,194,263]. To predict spatial and temporal distributions of vitrifiability, Nadia Shardt used the statistical model developed by Weiss *et al. via* fitting to experimental results of 5 mL cryoprotectant solutions with concentrations between 6 M and 9 M

placed in 10 mL polypropylene tubes and plunged in liquid nitrogen (a ~60 K/min cooling rate[112,239]) for 30 min, followed by warming in a 37 °C water bath[239]. Nadia Shardt used vitrifiability as the criterion for assessing the predicted success of a protocol, because it can be used to screen protocols with various cryoprotectant types and concentrations, as we showed in our previous work on cartilage dowels[208]. Based on this criterion of achieving a minimum level of vitrifiability throughout the cube, Nadia Shardt and Janet Elliott developed two new protocols (Protocol E–D–P and Protocol E–D) for 1 mm^3 particulated cartilage cubes, as summarized in Fig. 2.1B, with more details of the design process outlined in the **Methods**. Fig. 2.1C shows the spatial distribution of cryoprotectant concentration, freezing point, and vitrifiability at the end of each loading step for Protocol E–D–P and Protocol E–D. By the end of the second loading step, both protocols are predicted to exceed the minimum vitrifiability criterion ($\alpha_1 = 167.6$) at all locations in the cartilage from the center of the cube to the edge in contact with the cryoprotectant solution.

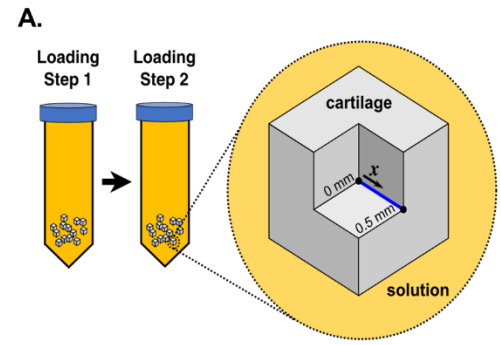

B. Cryoprotectant concentrations, loading times, and temperatures for each step of Protocol E–D–P and Protocol E–D.

	Protocol E–D–P			Protocol E–D		
Loading Step 1	3 M EG 3 M DMSO	10 min	0 °C	3 M EG	20 min	0 °C
Loading Step 2	3 M EG 3 M DMSO 2 M PG	20 min	−10 °C	4 M EG 4 M DMSO	15 min	−5 °C

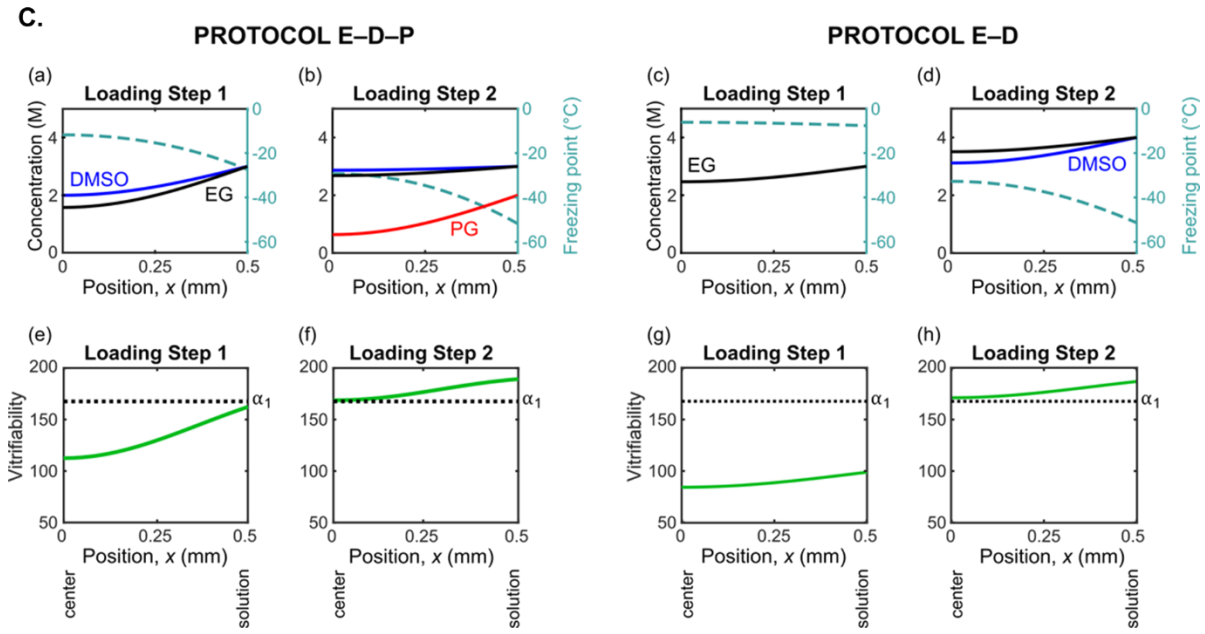

Figure 2.1 Overview of theoretical calculations. A. Schematic of the 1 mm^3 articular cartilage cubes. For our theoretical calculations, Nadia Shardt considered a one-dimensional line for diffusion with length 0.5 mm extending from the center of the cube to the edge of the cube that is in contact with the cryoprotectant solution. **B. Summary of cryoprotectant concentrations, loading times, and temperatures for each step of Protocol E–D–P and Protocol E–D.** Each protocol consists of two steps, with the second step introducing an additional cryoprotectant at a reduced temperature. **C. Calculations of the spatial distribution of cryoprotectant concentration, solution freezing point, and vitrifiability at the end of each loading step.** For these calculations, Nadia Shardt used Fick's law of diffusion, the multi-solute osmotic virial

equation combined with the Gibbs–Duhem equation[194,263], and a statistical model of vitrifiability[239]. In panels (e)–(h), α_1 indicates the minimum vitrifiability score required for vitrification under the experimental conditions described in Weiss *et al*[239].

2.4.2 Experimental vitrification of articular cartilage cubes

Based on the modelling results (Fig. 2.1) for cryoprotectant permeation into particulated articular cartilage, we developed the processing protocol to vitrify, store and warm particulated articular cartilage, illustrated in Fig. 2.2. Briefly, after harvesting articular cartilage from healthy femoral condyles it is sliced into 1 mm^3 cubes under sterile conditions (see Fig. 2.2A). Approximately 0.5–0.8 g wet weight of particulated articular cartilage per protocol treatment were loaded in 50 mL of multi-cryoprotectant cocktail solution in 50-mL Falcon tubes. Then two 2-step cryoprotectant loading protocols (Protocol E–D–P and Protocol E–D in Fig. 2.1B) with calculated loading times and preset temperatures at each step were followed to permeate sufficient amounts of cryoprotectants into the cartilage cubes. After the cryoprotectant permeation procedure, the particulated cartilage cubes were quickly removed from the Falcon tubes with the mesh strainer and transferred into a sterile 1.8 mL Cryovial tube with a residual amount of cryoprotectants remaining with the cartilage cubes, then plunged into liquid nitrogen on a cryovial cane (see Fig. 2.2B). After storage in liquid nitrogen at −196°C for the desired experimental time period (one tube warmed at Day 0 and one tube warmed at Day 180), the cryovial tube containing vitrified cartilage cubes was quickly removed from the liquid nitrogen and rewarmed in a 37 °C water bath until the glass was melted, which took approximately 30 s for warming (see Fig. 2.2C). The cartilage cubes were extracted with a sterile lab spoon and washed in a beaker filled with 25 mL

fresh medium (see **Methods**) to remove the cryoprotectants at 4 °C for 30 min and the wash was repeated three times before chondrocyte assessments.

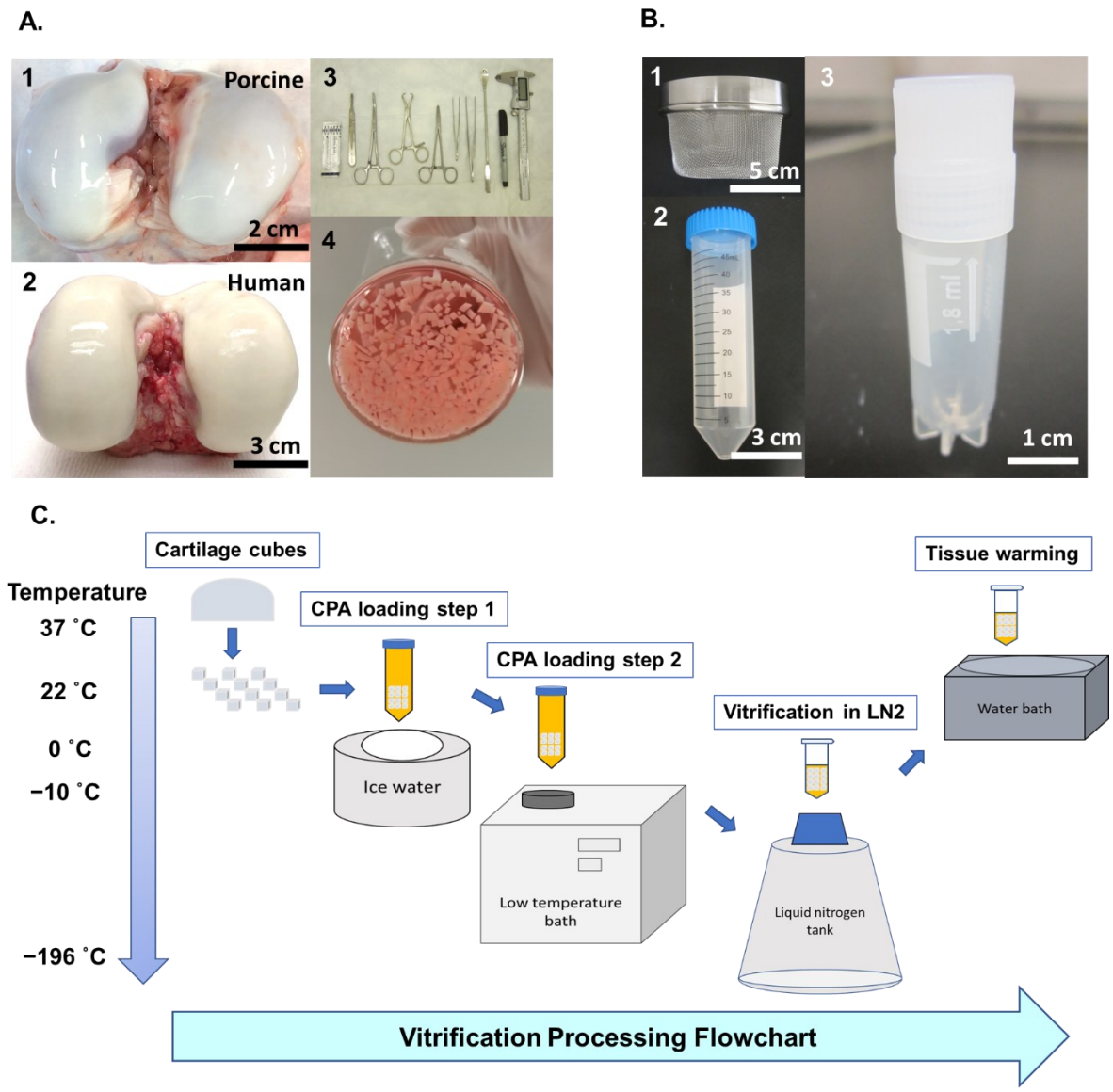

Figure 2.2 Vitrification process of particulated articular cartilage.

A. Harvesting articular cartilage cubes from fresh healthy knee joints. 1. A typical porcine stifle joint with exposed fresh healthy femoral condyles; 2. A typical human knee with exposed fresh healthy femoral condyles; 3. The surgical tool set, from left to right: #20 steel surgical blade,

surgical scalpel handle, curved forceps, towel forceps, straight forceps, non-toothed tissue forceps, toothed tissue forceps, double-ended spoon, Sharpie marker, and digital caliper; 4. Cartilage prepared into 1 mm^3 pieces and placed in medium before vitrification. **B. The vitrification tool set.** 1. Mesh strainer used for transferring cartilage cubes; 2. The 50 ml Falcon tube for cryoprotectant loading into articular cartilage; 3. 1.8 ml Cryovial for sample vitrification and storage in liquid nitrogen. **C. Flowchart of the vitrification process for articular cartilage.** Weighed cartilage cubes were transferred into a 50 ml prepared multi-cryoprotectant solution at the concentration, time, and temperature listed in Fig. 1B under Loading Step 1, followed by a second solution at the condition listed under Loading Step 2 in Fig. 1B. Once cryoprotectant permeation was finished, cartilage cubes were quickly transferred into a 1.8 ml Cryovial tube and plunged into liquid nitrogen on a Cryovial cane. Upon cartilage rewarming on Day 0 or on Day 180, the Cryovial tube was removed from the liquid nitrogen and plunged into a 37 °C water bath for warming the glassy cartilage, following by cryoprotectant removal and chondrocyte assessments.

2.4.3 Assessment of chondrocytes after vitrification/tissue rewarming

After vitrifying and rewarming porcine and human particulated cartilage, we assessed the viability and function of chondrocytes both in situ in intact cartilage and after isolation from the cartilage matrix. We quantified chondrocyte membrane integrity, metabolic activity, migration ability, and matrix productivity.

2.4.3.1 Chondrocyte membrane integrity stain of post-vitrified articular cartilage

Maintaining a high chondrocyte viability after storage is vital for articular cartilage transplantation, where a cell viability greater than 70% facilitates improved outcomes in the clinical scenario[37,242]. To evaluate chondrocyte viability after our proposed vitrification protocols, we used fluorescent dyes (Syto 13 and propidium iodide) to quantify the percentages of chondrocytes with intact or disrupted membranes. For porcine particulated articular cartilage (see Fig. 2.3A-B), the fresh positive control group had an absolute cell membrane integrity of 94.2 ± 4.8% (Mean ± SD), and the experimental groups treated with either Protocol E–D–P or Protocol E–D had 85–90% cell membrane integrity (see Supplemental Table 2.S3 for numeric data). After vitrification and warming, approximately 90% normalized chondrocyte membrane integrities were maintained in both Protocol E–D–P and Protocol E–D groups. Importantly, there were no statistically significant differences in chondrocyte viability between Protocol E–D–P and Protocol E–D groups after vitrification and warming at Day 0. After 6 months of storage in liquid nitrogen, the chondrocyte viability of porcine particulated articular cartilage remained as high as that vitrified and warmed at Day 0 using either Protocol E–D–P or Protocol E–D. For human particulated articular cartilage (see Fig. 2.5A-B), the absolute chondrocyte viability of the fresh positive control group was 91.6 ± 4.0%. After vitrification and warming, greater than 80% normalized chondrocyte membrane integrities were maintained in both Protocol E–D–P and Protocol E–D groups (see Supplemental Table 2.S4 for numeric data). There were no statistically significant differences in the absolute chondrocyte viability between Protocol E–D–P and Protocol E–D groups at Day 0. Storage of human particulated articular cartilage for 6 months in liquid nitrogen showed no statistically significant differences using either Protocol E–D–P or Protocol E–D when compared to the particulated articular cartilage that had been vitrified and warmed at Day 0.

2.4.3.2 Chondrocyte metabolic activity of post-vitrified articular cartilage

A defining function of viable chondrocytes is their metabolic activity associated with various physiologic pathways within the normal cellular contents. We used alamarBlue to determine metabolic activity of viable chondrocytes indicated by a change from non-fluorescent resazurin (blue color) to highly-fluorescent resorufin (red color) through the reduction reaction of active living cells[213,258]. Porcine particulated articular cartilage vitrified using either Protocol E–D–P or Protocol E–D and warmed at Day 0 demonstrated a similar metabolic activity to the fresh positive control after 48 hr, and showed a higher cell metabolic activity than the positive control after 96 hr. These findings are consistent with our recent work[113,248], which showed that articular cartilage that maintained high chondrocyte viability after vitrification had a level of chondrocyte metabolic activity that was activated or enhanced upon sample warming, possibly due to some sort of hypermetabolic rebound from cryogenic temperatures accompanied with mitochondrial repair inside the post-vitrified chondrocytes. A confirmatory low chondrocyte metabolic activity was observed in the negative control which remained a blue color for both 48 hr and 96 hr time points (see Fig. 2.3C-D, for numeric data see Supplemental Table 2.S5). Similarly, human particulated articular cartilage vitrified using either Protocol E–D–P or Protocol E–D and rewarmed at Day 0 demonstrated similar metabolic activity to the fresh positive control after 48 hr or after 96 hr incubation (see Fig. 2.5C-D, for numeric data see Supplemental Table 2.S6). A similar hypermetabolic rebound was observed in the post-vitrified human chondrocytes using either Protocol E–D–P or Protocol E–D and rewarmed after 6 months. The alamarBlue results showed that both porcine and human particulated articular cartilage vitrified in liquid nitrogen and warmed

after 6 months maintained a high level of metabolic activity comparable to the articular cartilage vitrified in liquid nitrogen and warmed at Day 0 and to fresh positive controls.

2.4.3.3 Chondrocyte migrating ability from post-vitrified articular cartilage

In order for articular cartilage repair to occur after implantation, chondrocytes must maintain their ability to migrate from the cartilage matrix and proliferate[159,233]. An *in vitro* culture of porcine particulated articular cartilage showed chondrocytes migrating from the cartilage matrix between two cartilage cubes (see Fig. 2.3E). This observation demonstrated that chondrocytes maintained good cellular function, an important characteristic for orthopaedic surgeons to consider in the clinical scenario[233]. To further confirm that chondrocytes from vitrified articular cartilage maintained a high functionality, we evaluated the ability of chondrocytes isolated from the cartilage matrix to proliferate *in vitro*. Isolated chondrocytes from articular cartilage cubes were seeded on a 24-well culture plate and grown with culture medium as described in the **Methods** section. Both porcine and human chondrocytes isolated after vitrification using either Protocol E–D–P or Protocol E–D demonstrated a similarly strong proliferating ability to become confluent in the culture plates after 168 hr (see Fig. 2.3F, Fig. 2.5F). To further investigate the migration ability of chondrocytes, a 1-mm wide section of expanded cells was removed by scratching and then followed by another 48-hr cell culture in the incubator, during which time the viable and active chondrocytes migrated to fill the gap. The results confirmed that our vitrification approaches for articular cartilage storage up to 6 months do not impair chondrocyte migration ability as shown in Fig. 2.3G and Fig. 2.5G.

2.4.3.4 Cartilage matrix productivity by chondrocytes after vitrification

The properties of the articular cartilage matrix generated by chondrocytes are important criteria to evaluate the functionality of viable chondrocytes. First, after culture for 21 days, we compared the wet weight of the cultured pellets to represent the amount of extracellular matrix produced. For both the porcine and human chondrocyte pellets, there were no significant differences between the fresh positive control, Protocol E–D–P and Protocol E–D groups, as shown in Figs. 2.4A and 2.6A. Secondly, Fig. 2.4B and Fig. 2.6B show the gross morphology of chondrocyte pellets with pink-colored Safranin-O staining for sulfated glycosaminoglycans (sGAG) of cartilage sections after the 21-day culture period. Glycosaminoglycan production is essential in maintaining the integrity of normal cartilage. A similar pink color was observed for the fresh positive control groups and the vitrified groups: Protocol E–D–P and Protocol E–D. Thirdly, the amount of GAG per DNA is an important parameter to evaluate the chondrocyte synthesis functionality. To document this, we quantified the GAG content using a dimethylmethylene blue (DMMB) assay to detect the amount of GAG being produced by post-vitrified chondrocytes, and the DNA content in the pellets using a DNA kit (see **Methods**). There were no statistically significant differences between the fresh positive control, Protocol E–D–P and Protocol E–D groups for both porcine and human chondrocyte pellets, as shown in Fig. 2.4C–E and 2.6C–E.

A. Porcine live–dead cell membrane integrity stain

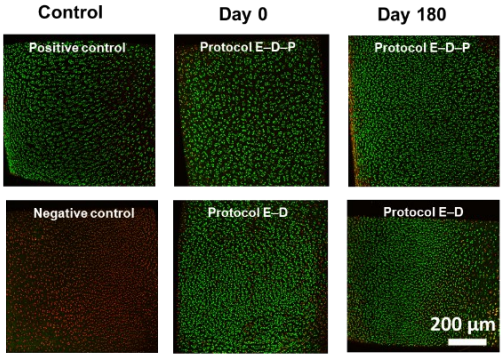

B. Porcine chondrocyte viability in articular cartilage after vitrification (Mean ± SD)

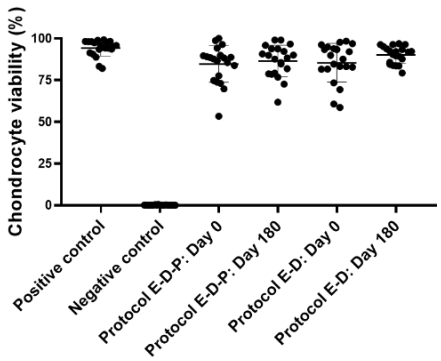

C. Porcine chondrocyte metabolic activity by alamarBlue

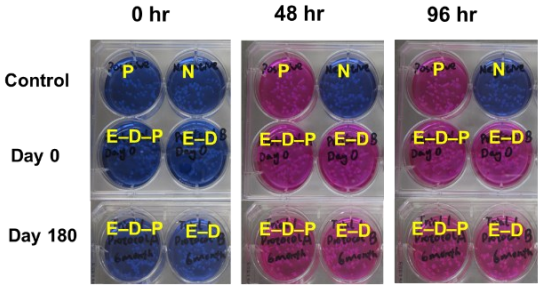

D. Chondrocyte metabolic activity of porcine articular cartilage after vitrification (Mean ± SD)

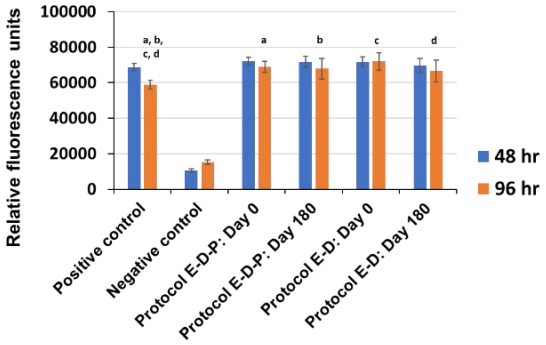

E. Porcine chondrocytes migrating out from matrix

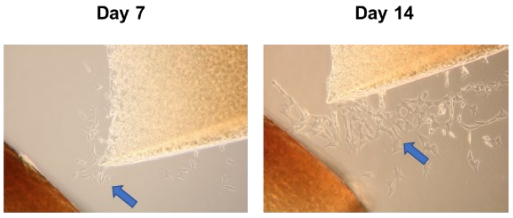

F. Isolated porcine chondrocyte proliferation after 168-hr culture

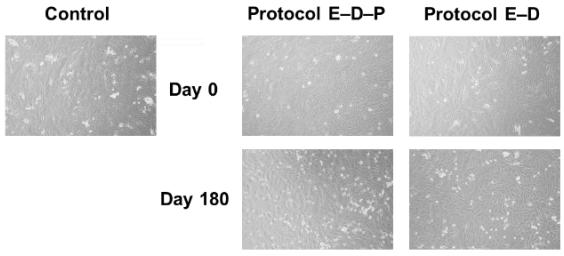

G. Isolated porcine chondrocyte migration after scratching (Mean ± SD)

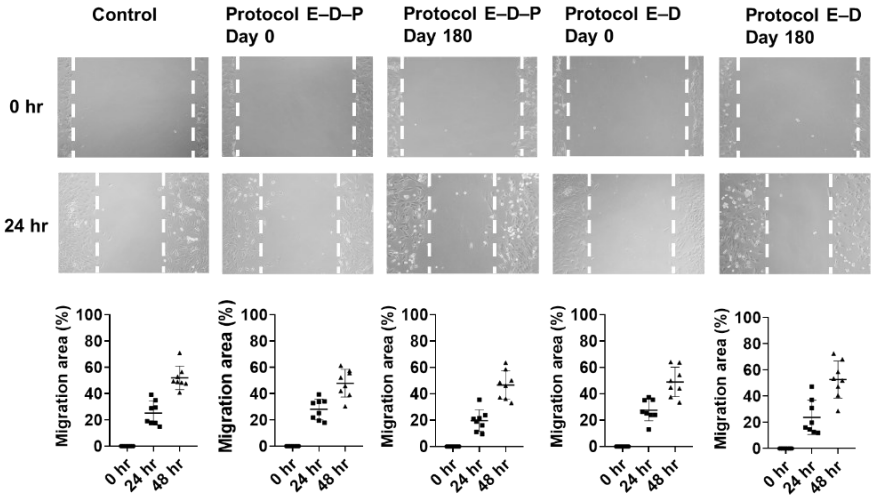

Figure 2.3 Assessment of porcine chondrocytes after vitrification and subsequent rewarming.

A: Representative images of porcine cartilage samples showing live (green) and dead (red) chondrocytes by a cell membrane integrity stain using two fluorescent dyes: Syto 13 and propidium iodide and imaged by a laser scanning confocal microscope (×100 magnification); **B:** Quantification of porcine chondrocyte viability of the positive control, negative control, Protocol E–D–P at Day 0, Protocol E–D–P at Day 180, Protocol E–D at Day 0, and Protocol E–D at Day 180 (n = 21 replicates per group: no statistical differences between the protocols and the storage times, $p = 0.261$, based on two–way ANOVA); **C:** Representative images of the alamarBlue assay showing porcine chondrocyte metabolic activity from particulated articular cartilage after vitrification at 0 hours, 48 hours and 96 hours; **D:** Quantification of porcine chondrocyte metabolic activity (n = 7 replicates per group: significant rebound of chondrocyte metabolic activity at 96 hours in the experimental groups compared to the positive control, $p_a = 0.003$; $p_b = 0.011$; $p_c < 0.001$; $p_d = 0.035$, based on two–way ANOVA and Tukey's test); **E:** Active porcine chondrocytes from particulated articular cartilage migrated from the cartilage matrix and proliferated *in vitro* culture at Day 7 and Day 14; **F:** Isolated porcine chondrocytes from post-vitrified articular cartilage dedifferentiated into fibroblast-like cells and migrated to the center of the culture plates (×100 magnification); **G:** Isolated porcine chondrocytes from particulated articular cartilage migrated at similar speed to heal the wound scratch when cultured *in vitro* (n = 8 replicates per group: $p = 0.811$, based on two–way ANOVA).

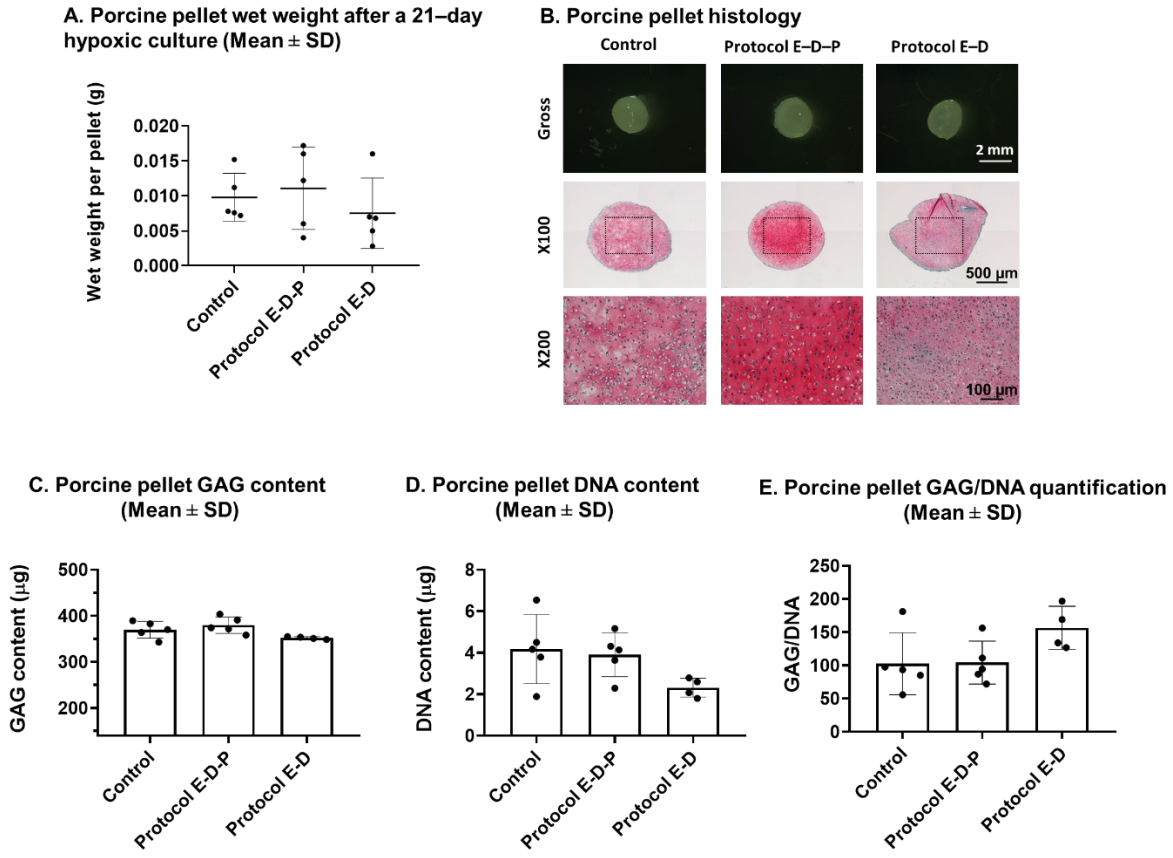

Figure 2.4 Assessment of porcine chondrocyte matrix productivity.

A: Porcine pellets after a 21-day culture show a similar wet weight among the control, Protocol E–D–P, and Protocol E–D groups (n = 5 replicates per group, p = 0.074, based on one–way ANOVA). **B:** Representative histological images showing the gross appearance of pellets after a 21-day culture with chondrogenic media under hypoxic conditions (3% O_2, 5% CO_2 at 37 °C). Safranin-O stain showing GAG content synthesized by viable and active chondrocytes for the control, Protocol E–D–P, and Protocol E–D groups. **C.** GAG content in the porcine pellets among the control, Protocol E–D–P, and Protocol E–D groups after a 21-day culture and measured *via* dimethylmethylene blue (DMMB) assay. **D.** DNA content in the porcine pellets quantified by CyQUANT^{TM} proliferation assay. **E.** GAG/DNA quantification of porcine pellets show similar

matrix productivity among the control, Protocol E–D–P, and Protocol E–D groups (n = 4~5 replicates per group, $p = 0.106$, based on one–way ANOVA).

A. Human live–dead cell membrane integrity stain

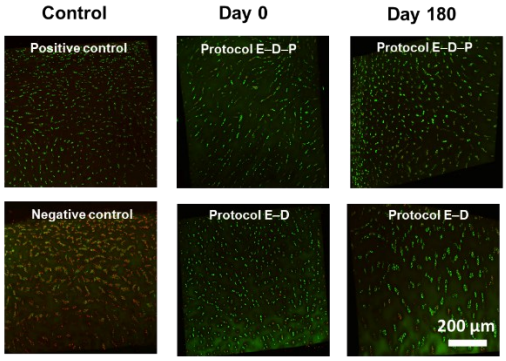

B. Human chondrocyte viability in articular cartilage after vitrification (Mean ± SD)

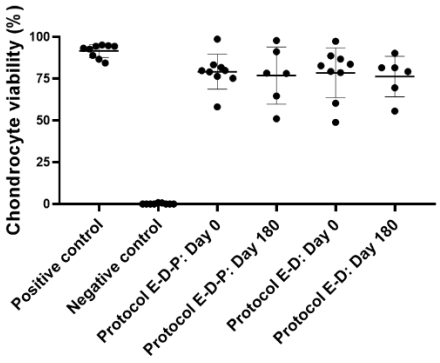

C. Human chondrocyte metabolic activity by alamarBlue

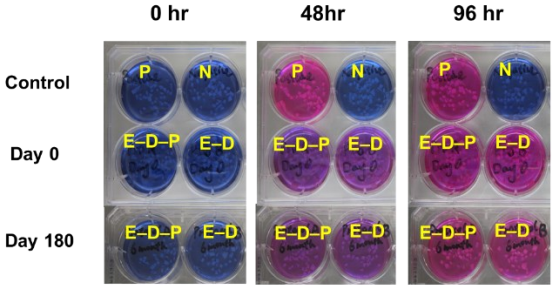

D. Chondrocyte metabolic activity of human articular cartilage after vitrification (Mean ± SD)

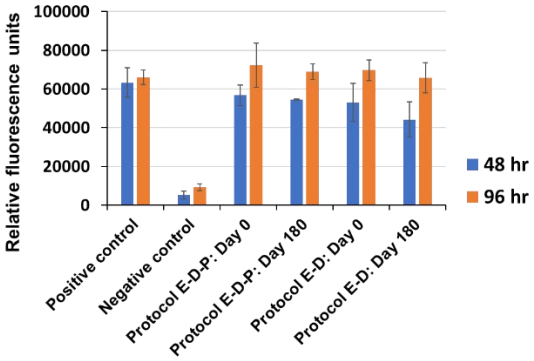

E: Donor info: age, sex and body mass index

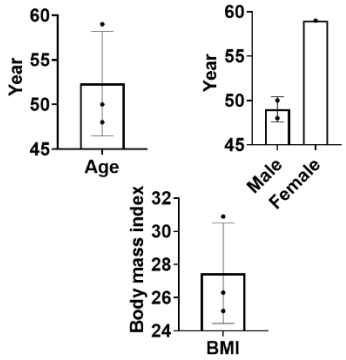

F. Isolated human chondrocyte proliferation after 168-hr culture

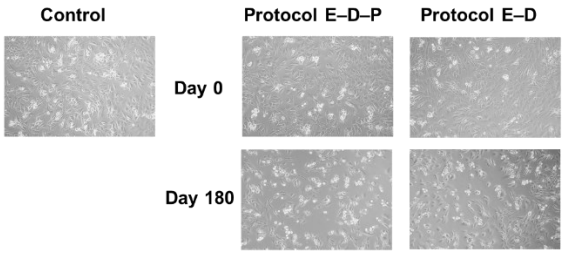

G. Isolated human chondrocyte migration after scratching (Mean ± SD)

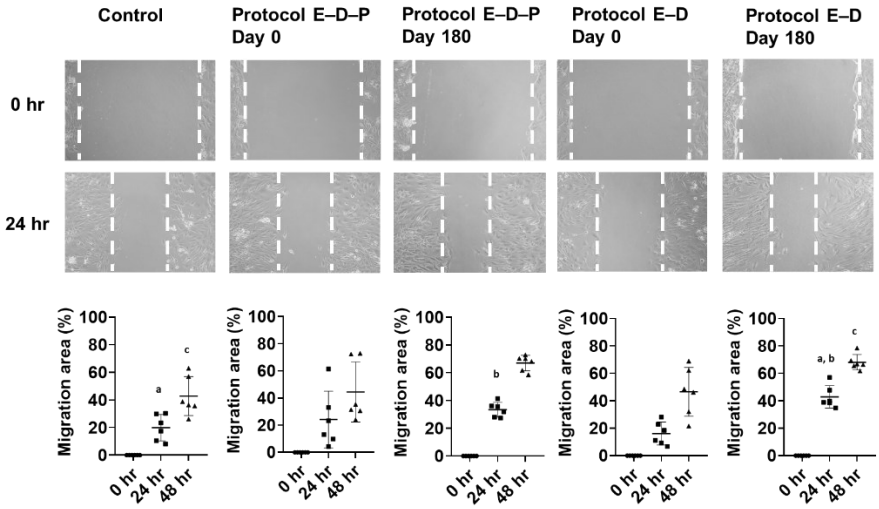

Figure 2.5 Assessment of human chondrocytes after vitrification and subsequent rewarming. **A:** Representative images of human cartilage samples showing live (green) and dead (red) chondrocytes by a cell membrane integrity stain using two fluorescent dyes: Syto 13 and propidium iodide and imaged by a laser scanning confocal microscope (×100 magnification); **B:** Quantification of human chondrocyte viability of the positive control, negative control, Protocol E–D–P at Day 0, Protocol E–D–P at Day 180, Protocol E–D at Day 0, and Protocol E–D at Day 180 (n = 6–9 replicates per group: no statistical differences between the protocols and the storage times, p = 0.706, based on two–way ANOVA); **C:** Representative images of the alamarBlue assay showing human chondrocyte metabolic activity from particulated articular cartilage after vitrification at 0 hours, 48 hours and 96 hours; **D:** Quantification of human chondrocyte metabolic activity with a similar level comparing the experimental groups to the positive control (n = 3 replicates per group, p = 0.823, based on two–way ANOVA) and a hypermetabolic rebound between 48 hours and 96 hours in both Protocol E–D–P and Protocol E–D groups; **E:** Age, sex and body mass index of human articular cartilage donors; **F:** Isolated human chondrocytes from post-vitrified articular cartilage dedifferentiated into fibroblast-like cells and migrated to the center of the culture plates (×100 magnification); **G:** When samples were stored for 6 months, isolated human chondrocytes from particulated articular cartilage using Protocol E–D migrated to heal the wound scratch with a faster migrating speed than the positive control, and the Protocol E–D group showed a faster migration than the Protocol E–D–P group at 24 hours when cultured *in vitro* (n = 6 replicates per group, $p_a = 0.016$, $p_b = 0.004$, $p_c = 0.043$, based on two–way ANOVA with Tukey's test).

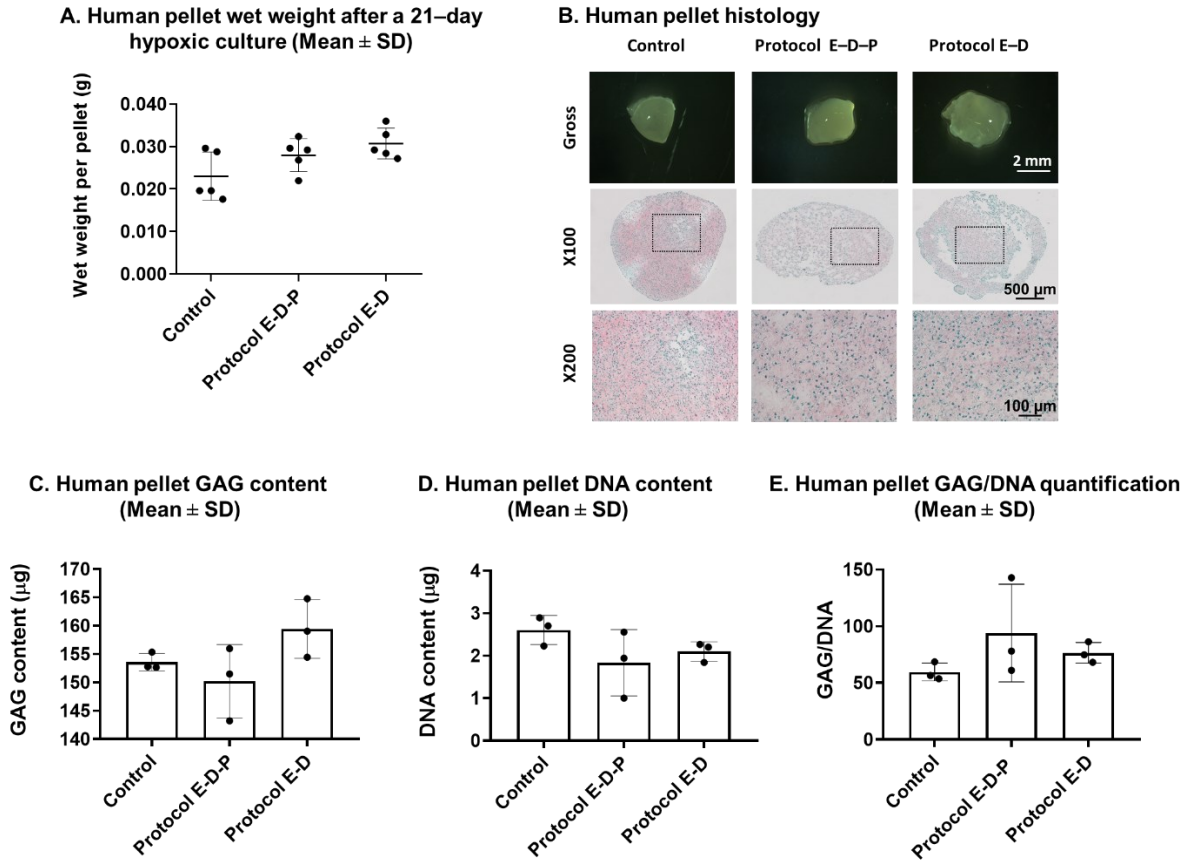

Figure 2.6 Assessment of human chondrocyte matrix productivity.

A: Human pellets after a 21-day culture show a similar wet weight among the control, Protocol E–D–P, and Protocol E–D groups (n = 5 replicates per group, p = 0.054, based on one–way ANOVA). **B:** Representative histological images showing the gross appearance of pellets after a 21-day culture with chondrogenic media under hypoxic conditions (3% O_2, 5% CO_2 at 37 °C). Safranin-O stain showing GAG content synthesized by viable and active chondrocytes for the control, Protocol E–D–P, and Protocol E–D groups. **C.** GAG content in the human pellets among the control, Protocol E–D–P, and Protocol E–D groups after a 21-day culture and measured *via* dimethylmethylene blue (DMMB) assay. **D.** DNA content in the human pellets quantified by CyQUANT^{TM} proliferation assay. **E.** GAG/DNA quantification of human pellets show similar

matrix productivity among the control, Protocol E–D–P, and Protocol E–D groups (n = 3 replicates per group, p = 0.334, based on one–way ANOVA).

2.5 Discussion

Our approach lengthens the time available for clinical transplantation to six months, compared to the current standard of 28 days[242], providing an extended period of time for arranging surgical procedures. This six-month storage time will alleviate the shortage of grafts and thus permit a larger number of particulated articular cartilage transplantations to take place, which is a clinically significant advance. Theoretically, storage as proposed in this paper can be indefinite without any expected change in results due to the absence of chemical and biologic activity at the storage temperature but we only tested out to six months to prove the concept. According to the United States Food and Drug Administration (FDA) guideline for donor eligibility, tissue donors for clinical transplantation are required to be screened and identified for the potential of transmission diseases[83,84,141]. The testing is performed on every tissue to confirm the safety of the tissue donated for clinical transplantation. However, these tests take about 14 days to complete, which, given the decline in chondrocyte function and viability after this time, makes the time frame for scheduling operations very short for surgeons in practice. In our study, we validated a stepwise vitrification approach using porcine articular cartilage, and further translated the method to human articular cartilage, providing a promising outcome that meets the requirement of 70% chondrocyte viability for clinical transplantation: our vitrification approach yields a high (> 80%) normalized chondrocyte viability in human particulated articular cartilage, a critical result for successful clinical implementation and use.

Particulated articular cartilage grafting is an accepted method of clinical chondral repair. Performed as a single stage procedure, small particulated articular cartilage allograft (from a deceased donor) is used to fill cartilage defects using fibrin fixation, such that a new articulating surface is developed in joints such as knees, and ankles[93,200]. Currently, the most used particulated cartilage grafts are provided by Zimmer, branded as DeNovo® NT (natural tissue) graft. A follow-up of 25 patients age 37 ± 11 years reported significant improvement in clinical outcomes as well as histologically indicated repair of hyaline-like cartilage after 24 months[72]. Another mid-term follow up study showed a progressive improvement in sequential MRIs with 70% achieving complete filling of knee cartilage defects in 26 patients after 4.4 years[182]. Although many cases using particulated articular cartilage have been performed on patients with full-thickness chondral defects, this treatment is limited by the availability of viable articular cartilage. In this study, based on engineering modelling we provide effective protocols to preserve particulated articular cartilage (approximately 1 mm^3 in size) with high viability of chondrocytes in porcine and human articular cartilage and validate their functionalities experimentally. Chondrocytes in porcine particulated articular cartilage migrated out of the cellular matrix and proliferated *in vitro* as shown in Fig. 2.3E; this evidence is consistent with the experiments reported by Tompkins *et al.*[233] for human particulated articular cartilage, an important property for cartilage repair. In our study, we further isolated the chondrocytes from vitrified articular cartilage to assess their proliferation and synthesis capacities: our results showed that the chondrocytes isolated from vitrified articular cartilage of both porcine and human species maintain a similar capacity when compared to their respective fresh control chondrocytes that did not undergo vitrification and rewarming. With our

current findings, vitrified particulated articular cartilage can be a potential source of tissue for use in clinical cartilage repair.

The chondrocyte viability of human particulated articular cartilage declined by ~15–20% after vitrification when compared to the fresh control group. In contrast, the porcine samples' viability declined only by ~5–10%. This difference may be attributed to the quality of the donated human tissue (although we have healthy articular cartilage with a positive control viability > 90%), one factor that may affect cartilage quality being the age of donor. Articular cartilage becomes mature in humans at the age of 20 years[128,228], characterized by a significant deposition of glycosaminoglycans in the extracellular matrix. As age increases to 50–60 years old, proteoglycans start to degenerate[240] and chondrocyte density decreases in comparison to articular cartilage in children aged younger than 13 years[233]. Over time, aged chondrocytes undergo slow apoptosis that worsens with more frequent and more intense daily activity accumulated over several decades, with a significant loss of water content in the cartilage matrix[144]. These changes to the cartilage increase the sensitivity and survival of chondrocytes when exposed to extracellular stimuli compared to that of chondrocytes in juvenile articular cartilage. In this study, we collected human articular cartilage from three donors (two male and one female, age 48, 50, 59 years, see Fig. 2.5E), ages at which cartilage quality would be expected to have declined. Conversely, the pigs are sexually mature but would be considered the equivalent to teenagers or young adults relative to humans. Second, the length of time between tissue harvesting and laboratory use can be detrimental to cell survival. In this study, the human articular cartilage from the three donors was harvested approximately 24 hours after donor death and kept in the tissue bank before same day delivery to the lab. Our previous research showed that porcine articular cartilage stored at 4 °C for

24 hours after slaughter and harvest had a lower tolerance to the chemical toxicity of a high concentration of cryoprotectants[247], when compared to those slaughtered and delivered to the lab within 6 hours, which could be due to the reactive oxidative species produced during the cryoprotectant loading procedure[89]. Therefore, it is likely that the lower chondrocyte viability of human tissues compared to porcine tissues in this study is due to both donor age and processing time of human articular cartilage. To improve chondrocyte viability in the clinical setting, juvenile or young adult articular cartilage could be vitrified, and a processing protocol in the tissue bank to guide the vitrification of human articular cartilage needs to be established in a future investigation.

2.6 Supplemental Information

Calculations from Engineering Modelling

Table 2.S3 Minimum cryoprotectant concentrations and vitrifiability scores, as well as maximum freezing point, calculated at the end of each loading step in Protocol E–D–P. These quantities are at the center of the cartilage cube where $x = 0$ mm.

Protocol E–D–P	Minimum Concentrations	Minimum Vitrifiability Score	Maximum Freezing Point
Loading Step 1	1.57 M EG 1.99 M DMSO	113	−12 °C
Loading Step 2	2.68 M EG 2.87 M DMSO 0.64 M PG	169	−29 °C

Table 2.S4 Minimum cryoprotectant concentrations and vitrifiability scores, as well as maximum freezing point, calculated at the end of each loading step in Protocol E–D. These quantities are at the center of the cartilage cube where $x = 0$ mm.

Protocol E–D	Minimum Concentrations	Minimum Vitrifiability Score	Maximum Freezing Point
Loading Step 1	2.47 M EG	84	−6 °C
Loading Step 2	3.51 M EG 3.12 M DMSO	171	−33 °C

Table 2.S3 Absolute chondrocyte viability of porcine particulated articular cartilage after vitrification and assessment with a cell membrane integrity stain.

Chondrocyte viability (%)	**Mean**	**Standard Deviation**	**95% Confidence Interval**
Positive control	94.2	4.8	[92.0, 96.4]
Negative control	0.1	0.1	[0, 0.1]
Protocol E–D–P: Day 0	84.7	11.0	[79.7, 89.7]
Protocol E–D–P: Day 180	86.5	9.4	[82.2, 90.8]
Protocol E–D: Day 0	85.4	11.6	[80.1, 90.7]
Protocol E–D: Day 180	90.2	5.1	[87.9, 92.6]

Table 2.S4 Absolute chondrocyte viability of human particulated articular cartilage after vitrification and assessment with a cell membrane integrity stain.

Chondrocyte viability (%)	Mean	Standard Deviation	95% Confidence Interval
Positive control	91.6	4.0	[88.6, 94.6]
Negative control	0.2	0.4	[−0.1, 0.6]
Protocol E–D–P: Day 0	79.1	10.4	[71.1, 87.1]
Protocol E–D–P: Day 180	82.5	11.4	[70.5, 94.5]
Protocol E–D: Day 0	74.7	17.2	[61.4, 87.9]
Protocol E–D: Day 180	76.3	12.1	[63.6, 88.9]

Table 2.S5 Relative fluorescence units (mean ± standard deviation) of porcine particulated articular cartilage after vitrification and assessment by alamarBlue.

Relative fluorescence units	48 hr	96 hr
Positive control	68663 ± 1946	58913 ± 2497
Negative control	10636 ± 976	15140 ± 1215
Protocol E–D–P: Day 0	72026 ± 2283	68993 ± 3155
Protocol E–D–P: Day 180	71636 ± 3084	67789 ± 5754
Protocol E–D: Day 0	71763 ± 2815	71875 ± 4941
Protocol E–D: Day 180	69620 ± 4030	66602 ± 6100

Table 2.S6 Relative fluorescence units (mean ± standard deviation) of human particulated articular cartilage after vitrification and assessment by alamarBlue.

Relative fluorescence units	**48 hr**	**96 hr**
Positive control	63317 ± 7668	66137 ± 3752
Negative control	5309 ± 2022	9275 ± 1743
Protocol E–D–P: Day 0	56727 ± 5245	72280 ± 11261
Protocol E–D–P: Day 180	54577 ± 221	68845 ± 4047
Protocol E–D: Day 0	53159 ± 9816	69682 ± 5471
Protocol E–D: Day 180	44304 ± 9151	65784 ± 7895

Chapter Three: Comparison of three multi-cryoprotectant loading protocols for vitrification of porcine articular cartilage

Authors: Kezhou Wu[a,d], Nadia Shardt[b], Leila Laouar[a], Zhirong Chen[b], Vinay Prasad[b], Janet A. W. Elliott[b,c], Nadr M. Jomha[a]*

Affiliations:

[a]Department of Surgery, University of Alberta, Edmonton, Alberta, Canada

[b]Department of Chemical and Materials Engineering, University of Alberta, Edmonton, Alberta, Canada

[c]Department of Laboratory Medicine and Pathology, University of Alberta, Edmonton, Alberta, Canada

[d]Department of Orthopedic Surgery, First affiliated hospital of Shantou University Medical College, Shantou, Guangdong, China

*Corresponding author. Address: 2D2.32 WMC Department of Surgery, University of Alberta Hospital, Edmonton, Alberta, Canada T6G 2B7, Fax: +17804072819. Email address: njomha@ualberta.ca (Nadr M. Jomha)

This chapter has been published in *Cryobiology* as: Kezhou Wu, Nadia Shardt, Leila Laouar, Zhirong Chen, Vinay Prasad, Janet A. W. Elliott, and Nadr M. Jomha. "Comparison of three multi-cryoprotectant loading protocols for vitrification of porcine articular cartilage." *Cryobiology* 92 (2020): 151-160. doi:10.1016/j.cryobiol.2020.01.001.

3.1 Abstract

Vitrification is a cryopreservation technique for the long-term storage of viable tissue, but the success of this technique relies on multiple factors. In 2012, our group published a working vitrification protocol for intact human articular cartilage and reported promising chondrocyte recovery after using a four-step multi-cryoprotectant (CPA) loading method that required 570 min. However, this protocol requires further optimization for clinical practice. Herein, we compared three multi-step CPA loading protocols to investigate their impact on chondrocyte recovery after vitrification of porcine articular cartilage on a bone base, including our group's previous four-step protocol (original: 570 min), and two shorter three-step protocols (optimized: 420 min, and minimally vitrifiable: 310 min). Four different CPAs were used including glycerol, dimethyl sulfoxide, ethylene glycol and propylene glycol. As vitrification containers, two conical tubes (50 ml and 15 ml) were evaluated for their heat transfer impact on chondrocyte recovery after vitrification. Osteochondral dowels were cored into two diameters of 10.0 mm and 6.9 mm with an approximately 10-mm thick bone base, and then allocated into the twelve experimental groups based on CPA loading protocol, osteochondral dowel size, and vitrification container size. After vitrification at −196 °C and tissue warming and CPA removal, samples in all groups were assessed for both chondrocyte viability and metabolic activity. The optimized protocol proposed based on mathematical modelling resulted in similar chondrocyte recovery to our group's original protocol and it was 150 min shorter. Furthermore, this study illustrated the role of CPA permeation (dowel size) and heat transfer (container size) on vitrification protocol outcome.

3.2 Introduction

Articular cartilage is a connective tissue that lacks blood vessels, nerves, and lymphatic supply. Consequently, the ability of articular cartilage to regenerate or adapt to mechanical changes is very limited[33,87,184]. Large cartilage defects over 1 cm^2 often progress into osteoarthritis if not properly treated[35,98]. Osteochondral allograft transplantation has been proven to be an effective surgical procedure for large cartilage defect repair and prevents the development of osteoarthritis if performed in the early stage of disease progress[37,46,227]. This treatment can be used to postpone the timing of joint replacement in young patients with large articular cartilage defects, but it is limited by the availability of fresh donor joints[119,242]. To overcome the limited availability of fresh cartilage, harvested osteochondral grafts can be stored in a well-designed tissue banking system equipped with appropriate preservation protocols. Current cartilage storage is at hypothermic temperatures for a maximum of 28–42 days before significant cell deterioration begins[84,242]. This results in tight surgical timelines, extensive tissue wastage, and large costs[210], which could be better managed if storage time were extended. Long-term preservation of cells and tissues beyond the times achievable at hypothermic temperatures can be possible with vitrification, a process that achieves a glassy state at super-low temperatures. Successful vitrification of intact osteochondral tissue will enable ultra-long term storage (*i.e.* years), resulting in improved circumstances for clinical transplantation of articular cartilage for cartilage defect repair.

Vitrification of articular cartilage is a complex procedure relying on multiple factors[3], such as CPA permeation into articular cartilage, CPA toxicity on chondrocytes, heat transfer and sample packaging for storage at cryogenic temperatures. Previously, our group published a working vitrification protocol for intact human articular cartilage, reporting promising cell recovery after

using a four-step multi-CPA loading method that required 570 min[113]. A typical trial of articular cartilage vitrification involves three phases including CPA permeation, sample vitrification, and sample warming as shown in Fig. 3.1. Harvested osteochondral tissue is immersed in pre-cooled CPA cocktail solutions in a stepwise manner for CPA permeation in a series of low temperature baths (Phase 1). The osteochondral tissue is transferred into a container filled with vitrifiable CPA cocktail solution and plunged into liquid nitrogen for vitrification (Phase 2) and storage. Subsequently, osteochondral tissues are removed from the liquid nitrogen tank and quickly warmed in a water bath and washed in medium to remove the CPAs for further testing (Phase 3).

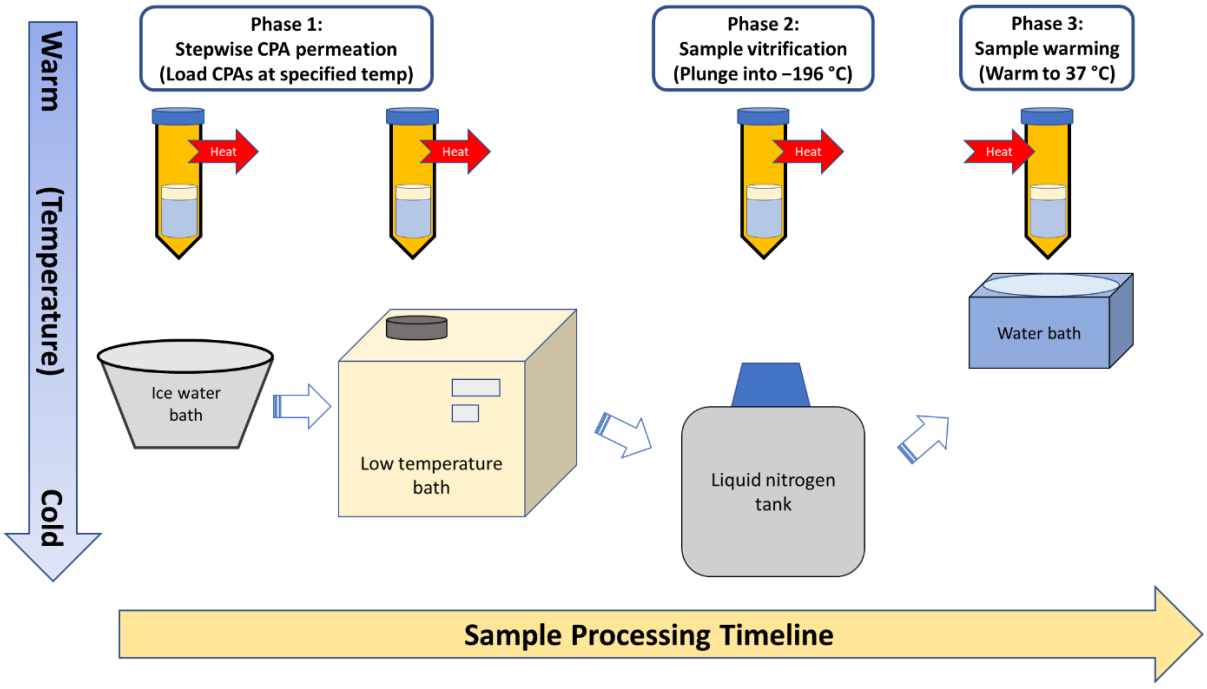

Figure 3.1 Processing flowchart for vitrification of osteochondral dowels. Phase 1 consists of stepwise CPA permeation, Phase 2 is the vitrification and storage of the sample in liquid nitrogen, and Phase 3 warms the sample for analysis.

Optimizing the vitrification of osteochondral tissue involves several challenges, such as to improve the CPA permeation into articular cartilage, or to improve the heat transfer during cooling and warming. CPA permeation is an essential step in a vitrification protocol, in which specified amounts of CPAs are loaded into the extracellular matrix and cells to achieve a glassy state after cooling at appropriate rates[69,198,218]. Pegg *et al.* developed the "liquidus tracking method" proposed by Farrant[73] and used a single CPA for CPA permeation at a series of temperatures[185]; while the approach of Fahy *et al.*[198] and Song *et al.*[218] was to use a multi-CPA solution for CPA permeation at one fixed temperature followed by programmed cooling for vitrification. The overall challenge of CPA permeation in articular cartilage is to load sufficient CPA into the cartilage tissue with minimal CPA toxicity while achieving vitrifiable concentrations throughout the whole tissue[25,66,113]. CPA toxicity to chondrocytes is a major concern related to CPA permeation into articular cartilage. Our group measured CPA toxicity to chondrocytes of both porcine and human articular cartilage[9,65,110] and developed a strategy to minimize the toxicity effects by using multiple permeating CPAs and adding antioxidative agents[89,247]. Our group proposed a vitrification method in 2012 that consisted of loading multiple types of CPAs sequentially into intact articular cartilage at a series of progressively lower temperatures, so as to minimize the chondrocyte toxicity of high concentrations of CPAs and to permeate vitrifiable concentrations of CPA within the whole articular cartilage tissue by the end of the multi-step loading. However, our group's vitrification protocol required 570 min for sufficient CPA permeation into the articular cartilage, which was not ideal for practical use in tissue banks. Therefore, shortening the loading protocol is desired to provide a reasonable processing time frame. In this study, we compared three multi-step CPA loading protocols to evaluate their effectiveness in the vitrification of porcine osteochondral tissue. The first protocol was the original 570-min loading protocol from our group's previous paper[113].

The next two protocols were shorter loading protocols targeted for clinical practice. One 420-min optimized protocol was determined with mathematical modelling of permeation, vitrifiability, and freezing point[208]. The final 310-min protocol was an *ad hoc* protocol chosen as one expected to be minimally vitrifiable for intact articular cartilage. Unlike the original protocol, both shortened protocols make use of multi-CPA solutions in the first step and avoid use of a very high concentration CPA in the first step, a strategy aimed at reducing CPA toxicity[9,65,67,68]. In addition, glycerol was removed from both shortened protocols since its potential toxicity when used in articular cartilage vitrification protocols was significant[65]. The size of the tissue sample is an important property that effects the extent of CPA permeation for a given protocol. Thus, we studied the effect of each protocol on two different tissue sample sizes.

Along with CPA permeation, another consideration is that of heat transfer: how quickly the tissue can be cooled when it is immersed in liquid nitrogen, followed by how quickly it can be warmed after storage. If the rate of heat transfer during cooling and warming is too slow, ice can form and cell recovery can be compromised[27,58,59,152,153]. Factors that contribute to the rate of heat transfer can be divided into the amount of sample to be vitrified (tissue plus vitrification solution) and the properties of the container used for vitrification. As the size of the tissue sample grows, the required volume to be vitrified grows accordingly, which increases the time taken for cooling/warming to occur. That is, insufficiently fast heat transfer places a limit on the size of a sample that is amenable to conventional cooling and warming in vitrification processes[58,59]. Together with container size, container material affects the process of heat transfer. For instance, to achieve better heat transfer, Bos-Mikich *et al.*[28] used a metal container to enhance mouse ovary recovery while Kim *et al.*[129] found that a paper container was beneficial for vitrifying bovine

blastocytes. In this study, we focused on comparing two vitrification container sizes to evaluate the impact of their different heat transfer on vitrification of porcine osteochondral tissue. This will provide knowledge about heat transfer in the design of vitrification protocols for articular cartilage.

We hypothesized that a mathematically modeled shortened protocol would provide biologic results as determined by cell viability and metabolic activity equal to, or better than, our group's previously published protocol and that tissue sample size and container size would have a significant effect on these results. To investigate this, we compared three vitrification protocols (original, optimized, and minimally vitrifiable), two tissue sample sizes, and two container sizes.

3.3 Materials and Methods

3.3.1 Study design and method flowchart

This study compared chondrocyte recovery from porcine osteochondral tissue after vitrification using three multi-step multi-CPA loading protocols. We investigated the impact of CPA loading protocol, osteochondral dowel size, and vitrification container size on cell recovery after vitrification in liquid nitrogen (LN_2 at −196 °C). The method flowchart below (Fig. 3.2) shows the experimental preparation of the osteochondral tissue, the processes of CPA loading, sample vitrification, sample thawing and CPA removal. Chondrocyte recovery was determined by a cell membrane integrity fluorescent dual stain and a mitochondrial activity functional assay.

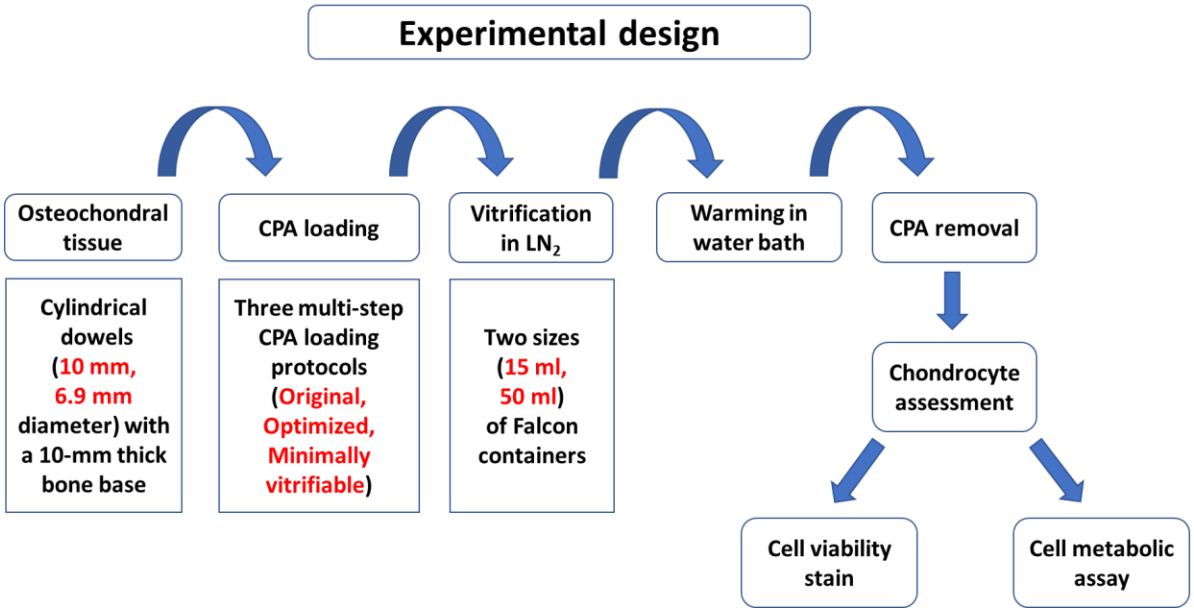

Figure 3.2 Method flowchart for the vitrification of porcine osteochondral dowels highlighting the experimental variables in red

3.3.2 Porcine osteochondral dowel preparation

Hind legs with joints from sexually mature pigs were obtained from a slaughter house in Wetaskiwin, Canada. All porcine stifle joints were from meat-processing plants and no animals were specifically euthanized for this research. An electric saw was used to split the condyles from the porcine femora and then these condyles were cored into osteochondral dowels consisting of two diameter sizes (10.0 mm and 6.9 mm) with bone bases that were approximately 10 mm thick. All osteochondral dowels were cleaned for 15 minutes by incubation in sterile phosphate-buffered saline (PBS) supplemented with 100 units/ml penicillin, 100 µg/ml streptomycin, and 0.25 µg/ml amphotericin B (Gibco) under sterile conditions. Osteochondral dowels were randomly divided into the 12 experimental groups and incubated in a complete medium (DMEM complete: Dulbecco's Modified Eagle Medium F12 (Gibco)) supplemented with 10% calf serum (Gibco),

100 units/ml penicillin, 100 μg/ml streptomycin, 0.25 μg/ml amphotericin B, and 1 mM sodium pyruvate (Gibco) at 4 °C for less than 24 hours prior to vitrification.

3.3.3 Multi-cryoprotectant loading protocols

Three multi-step CPA loading protocols were used (Fig. 3.3): our group's previously established four-step protocol (the original protocol; 570 min[113]), and two shorter three-step protocols, the optimized protocol (420 min, calculated by mathematical modelling[208]) and the minimally vitrifiable protocol (310 min, an *ad hoc* protocol). Four CPAs were used to make the CPA cocktail solutions in this study including glycerol (Gly), dimethyl sulfoxide (DMSO), ethylene glycol (EG) and propylene glycol (PG). The multi-step CPA loading procedure for each protocol was completed as follows. All CPA cocktail solutions were prepared in DMEM supplemented with 0.1 mg/ml chondroitin sulfate. After the CPA loading in step 1, the osteochondral dowel was quickly transferred to the pre-cooled solution for step 2, followed by step 3 and step 4 if indicated. After the loading procedure, whole osteochondral dowels within the CPA loading containers were rapidly plunged into liquid nitrogen (−196 °C) for vitrification. The final volume in the 50 ml containers is 15 ml including the osteochondral dowel and surrounding CPAs; while the final volume in the 15 ml containers is 5 ml including the osteochondral dowel and surrounding CPAs.

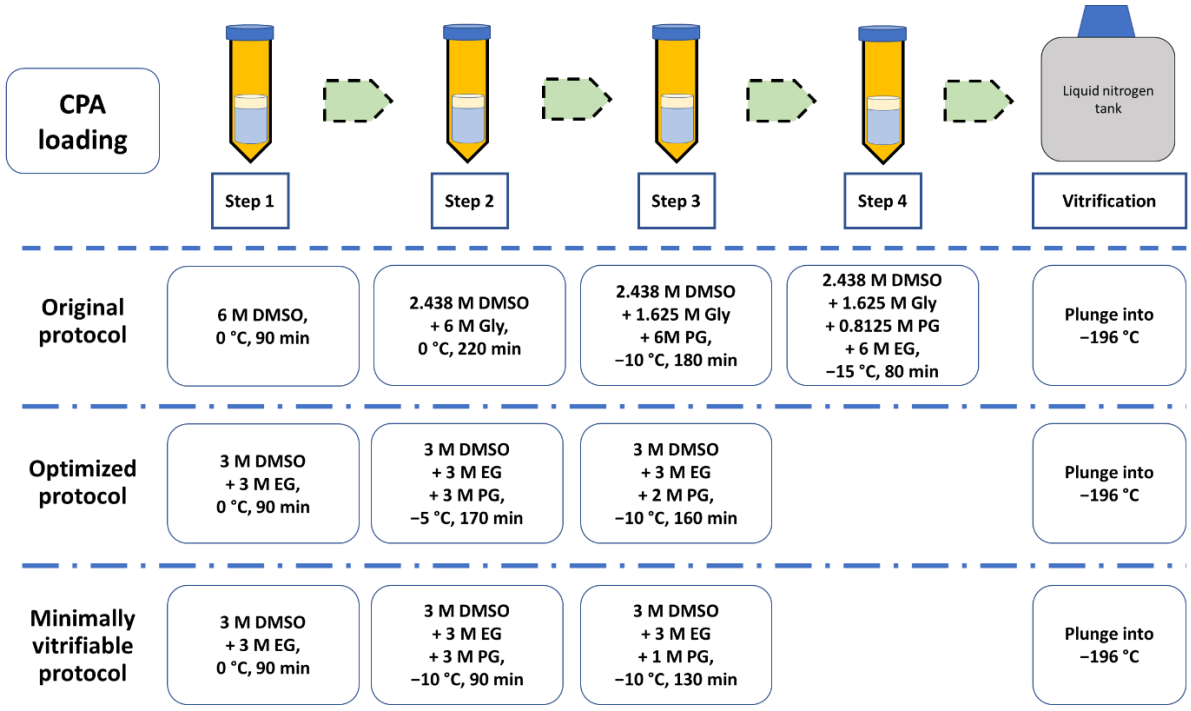

Figure 3.3 Cryoprotectant concentrations, times, and temperatures for each step of three cryoprotectant loading protocols: the original protocol, an optimized protocol, and a minimally vitrifiable protocol

3.3.4 Vitrification storage and warming procedure

After vitrification and storage in liquid nitrogen for at least 72 hours, samples were removed from liquid nitrogen (−196 °C) and warmed in a 37 °C water bath. Once the glassy CPA surrounding the osteochondral dowel melted, the osteochondral dowels were quickly removed from the tubes, patted dry and placed into 25 ml DMEM plus chondroitin sulphate (0.1 mg/mL) for CPA removal at 4 °C for 30 min. The osteochondral dowels were then placed in another 25 ml of fresh DMEM with chondroitin sulphate for a second 30 min at 4 °C, followed by a third wash of 30 min at 4 °C.

3.3.5 Experimental groups

In the present study, three vitrification protocols with different total lengths of time were tested for successful vitrification of porcine articular cartilage. Two sizes of conical tubes as CPA loading/sample vitrification containers and two dowel sizes were used to investigate how the container and dowel sizes impacted chondrocyte recovery for the three vitrification protocols. Dissected dowels were allocated into the experimental groups based on CPA loading protocol (original, optimized, or minimally vitrifiable protocol), osteochondral dowel size (10.0 mm or 6.9 mm diameter) and container size (50 ml or 15 ml volume) (n = 4 replicate dowels per group). Dimensions of the sample container tubes (Falcon™, Fisher Scientific) and osteochondral dowels are shown in Fig. 3.4.

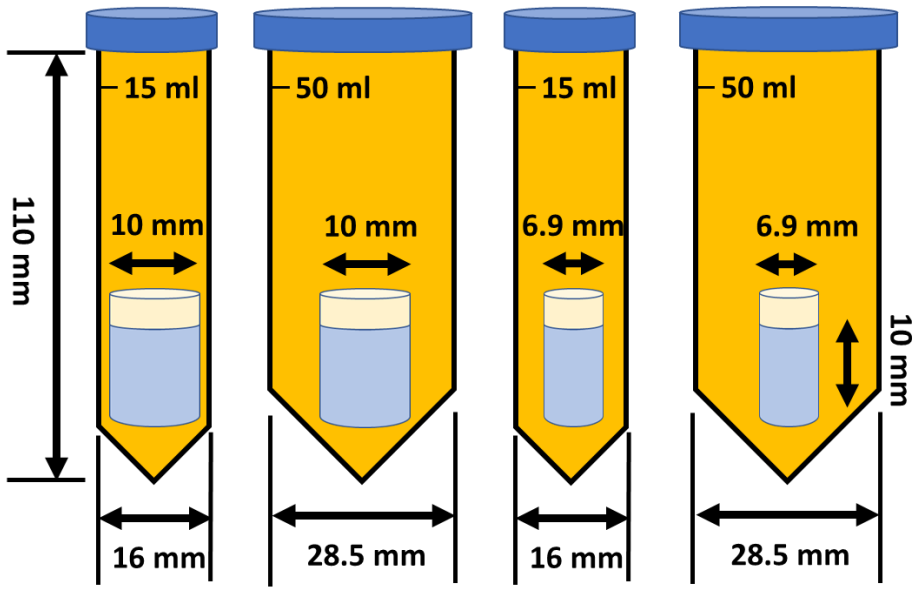

Figure 3.4 Dimensions of sample containers and osteochondral dowels

3.3.6 Chondrocyte assessment

The inclusion criteria for a healthy cartilage tissue sample was a minimum of 85% absolute chondrocyte viability in the fresh controls before CPA exposure. Following CPA removal, chondrocyte viability was quantified by a dual live–dead cell membrane integrity stain and the chondrocyte metabolic activity was measured by alamarBlue.

3.3.6.1 Live–dead cell membrane integrity staining

Chondrocyte viability was quantified using live–dead cell fluorescent microscopy based on cell membrane integrity stains (6.25 µM Syto 13 and 9.0 µM propidium iodide mixed in PBS). Syto 13 (Syto 13; Molecular Probes) is a live cell nucleic acid dye that fluoresces green, and propidium iodide (PI; Invitrogen) is a membrane-impermeant dye that penetrates membrane-damaged cells and fluoresces red. Cartilage slices from each dowel were sectioned into 85-µm thick slices using a vibratome-1500 machine (The Vibratome Company, St. Louis, MO) and kept in PBS before staining. After sectioning, cartilage slices were placed on glass slides and gently patted dry with Kimwipes. Each slice was overlaid with approximately 50 µl of stain mixture and covered with a coverslip, then incubated in the dark for 15 min before imaging. Cartilage slices were observed under an inverted fluorescent microscope (model: Nikon ECLIPSE Ti-5) using a dual filter (excitation/emission: 488 nm/503 nm and 535 nm/617 nm) and imaged with a digital camera (model: Nikon DS-Fi2). Cell viability within slices was determined by counting the numbers of green-stained (viable) cells and red-stained (non-viable) cells, using a custom-made software Viability 3.2[111]. The chondrocyte viability after vitrification was normalized to its own fresh control before CPA loading. The normalized cell viability of the experimental samples was determined according to the following formula:

$$\text{Normalized cell viability (\%)} = \frac{\frac{\#\text{ of green cells after vitrification}}{\#\text{ of green cells} + \#\text{ of red cells after vitrification}}}{\frac{\#\text{ of green cells before CPA loading}}{\#\text{ of green cells} + \#\text{ of red cells before CPA loading}}} \times 100\% \quad (1)$$

3.3.6.2 Chondrocyte metabolic activity by alamarBlue

Chondrocyte metabolic activity was assessed by alamarBlue using our group's previously published method[113]. AlamarBlue (Invitrogen, Burlington, Canada) is a cell viability indicator in which the non-fluorescent resazurin (blue colour) is converted to highly fluorescent resorufin (red colour) *via* the reduction reaction of metabolically active cells[180,213,258]. After the warming procedure, cartilage disks from each experimental group were shaved off the bone and approximately 0.2 g of cartilage samples per group were washed with 5 ml sterile PBS supplemented with antibiotics for 15 minutes. The cartilage samples were then incubated in 5 ml DMEM complete for 5 days. Cartilage samples were then incubated in an alamarBlue assay solution containing 5 ml X-VIVO 10 (a serum-free medium (Lonza, California, USA)) supplemented with 0.1 mM ascorbic acid, 100 nM dexamesasone, and 10 ng/ml transforming growth factor (TGF) beta 1 that was mixed with 500 µl alamarBlue in a 6 well plate and incubated at 37 °C. Fluorescence was measured in duplicate for each sample per experimental group at 24 hr, 48 hr, 72 hr, 96 hr, 120 hr, 144 hr and 168 hr. Positive controls consisted of articular cartilage that was neither exposed to CPAs nor vitrified. The average of two readings of blank samples (alamarBlue assay solution without cartilage samples) was subtracted from the average of the experimental samples to yield a value in relative fluorescent units (RFU) divided by weight in grams of articular cartilage. The Cytofluro 2.0 software was used to read the plates with fluorescence parameters set to emission wavelengths of 580/50 nm, excitation wavelengths of 485/20 nm and a gain of 45 for fluorescent intensity. The RFU readings of chondrocytes after vitrification were normalized to their own fresh positive controls and presented as a percentage.

3.3.7 Statistical analysis

The numerical data are presented as the means ± standard error (SE). The analysis of variance (ANOVA) with Tukey's multiple-comparison post hoc test was performed on cell recovery if the variances of variables were equal as determined by Levene's test. Otherwise, the nonparametric Kruskal–Wallis or Mann–Whitney *U* test was performed on cell recovery under different experimental conditions using SPSS 20.0 software. The *p*-values are reported in the results section and numerical data with standard error are presented in the Supplemental Tables. In general, statistical significance in all the figures is indicated with asterisks: * indicates $p < 0.05$, and ** indicates $p < 0.01$.

3.4 Results

3.4.1 Chondrocyte viability by a cell membrane integrity stain

The representative images in Fig. 3.5 show the chondrocytes *in situ* after staining with live–dead cell membrane integrity dyes. Fig. 3.5A shows an almost 100% chondrocyte viability of articular cartilage sections from fresh porcine joints without CPA permeation nor having been plunged into liquid nitrogen. Fig. 3.5B shows a 0% chondrocyte viability of articular cartilage sections after having been plunged into liquid nitrogen without CPA permeation. Fig. 3.5C shows approximately 80% (high) chondrocyte viability of articular cartilage sections after CPA permeation with a vitrifiable CPA loading protocol and having been plunged into liquid nitrogen for vitrification. Fig. 3.5D shows approximately 30% (low) chondrocyte viability of articular cartilage sections after

CPA permeation with a non-suitable CPA loading protocol and having been plunged into liquid nitrogen for vitrification. Chondrocyte viability was quantified by counting the green stained (live) chondrocytes and red or orange stained (dead) chondrocytes using a custom-made software Viability 3.2.

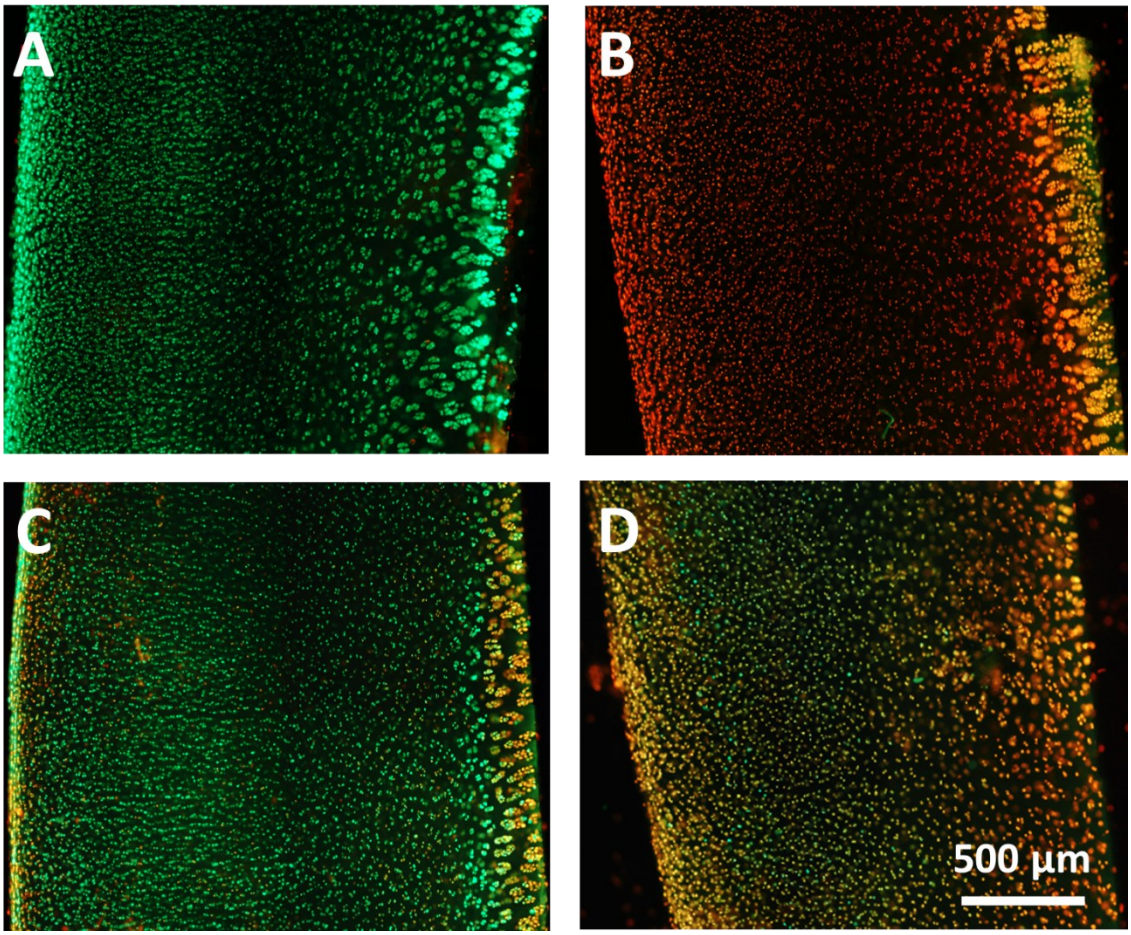

Figure 3.5 Chondrocytes labelled with a live–dead cell membrane integrity stain

A: Representative image of positive fresh control articular cartilage sections before cryoprotective agent permeation.

B: Representative image of negative control articular cartilage sections after having been plunged into liquid nitrogen without cryoprotective agent permeation.

C: Representative image of high chondrocyte survival articular cartilage sections after cryoprotective agent permeation with the optimized protocol and plunging into liquid nitrogen for vitrification.

D: Representative image of low chondrocyte survival articular cartilage sections after cryoprotective agent permeation with the minimally vitrifiable protocol and plunging into liquid nitrogen for vitrification.

Fig. 3.6 shows the viability results of this study grouped according to each sample size and container size combination. The chondrocyte viability after vitrification of 10.0 mm diameter dowels in 15 ml sample containers using the optimized protocol was similar when compared to the original protocol ($p = 0.063$); while the chondrocyte viability was significantly higher using the optimized protocol when compared to the minimally vitrifiable protocol ($p^{**} = 0.008$) (Fig. 3.6A). The chondrocyte viability after vitrification of 10.0 mm diameter dowels in 50 ml sample containers was significantly higher for both the original protocol and the optimized protocol when compared to the minimally vitrifiable protocol ($p^{*} = 0.048$ and $p^{**} = 0.006$, respectively) (Fig. 3.6B). The chondrocyte viability after vitrification of 6.9 mm diameter dowels in 15 ml sample containers showed no significant differences between the original, the optimized, or the minimally vitrifiable protocols ($p = 0.130$) (Fig. 3.6C). The chondrocyte viability after vitrification of 6.9 mm diameter dowels in 50 ml sample containers was significantly higher for the optimized protocol compared to the minimally vitrifiable protocol ($p^{*} = 0.015$) (Fig. 3.6D). (For numeric data, see Supplemental Table 3.S1.)

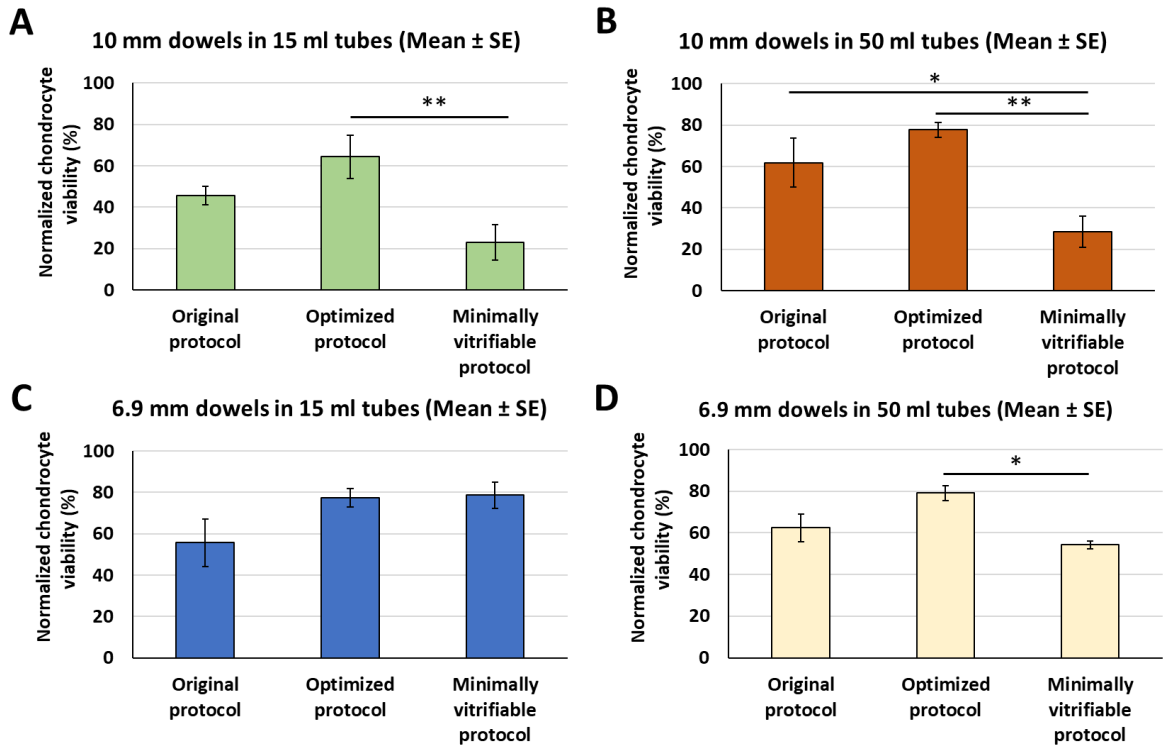

Figure 3.6 Comparison of chondrocyte viability by vitrification protocol for each tissue sample size/container size combination

A: The chondrocyte viability after vitrification of 10.0 mm diameter dowels in 15 ml sample containers was significantly higher for the optimized protocol compared to the minimally vitrifiable protocol.

B: The chondrocyte viability after vitrification of 10.0 mm diameter dowels in 50 ml sample containers was significantly higher for both the original protocol and the optimized protocol when compared to the minimally vitrifiable protocol.

C: The chondrocyte viability after vitrification of 6.9 mm diameter dowels in 15 ml sample containers did not show significant differences between the original, the optimized, or the minimally vitrifiable protocols.

D: The chondrocyte viability after vitrification of 6.9 mm diameter dowels in 50 ml sample containers was significantly higher for the optimized protocol when compared to the minimally vitrifiable protocol.

Fig. 3.7 shows the viability results of this study grouped according to CPA loading protocol. Chondrocyte viability after vitrification using the original protocol or the optimized protocol did not show statistically significant differences between 10.0 mm and 6.9 mm diameter dowels whether CPA was loaded in 15 ml or 50 ml sample containers ($p > 0.05$) (Fig. 3.7A-B). Using the minimally vitrifiable protocol, the chondrocyte viability after vitrification of 6.9 mm diameter dowels in both 15 ml ($p^{**}_{15\text{ ml}} = 0.002$) and 50 ml ($p^{*}_{50\text{ ml}} = 0.016$) sample containers was significantly higher than that for the 10.0 mm diameter dowels, respectively; and chondrocyte viability after vitrification of 6.9 mm diameter dowels was significantly higher in 15 ml sample containers than in 50 ml sample containers ($p^{*}_{6.9\text{ mm}} = 0.027$) (Fig. 3.7C). (For numeric data see Supplemental Table 1.)

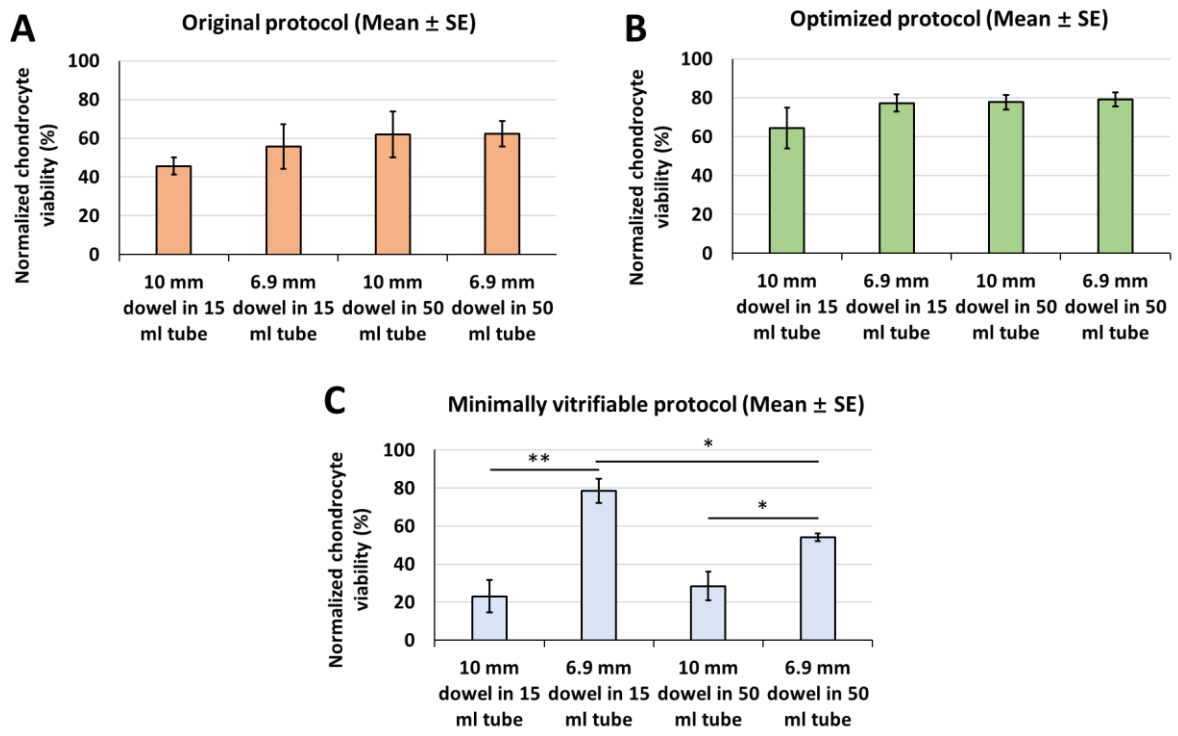

Figure 3.7 Comparison of chondrocyte viability by sample size/container size combination for each vitrification protocol

A: Using the original protocol, there were no significant differences in chondrocyte viability after vitrification between 15 ml and 50 ml sample containers for both 6.9 mm and 10.0 mm dowels.

B: Using the optimized protocol, there were no significant differences in chondrocyte viability after vitrification between 15 ml and 50 ml sample containers for both 6.9 mm and 10.0 mm dowels.

C: Using the minimally vitrifiable protocol, the chondrocyte viability after vitrification of 6.9 mm diameter dowels was significantly higher than that for 10.0 mm diameter dowels in both 15 ml and 50 ml sample containers; the chondrocyte viability after vitrification of 6.9 mm diameter dowels was significantly higher in 15 ml sample containers compared to 50 ml sample containers.

3.4.2 Chondrocyte metabolic activity by alamarBlue

The chondrocyte metabolic activity of each experimental group was quantified by alamarBlue fluorescence normalized by each group's positive control for 7 days at intervals of 1 day. The gradual increase in fluorescence, "normalized metabolic activity" of each experimental group showed continued mitochondrial function of chondrocytes after vitrification (Fig. 3.8). (For numeric data see Supplemental Table 3.S2.)

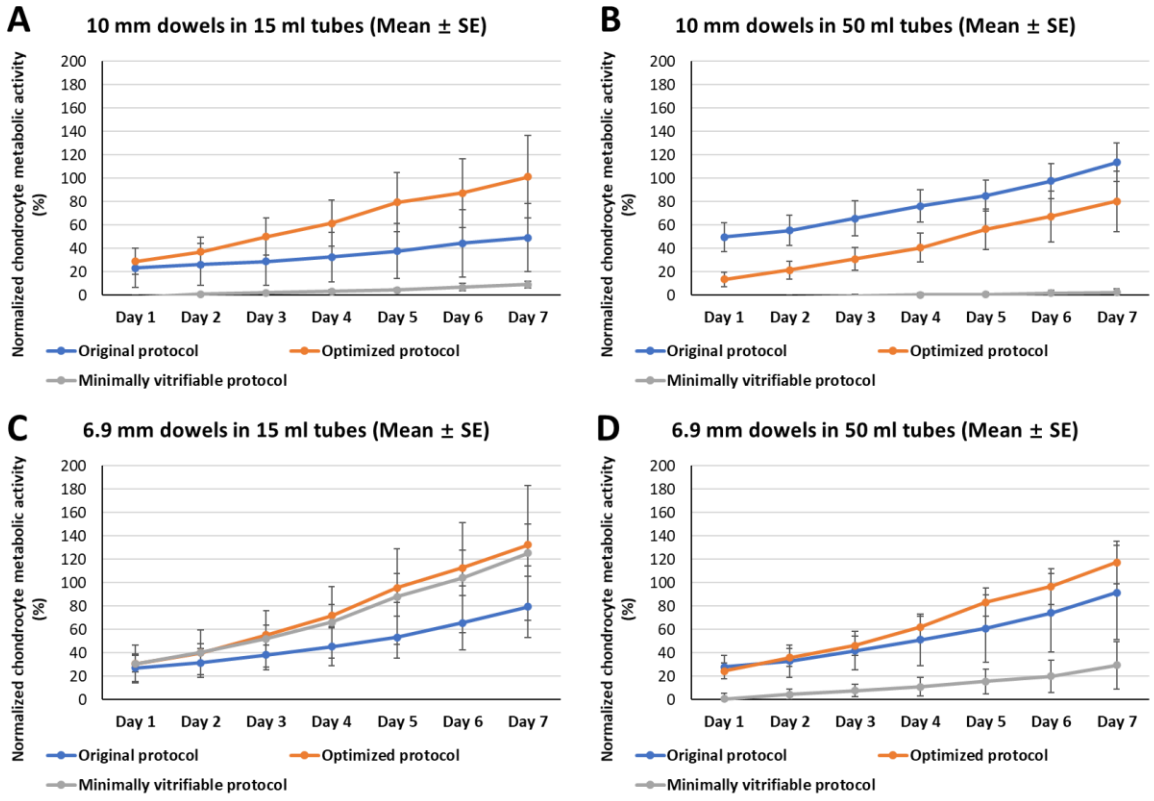

Figure 3.8 Chondrocyte metabolic activity assessed by alamarBlue

A: For samples in 15 ml containers, the normalized metabolic activity of 10.0 mm diameter dowels appeared to show increased chondrocyte metabolic activity for the optimized protocol compared to the original protocol, while the minimally vitrifiable protocol resulted in almost no chondrocyte metabolic activity from Day 1 to Day 7.

B: For samples in 50 ml containers, the normalized metabolic activity of 10.0 mm diameter dowels appeared to show increased metabolic activity for the original protocol compared to the optimized protocol, while the minimally vitrifiable protocol resulted in almost no chondrocyte metabolic activity from Day 1 to Day 7.

C: For samples in 15 ml containers, the normalized metabolic activity of 6.9 mm diameter dowels appeared to show similar trends for the optimized protocol and the minimally vitrifiable protocol, and both the optimized protocol and the minimally vitrifiable protocol appeared to show increased metabolic activity compared to the original protocol from Day 1 to Day 7.

D: For samples in 50 ml containers, the normalized metabolic activity of 6.9 mm diameter dowels appeared to show similar trends for the original protocol and the optimized protocol, while both the original protocol and the optimized protocol appeared to show increased metabolic activity compared to the minimally vitrifiable protocol from Day 1 to Day 7.

Note: In all graphs in Figure 3.8, statistical significance was not achieved for metabolic assays due to the high variability and small sample size. However, the trends are consistent with the membrane integrity results.

3.5 Discussion

Vitrification is a complex, but promising, long-term preservation method for storing viable articular cartilage at cryogenic temperatures. Vitrification of articular cartilage is a stepwise procedure relying on multiple key factors: CPA permeation, CPA vitrifiability, CPA toxicity, and heat transfer. Our group has investigated methods of achieving optimal concentrations of CPAs[110,113], CPA loading timings[114], CPA loading temperatures[63,211] and calculating the CPA

permeation kinetics[4,208,209,211,257] and vitrifiability[208,239] for the vitrification of articular cartilage. The investigation of CPA permeation and heat transfer in articular cartilage during the vitrification process can contribute to the design of successful vitrification protocols for articular cartilage.

CPA permeation planning using our group's mathematical approach[208] (for calculating the required amount of CPA permeation within articular cartilage tissue to reach a vitrifiability target) is a new tool for developing successful vitrification protocols. Mathematical modelling is a critical tool because of its ability to quickly identify potential CPA loading protocols that minimize the total time required for CPA permeation, and in doing so, mathematical modelling importantly bypasses the need for a large number of empirical experiments [25,53,208]. In our companion paper[208] to the current study, Nadia Shardt used engineering modelling to predict the spatially- and temporally-resolved CPA concentrations, solution vitrifiability, and solution freezing point for the three protocols. In that work [208], it was determined that the original and optimized protocols were both expected to reach a vitrifiable quantity of CPAs at all locations in the cartilage from the bone to the cartilage–solution boundary by the end of each loading protocol, while less than half of the cartilage thickness was predicted to be vitrifiable for the minimally vitrifiable protocol. These theoretical predictions of vitrifiability aligned well with the experimental data presented herein: porcine osteochondral dowels vitrified using either the original protocol or the optimized protocol demonstrated significantly higher chondrocyte viability compared to the minimally vitrifiable protocol when vitrifying the 10.0 mm dowels in either 15 ml or 50 ml volume containers (Fig. 3.6A-B). This was supported by the evident chondrocyte metabolic activity of each experimental treatment as seen in Fig. 3.8A-B that showed similar trends to chondrocyte viability in Fig. 3.6A-B, indicating that a significant number of chondrocytes remained intact and functional after the

stress of vitrification. Thus, this experiment demonstrated that optimized CPA loading protocols can be generated using an engineering modeling approach and the protocol used herein resulted in high cell viability and function.

Another important variable for optimization of vitrification protocols is the rate of heat transfer from/to the sample during the cooling/warming phases. Heat transfer has been extensively studied for cryopreservation of tissues and organs[58,59,152]. Slow warming may cause crystallization in the specimen and result in cell death[157]. Radio frequency heating or laser nanowarming devices have been developed for ultrafast warming for cryopreservation of many tissue types[27,50,64,152]. However, these emerging technologies are not yet applicable in vitrification of articular cartilage, possibly due to the high cellular toxicity and poor permeability of iron nanoparticles into articular cartilage matrix[135]. Using convective heat transfer is still the mainstream method for cooling and warming articular cartilage samples for vitrification; thus, our group's approach has been to develop protocols that vitrify consistently with convective cooling/warming.

One novelty in this study is that we explored the relationship between the post-vitrified cell recovery and two variables that affect cell recovery: tissue size and vitrification container size. In the current study, two tissue sample sizes were tested in two container sizes as shown in Fig. 3.4. For the 10.0 mm diameter dowels, chondrocyte viability was significantly higher in the original protocol and the optimized protocol when compared to the minimally vitrifiable protocol using a 50 ml CPA loading container (Fig. 3.6B). Importantly, this difference did not exist in the 6.9 mm diameter dowels using the 15 ml CPA loading containers (Fig. 3.6C). We emphasize that larger tissue sample sizes may have less CPA permeation for a given loading protocol while larger

vitrification containers slow down the heat transfer during cooling and warming. These factors need to be considered when considering clinical translation of a vitrification protocol.

After evaluating the effect of changing loading protocols for each osteochondral dowel size and container size, we examined how the success of each loading protocol changed with changing dowel and container size. Differences in chondrocyte viability among the two dowel sizes and container sizes became significant when using the minimally vitrifiable protocol (Fig. 3.7C). The minimally vitrifiable protocol was successful in vitrifying 6.9 mm diameter dowels in the 15 ml container tube, with a chondrocyte recovery comparable to that achieved using the original or the optimized protocol with the same dowel size and same container size (Fig. 3.6C). This finding indicates that a favorable combination of experimental factors may result in a good outcome for vitrification of articular cartilage, that is a smaller tissue sample size for enhanced CPA permeation and a smaller container size for enhanced heat transfer. The cell viability results were supported by the chondrocyte metabolic activity measurements (Fig. 3.8) between the three CPA loading protocols, although not to the same statistical significance. It appears that after vitrification with a suitable protocol, cells were intact and functional which is important in the transplantation scenario.

From the findings in this study, we conclude that CPA permeation and heat transfer during cooling/warming together contribute to the final chondrocyte recovery of post-vitrified articular cartilage. In this study, we identify three vitrification scenarios. In the best case (Fig. 3.6C; small dowel (6.9 mm diameter) in a small container (15 ml tube)), increased CPA permeation and faster heat transfer make it easier to vitrify articular cartilage successfully, possibly with less exposure of the chondrocytes to CPAs. For example, the minimally vitrifiable protocol showed similar

chondrocyte viability to the optimized protocol, and both were better than the original protocol. The original protocol may have higher CPA toxicity due to the longer duration of CPA exposure during loading. In the worst case (Fig. 3.6B; big dowel (10 mm diameter) in a big container (50 ml tube)), the slower heat transfer is compensated by the slightly greater CPA permeation of the optimized protocol and the original protocol. Conversely, in the minimally vitrifiable protocol, there is insufficient CPA permeation to counter the detrimental effects of the slower heat transfer resulting in lower chondrocyte viability. In the intermediate cases (Fig. 3.6A; big dowel (10 mm diameter) in a small container (15 ml tube) with less CPA permeation but faster heat transfer in articular cartilage), or (Fig. 3.6D; small dowel (6.9 mm diameter) in a big container (50 ml tube) with more CPA permeation but slower heat transfer in articular cartilage), chondrocyte viability after the optimized protocol is always better than that after the minimally vitrifiable protocol. One possible explanation for poor CPA permeation in big osteochondral dowels is that CPA permeation into the central portion of the cartilage on a bone base takes longer due to the longer distance for permeation from the peripheral cut edges and the greater volume to surface area ratio. This finding is consistent with the result published in 2002[110] that CPA permeation throughout the three articular cartilage layers of different locations contributed differently to their chondrocyte viabilities after rapid cooling and warming. In addition, cooling/warming osteochondral dowels to/from −196°C is faster in the small container compared to the big container. The heat transfer for cartilage cooling/warming in a 15 ml container is faster compared to that in a 50 ml container, which indicates that a large container can prevent heat transfer from occurring quickly enough during the cooling/warming procedures that can be damaging to the chondrocytes. Our result here is consistent with the findings in literature that small volumes (e.g., 1 ml) over large volumes (e.g., 50 ml) are easier to successfully warm by convective heat transfer[152,153].

3.6 Conclusions

Chondrocyte viability and metabolic activity of osteochondral dowels after vitrification and warming rely on the several key variables: CPA loading protocol, tissue sample size, and container size. This study provides *in vitro* experimental data from porcine articular cartilage that confirm success of a vitrification CPA loading protocol predicted by mathematical modelling[208]. These findings demonstrate the effectiveness of mathematical modeling in shortening the cryoprotectant loading time while maintaining similar chondrocyte recovery after vitrification. A further advantage of our successful optimized protocol is its simplicity for clinical practice. With the presented experimental results, the new optimized protocol (420 min) shows comparable chondrocyte recovery to the original protocol (570 min), but it is one step less in manipulation and 150 min shorter in duration. These improvements make this "optimized" protocol possible to complete within one 8-hour work shift in tissue banks. This study provides useful knowledge for the design of practical, successful vitrification protocols to aid in the long-term storage of articular cartilage.

3.7 Supplemental Information

Supplemental Table 3.S1 Chondrocyte viability

Groups	Normalized chondrocyte viability (%) Mean ± SE		
	Original protocol	Optimized protocol	Minimally vitrifiable protocol
10 mm dowel; 15 ml tube	45.6 ± 4.4	64.4 ± 10.4	23.1 ± 8.6
10 mm dowel; 50 ml tube	61.9 ± 11.9	77.7 ± 3.7	28.5 ± 7.5
6.9 mm dowel; 15 ml tube	55.7 ± 11.5	77.3 ± 4.5	78.6 ± 6.4
6.9 mm dowel; 50 ml tube	62.5 ± 6.6	79.1 ± 3.5	54.2 ± 2.0

Supplemental Table 3.S2 Chondrocyte metabolic activity

Normalized chondrocyte metabolic activity (%) Mean ± SE							
10 mm dowel; 15 ml tube	**Day 1**	**Day 2**	**Day 3**	**Day 4**	**Day 5**	**Day 6**	**Day 7**
Original protocol	23.4 ± 16.7	26.3 ± 17.9	28.9 ± 20.5	32.7 ± 21.0	37.7 ± 23.6	44.4 ± 28.8	49.2 ± 29.1
Optimized protocol	29.0 ± 11.1	37.2 ± 12.7	50.1 ± 15.9	61.7 ± 19.5	79.5 ± 25.3	87.5 ±29.5	101.2 ± 35.2
Minimally vitrifiable protocol	-1.5 ± 1.6	0.9 ± 1.2	2.3 ± 1.0	3.3 ± 1.5	4.6 ± 1.7	6.9 ± 3.1	9.1 ± 3.2
10 mm dowel; 50 ml tube	**Day 1**	**Day 2**	**Day 3**	**Day 4**	**Day 5**	**Day 6**	**Day 7**
Original protocol	49.9 ± 12.4	55.5 ± 12.8	65.7 ± 15.0	76.3 ± 13.9	85.1 ± 13.3	97.8 ± 15.0	113.7 ± 16.7
Optimized protocol	13.5 ± 5.9	21.5 ± 7.5	31.1 ± 9.9	40.7 ± 12.2	56.6 ± 17.4	67.5 ± 21.7	80.4 ± 25.8
Minimally vitrifiable protocol	-3.8 ± 3.2	-1.9 ± 1.8	-0.7 ± 1.4	0.4 ± 1.9	0.6 ± 2.1	1.9 ± 2.7	2.4 ± 3.2
6.9 mm dowel; 15 ml tube	**Day 1**	**Day 2**	**Day 3**	**Day 4**	**Day 5**	**Day 6**	**Day 7**
Original protocol	27.3 ± 12.0	31.7 ± 12.4	38.3 ± 12.7	45.4 ± 16.2	53.4 ± 18.1	65.8 ± 23.4	79.5 ± 26.3
Optimized protocol	30.8 ± 7.0	40.1 ± 7.6	55.5 ± 8.4	71.9 ± 9.4	95.7 ± 12.3	112.7 ± 15.4	132.4 ± 18.1
Minimally vitrifiable protocol	30.8 ± 16.1	40.4 ± 19.0	52.3 ± 24.1	66.2 ± 30.7	88.1 ± 41.0	104.2 ± 47.0	125.4 ± 57.6
6.9 mm dowel; 50 ml tube	**Day 1**	**Day 2**	**Day 3**	**Day 4**	**Day 5**	**Day 6**	**Day 7**
Original protocol	28.1 ± 8.2	33.1 ± 9.4	42.0 ± 12.7	51.3 ± 14.0	61.0 ± 16.2	74.3 ± 19.7	91.6 ± 24.4
Optimized protocol	24.7 ± 10.1	36.1 ± 13.8	46.2 ± 16.6	62.3 ± 22.0	83.5 ± 28.7	96.9 ± 33.5	117.3 ± 40.4
Minimally vitrifiable protocol	0.7 ± 5.2	4.6 ± 4.5	7.9 ± 5.4	11.0 ± 7.9	15.6 ± 10.5	20.1 ± 13.9	29.4 ± 20.4

Chapter Four: Evaluation of five additives to mitigate toxicity of cryoprotectant agents on porcine chondrocytes

Authors: Kezhou Wu[a,d], Leila Laouar[a], Rachael Dong[a], Janet A. W. Elliott[b,c], Nadr M. Jomha[a*]

Affiliations:

[a]Department of Surgery, University of Alberta, Edmonton, Alberta, T6G 2B7, Canada

[b]Department of Chemical and Materials Engineering, University of Alberta, Edmonton, Alberta, T6G 1H9, Canada

[c]Department of Laboratory Medicine and Pathology, University of Alberta, Edmonton, Alberta, T6G 2R7, Canada

[d]Department of Orthopaedic Surgery, First affiliated hospital of Shantou University Medical College, Shantou, Guangdong, 515300, China

*Corresponding author. Address: 2D2.32 WMC Department of Surgery, University of Alberta Hospital, Edmonton, Alberta, Canada T6G 2B7, Fax: +17804072819. Email address: njomha@ualberta.ca (Nadr M. Jomha)

This chapter has been published in *Cryobiology* as: Kezhou Wu, Leila Laouar, Rachael Dong, Janet A. W. Elliott, and Nadr M. Jomha. "Evaluation of five additives to mitigate toxicity of cryoprotective agents on porcine chondrocytes." *Cryobiology* 88 (2019): 98-105. doi:10.1016/J.CRYOBIOL.2019.02.004.

4.1 Abstract

Cryoprotectant agents (CPAs) are used in cryopreservation protocols to achieve vitrification. However, the high CPA concentrations required to vitrify a tissue such as articular cartilage are a major drawback due to their cellular toxicity. Oxidation is one factor related to CPA toxicity to cells and tissues. Addition of antioxidants has proven to be beneficial to cell survival and cellular functions after cryopreservation. Investigation of additives for mitigating cellular CPA toxicity will aid in developing successful cryopreservation protocols. The current work shows that antioxidant additives can reduce the toxic effect of CPAs on porcine chondrocytes. Our findings showed that chondroitin sulfate, glucosamine, 2,3,5,6-tetramethylpyrazine and ascorbic acid improved chondrocyte cell survival after exposure to high concentrations of CPAs according to a live-dead cell viability assay. In addition, similar results were seen when additives were added during CPA removal and articular cartilage sample incubation post CPA exposure. Furthermore, we found that incubation of articular cartilage in the presence of additives for 2 days improved chondrocyte recovery compared with those incubated for 4 days. The current results indicated that the inclusion of antioxidant additives during exposure to high concentrations of CPAs is beneficial to chondrocyte survival and recovery in porcine articular cartilage and provided knowledge to improve vitrification protocols for tissue banking of articular cartilage.

Abbreviations:

AA: ascorbic acid; CPA: cryoprotectant agent; CS: chondroitin sulphate; DMEM: Dulbecco's Modified Eagle Medium; DMSO: dimethyl sulfoxide; EG: ethylene glycol; GlcN: glucosamine; PBS: phosphate buffered saline; PF-68: Pluronic F-68; PG: propylene glycol; TMP: 2,3,5,6-tetramethylpyrazine.

4.2 Introduction

Articular cartilage is a few-millimetres-thick tissue covering the bone end in articulating joints and it has very limited self-repair capacity[219]. Cartilage defects over 1 cm^2 often progress into osteoarthritis if not properly treated[33,100]. Cartilage allograft transplantation is an effective surgical procedure for large cartilage defects[86,87]; however, it is limited by the availability of fresh donor joint tissue. Cryopreservation of articular cartilage would enable banking of these tissues for clinical transplantation[3,30,113,114]. Vitrification, also called "ice-free" cryopreservation, is proven to be a useful method for long-term preservation of cells[30,42,113,187,198,261] and our group developed a working vitrification protocol for osteochondral tissue of human knee articular cartilage with promising chondrocyte recovery and cellular metabolic function[113]. Vitrification can be achieved by using high concentrations of cryoprotectant agents (CPAs) and a rapid cooling rate[30,69,113,185,187,198,218]. However, one of the major obstacles is toxicity of high concentrations of CPAs to cells[9,26,65,89,116]. Dimethyl sulfoxide (DMSO), ethylene glycol (EG), and propylene glycol (PG) are three CPAs commonly used in cryopreservation protocols[30,42,44,113,185,187,198,218]. These CPAs are toxic to cells when used at high concentrations[9,13,65,116]. There are several types of cell injury induced by CPAs, including membrane disruption and oxidative stress. Membrane disruption is induced by the high concentration of solutes outside the cell membrane, which is unavoidable in many current vitrification protocols[60,136,177]. Oxidative stress, an oxidative reaction between cells and CPAs, is one important toxic event during CPA loading[130,192,226,235]. Reducing oxidative reactions could improve cell recovery and benefit cryopreservation of cells and tissues[20,89,106,235]. To mitigate oxidative injuries, some researchers that employ vitrification have found that inclusion of antioxidant additives as supplements in the CPA loading solution can benefit cell viability after exposure to high concentrations of CPAs[32,40,89,106,130].

In the current study, five additive compounds including chondroitin sulphate (CS), glucosamine (GlcN), 2,3,5,6-tetramethylpyrazine (TMP), ascorbic acid (AA), and Pluronic F-68 (PF-68) were examined. Among these, four additives: CS[16,113], GlcN[11,229,251], TMP[71,120,143], and AA[14,45] were proven to be antioxidants in previous studies. However, their protective effects on porcine articular cartilage in multi-CPA cocktail solutions remain unknown. CS is a sulfated glycosaminoglycan composed of a chain of alternating sugars and is an important structural component of articular cartilage[75]. CS was used previously in a vitrification study of human articular cartilage by our group and shown to be beneficial to cell viability in the rewarmed cartilage[3,113]. GlcN is an amino sugar and is a precursor for glycosaminoglycan which is an important articular cartilage structural component[11,229]. GlcN has been proven to beneficially influence cartilage structure and to alleviate arthritis pain in clinics[102,229]. TMP is one of the alkaloids contained in *Ligusticum wallichii* and possesses anti-inflammatory and antioxidative activities[80,99,122] through inhibiting reactive oxygen species levels and increasing the antioxidant enzymes superoxide dismutase and catalase[80,88,238]. AA is an essential component in synthesis of collagen, a major component of cartilage extracellular matrix[14,45]. AA is a highly effective antioxidant, acting to lessen oxidative stress and is an enzyme cofactor for the biosynthesis of many important biochemicals[8,29,45,108,183]. All these effects of CS, GlcN, TMP, or AA could decrease the severity of CPA oxidation effects on chondrocytes. Although PF-68 is not reported to be antioxidative; it is a non-ionic surfactant reported to be effective in maintaining cell membrane integrity which could reduce the disruption of chondrocyte cell membranes[82]. Oxidative stress on chondrocytes may lead to cell death, followed by degradation of the extracellular skeleton and structural collagen[92,256]. Elimination of oxidative stress has been proven to be beneficial to the cryopreservation of cells and tissues[16,32,40,130,226],

because oxidation is one major reaction that can cause cell death. The objective of this study was to evaluate chondrocyte recovery after using these five additives during CPA exposure and removal. In this study, we hypothesized that the inclusion of additives could provide cell protection through the antioxidation effects on chondrocytes and by mitigating CPA toxicity due to the high concentration of CPAs. Investigating the effects of additives will aid in the development of successful vitrification protocols for articular cartilage.

4.3 Materials and Methods

4.3.1 Study design

This study investigated the protective effects of several additives on articular cartilage chondrocytes after CPA exposure at specified temperatures determined by a CPA loading protocol (see Table 4.1). In this study, we evaluated the effects of five additive compounds in a stepwise multi-temperature, multi-CPA addition protocol[3,113] using sexually mature porcine articular cartilage as a model. The objective of this study was to assess the abilities of these additives to mitigate chondrocyte cell toxicity during the exposure to high concentrations of CPAs at temperatures down to −10 °C, the final CPA loading temperature that would be used in a vitrification protocol before plunge cooling in liquid nitrogen.

Table 4.1 Table of variables

Study	Additives	When Added	Source	Cell viability Assessment Timepoint	Goals of Study
Experiment 1	1. CS 2. GlcN 3. TMP 4. AA 5. PF-68 6. Control	CPA exposure	Pooled	1. t_1: Cell viability after CPA exposure followed by CPA removal 2. t_3: Cell viability after 4-day DMEM incubation	Compare effects of additives during CPA exposure to control with no additive
Experiment 2	1. AA 2. TMP	1. CPA exposure 2. CPA removal 3. DMEM incubation	1. Early Source 2. Late Source	1. t_1: Cell viability after CPA exposure followed by CPA removal 2. t_2: Cell viability after 2-day DMEM incubation 3. t_3: Cell viability after 4-day DMEM incubation	1. Compare effects of sources 2. Compare effects of adding additive during CPA removal and DMEM incubation 3. Compare effects of 2-day incubation and 4-day incubation

4.3.2 Sample source and preparation

Hind legs with joints from sexually mature pigs aged over 54 weeks were obtained from 2 locations, a slaughter house in Wetaskiwin, Canada (Early Source), and from a deli store located in Edmonton, Canada (Late Source) (66 porcine hind legs resulting in 132 condyles were used in total). All joints were from meat-processing plants and no animals were specifically euthanized for this research. The joints from these two places were labelled as Early Source (< 6 hours post slaughter) and Late Source (> 24 hours post slaughter) based on the sample collection times after slaughtering. Porcine joints from the Early Source were harvested and immersed in phosphate buffered saline (PBS) immediately then transported to the research laboratory within 6 hours on the same day, while joints from the Late Source were hung for 24 hours after slaughtering in the butchery and stored in a 4 °C fridge before transportation to the laboratory. All joints were immersed in PBS prior to dissection. An electric saw was used to split the condyles from the femora and all condyles with approximately 20 mm thick bone base were cleaned by incubation in sterile PBS plus antibiotics [100 units/ml penicillin, 100 µg/ml streptomycin and 0.25 µg/ml amphotericin B (Gibco)] for 15 minutes under a biological safety cabinet. Condyles were randomly divided into the different experimental groups and incubated overnight in a complete medium plus antibiotics [DMEM complete: Dulbecco's Modified Eagle Medium F12 (Gibco) supplemented with 10% heat-inactivated Fetal Bovine Serum, 100 units/ml penicillin, 100 µg/ml streptomycin, 0.25 µg/ml amphotericin B and 1 mM sodium pyruvate] at 4 °C for less than 24 hours prior to CPA exposure.

4.3.3 Cryoprotective agent cocktail solutions preparation

Three fresh CPA cocktail solutions in DMEM were prepared the same day of the experiment into 175 ml final volume using the following concentrations of CPAs (M = molar): Solution One [3 M DMSO + 3 M EG], Solution Two [3 M DMSO + 3 M EG + 3 M PG], and Solution Three [3 M DMSO + 3 M EG + 1 M PG]. Additives were added to the CPA cocktail solutions based on preset experimental conditions (see Experimental design). All the CPA cocktail solutions were stirred vigorously at 4 °C using an electronic stirrer for 30 minutes, then cooled to the desired temperature before starting CPA exposure (Solution One at 0 °C, Solution Two at −10 °C, and Solution Three at −10 °C).

4.3.4 Stepwise CPA exposure protocol

A stepwise CPA exposure protocol with multiple CPAs added at progressively lower temperatures was used to mimic CPA-toxicity-minimizing strategies according to our group's previous research[9,65,89,116]. All condyles were paired and incubated stepwise in the three 175 ml CPA cocktail solutions: Solution One at 0 °C for 90 min, followed by Solution Two, at −10 °C for 90 min, and last in Solution Three at −10 °C for 130 min, then washed with 175 ml DMEM with or without additives at 4 °C for 45 min for CPA removal, then incubated with 100 ml DMEM with or without additives at 4 °C. Chondrocyte viability was assessed at four different time points: t_0 = after overnight incubation before CPA exposure (fresh control), t_1 = after the 3rd step CPA exposure followed by CPA removal in DMEM, t_2 = after 2 days incubation at 4 °C post CPA removal, and t_3 = after 4 days incubation at 4 °C post CPA removal (See Fig. 5.1). Percent cell

viability in each experimental sample was normalized to the percent cell viability of its own fresh control at t_0.

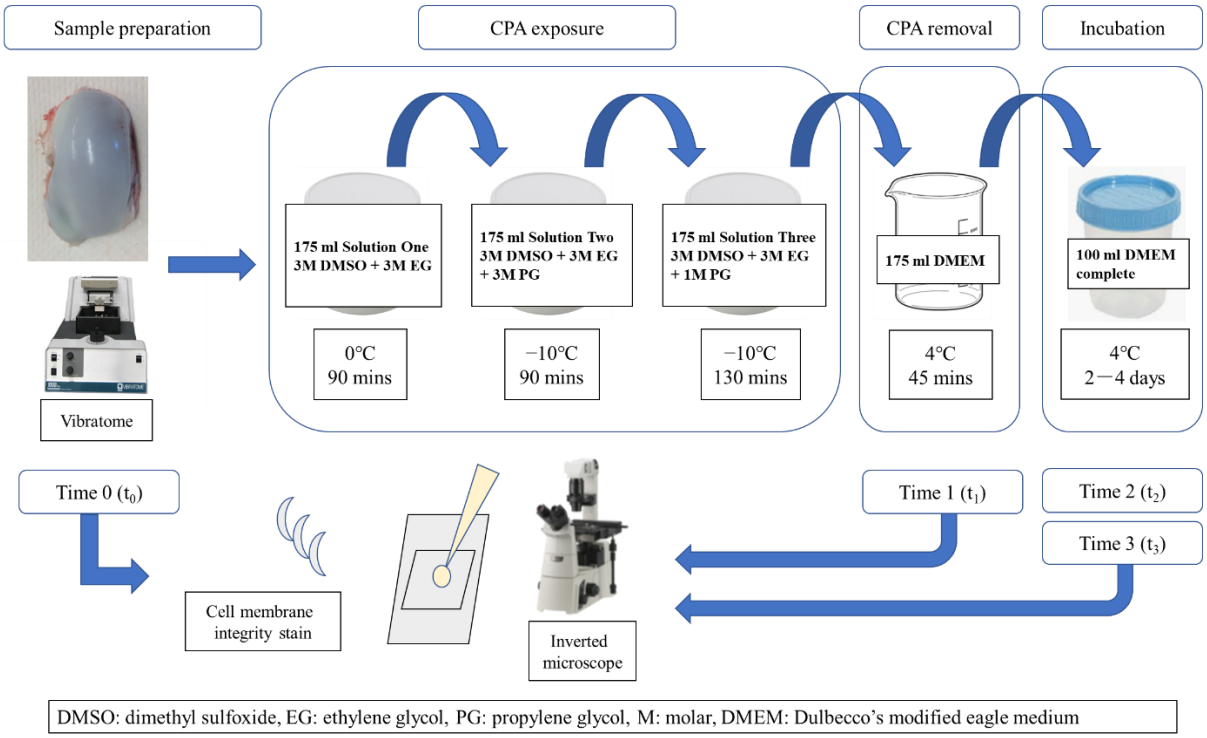

Figure 4.1 Description of multi-CPA stepwise exposure protocol: Chondrocyte viability of each condyle was determined by cell membrane integrity prior to any CPA exposure procedures (t_0). Subsequently, the condyle was incubated in 175 ml of Solution One at 0 °C on ice and water for 90 minutes with shaking. Then the condyle was quickly taken out from Solution One and excess CPA surrounding the condyle was removed using paper towels. The condyle was then moved to 175 ml of Solution Two held in a stirred alcohol bath at −10 °C for 90 minutes, then removed quickly, dried and moved to 175 ml of Solution Three at −10 °C for 130 minutes. After the three steps of CPA loading, the condyle was washed in 175 ml DMEM with shaking for 45 min for CPA removal (t_1). Condyles were then incubated in 100 ml sterile DMEM complete for 2 days (t_2) to 4 days (t_3) at 4 °C.

4.3.5 Experimental design

Experiment 1: Chondrocyte viability in experimental groups exposed to CPA solutions supplemented with additives compared to a control group exposed to CPA solutions without additives.

The objective of this experiment was to compare the effects of five additives, when added during the three-step CPA exposure, followed by CPA removal and a 4-day incubation without the presence of additives in the removal and incubation solutions. Porcine condyles were randomly divided into six groups (dissected joints from the two sources were pooled together, n = 14 condyles for each group). CPA cocktail solutions were prepared as described previously. Five additives were investigated separately in this study: 0.1 mg/ml CS (Sigma-Aldrich, St. Louis, Missouri), 400 μM GlcN (Medisca Pharmaceutique Inc., St-Laurent, Quebec), 400 μM TMP (Sigma-Aldrich, St. Louis, Missouri), 2000 μM AA (Sigma-Aldrich, St. Louis, Missouri), 0.1% PF-68 (vol/vol) (Gibco, Grand Island, New York), and compared with a control group exposed to CPA without additive. After the three-step CPA exposure for CPA permeation, condyles were washed in DMEM alone without additives for 45 min at 4 °C with shaking to remove the CPAs. A time of 45 min was expected to remove the majority of CPA based on our group's previous research[257]. Chondrocyte viability was measured at three time points: before CPA exposure (t_0), after the 3rd step CPA exposure followed by CPA removal in DMEM (t_1), and after 4 days incubation at 4 °C post CPA removal (t_3).

Experiment 2: Chondrocyte viability determination by tissue freshness and the effects of AA and TMP when added during CPA exposure, removal, and DMEM incubation.

The first objective of this experiment was to compare chondrocyte viability after CPA exposure in porcine condyles obtained from two sources. The second objective was to study the effect of TMP and AA separately during the CPA exposure period, post removal and after incubation for 2 and 4 days. Porcine joints collected from both the Early Source and the Late Source were dissected separately and condyles from the same source were randomly divided into four groups (n = 6 condyles for each group). In the AA +/− group, 2000 μM AA was added during CPA exposure but not during CPA removal or incubation. In the AA +/+ group, 2000 μM AA was added during CPA exposure, as well as during CPA removal and incubation. In the TMP +/− group, 400 μM TMP was added during CPA exposure but not during CPA removal or incubation. In the TMP +/+ group, 400 μM TMP was added during CPA exposure, as well as during CPA removal and incubation. Chondrocyte viability was measured at four time points: before CPA exposure (t_0), after the 3rd step CPA exposure followed by CPA removal in DMEM (t_1), after 2 days incubation (t_2), and after 4 days incubation at 4 °C post CPA removal (t_3).

4.3.6 Chondrocyte viability assessment

Eighty-five-μm-thick cartilage slices were cut from each condyle using a vibratome-1500 (The Vibratome Company, St. Louis, MO) filled with 500 ml pre-cooled PBS at 4 °C. Chondrocyte viability within slices was assessed by measuring cell membrane integrity with a dual stain using a fluorescent live cell nucleic acid stain (Syto 13; Molecular Probes) which is a cell permeant dye and propidium iodide (PI; Sigma) which is a membrane-impermeant dye that penetrates only into cells with disrupted cell membranes [6.25 μM Syto 13 and 15.0 μM PI mixed in PBS]. After collecting slices, the remaining condyles were removed from the vibratome and washed with sterile PBS plus antibiotics for 15 minutes under sterile conditions, then stored in sterile DMEM

complete (see sample source and preparation) at 4 °C until the next imaging time point. Slices were gently placed on glass slides and patted dry with Kimwipes. Each slice was overlaid with approximately 50 µl of stain mixture and covered with a coverslip, then incubated in the dark for 10 min. All slices were viewed under a Nikon inverted fluorescent microscope (model: ECLIPSE Ti-5) and imaged using a Nikon digital camera (model: DS-Fi2). The dual filters used to image all the slices in this study had the following spectra peak maxima: Excitation/Emission: 488 nm/503 nm and 535 nm/617 nm. Chondrocyte viability within slices was determined by counting the numbers of green-stained (viable) cells and red-stained (non-viable) cells, using a custom-made software Viability 3.2[111].

4.3.7 Data analysis

All data were analyzed using SPSS 20.0 software. A minimum 85% absolute cell viability in the fresh controls before CPA exposure (t_0 cell viability) was used as the inclusion criterion to identify healthy tissue samples. Normalized cell viability of the experimental samples was determined according to the following formula:

$$\text{Normalized cell viability (\%)} = \frac{\text{\% green cells after CPA exposure or DMEM incubation}}{\text{\% green cells before CPA exposure}} \times 100\%$$

The numerical data are presented as the means ± SE. The p values are reported in the figure legends. In general, statistical significance in all the figures was indicated with asterisks respectively: * indicates $p < 0.05$, ** indicates $p < 0.01$, *** indicates $p < 0.001$. The equality of variance for variables was determined by Levene's test before multiple comparisons. The analysis of variance (ANOVA) with *post hoc* tests (Tukey test for multiple comparisons), paired t-tests and two-tailed

independent t-tests were performed on sample cell viability under different experimental conditions depending on the sample configuration.

4.4 Results

4.4.1 Gross appearance of articular cartilage before and after CPA exposure and chondrocyte viability

All condyles were harvested from porcine stifle joints. All condyles were removed from the porcine femur with an electric saw, then allocated into different experimental groups randomly. Healthy condyles had a smooth and white hyaline cartilage surface (Fig. 4.2A). Fluorescent microscopy on slices from fresh healthy articular cartilage showed most chondrocytes stained green indicating viable cells (Fig. 4.2B). However, when cartilage was exposed to CPA, a percentage of chondrocytes were stained red indicating cell death due to cell toxicity during CPA exposure (Fig. 4.2C). All samples with fresh control cell viability < 85% were excluded from this study to screen out unhealthy donors. The chondrocyte viability of the included condyles prior to CPA exposure ranged from 85 to 99 %.

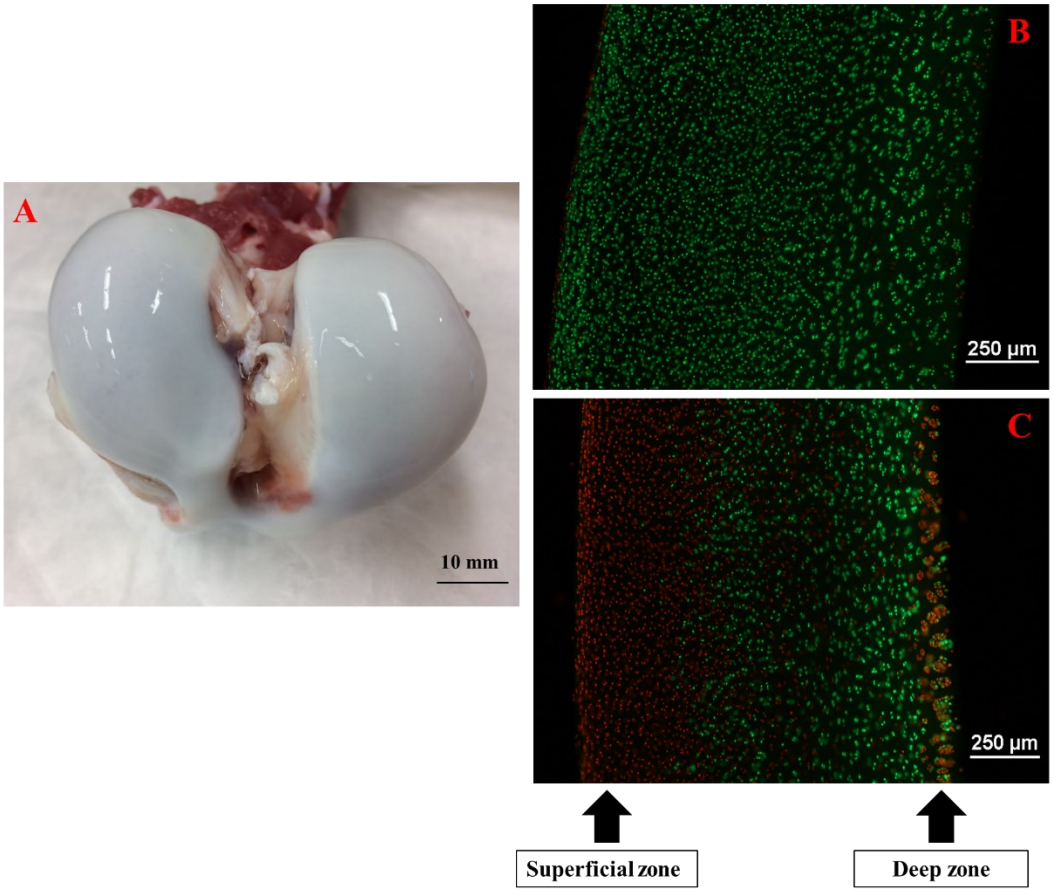

Figure 4.2 Gross appearance of the condyle morphology and chondrocyte viability based on Syto 13/PI membrane integrity staining: (A) In the fresh control condyles of porcine femora, the cartilage was smooth and intact; (B) In the fresh control condyle, fluorescent microscopy imaging of an 85-µm-thick slice showed mostly viable chondrocytes that stained green (Cross section, from left to right are the superficial to deep zones of articular cartilage, 100×); (C) In an experimental condyle exposed to CPAs, a percentage of cells died during CPA exposure, and dead cells were stained red (Cross section, from left to right are the superficial zone to deep zone of articular cartilage, 100×).

4.4.2 Chondrocyte viability assessment results

Experiment 1: Comparison of chondrocyte viability in experimental groups exposed to CPAs with additives to that of a control group exposed to CPA without additives.

Cartilage slices from condyles exposed to CPA solutions with additives showed significantly higher chondrocyte viability in TMP, AA, CS, and GlcN groups when compared to the control group exposed to CPA without additives (Fig. 4.3A). The TMP treated group showed the highest chondrocyte viability after CPA exposure followed by CPA removal (76.4 ± 9.1%) (Fig. 4.3A). After 4-day incubation in DMEM complete, chondrocyte viability in the CS and GlcN treated groups was significantly higher than the control group as shown in Fig. 3B. The CS treated group had the highest chondrocyte viability after incubation for 4-day post CPA removal (74.5 ± 10.7%) (Fig. 4.3B). However, the chondrocyte viability after 4-day incubation in TMP and AA groups was significantly lower when compared to the chondrocyte viability under the same conditions after CPA exposure followed by CPA removal (Fig. 4.3C).

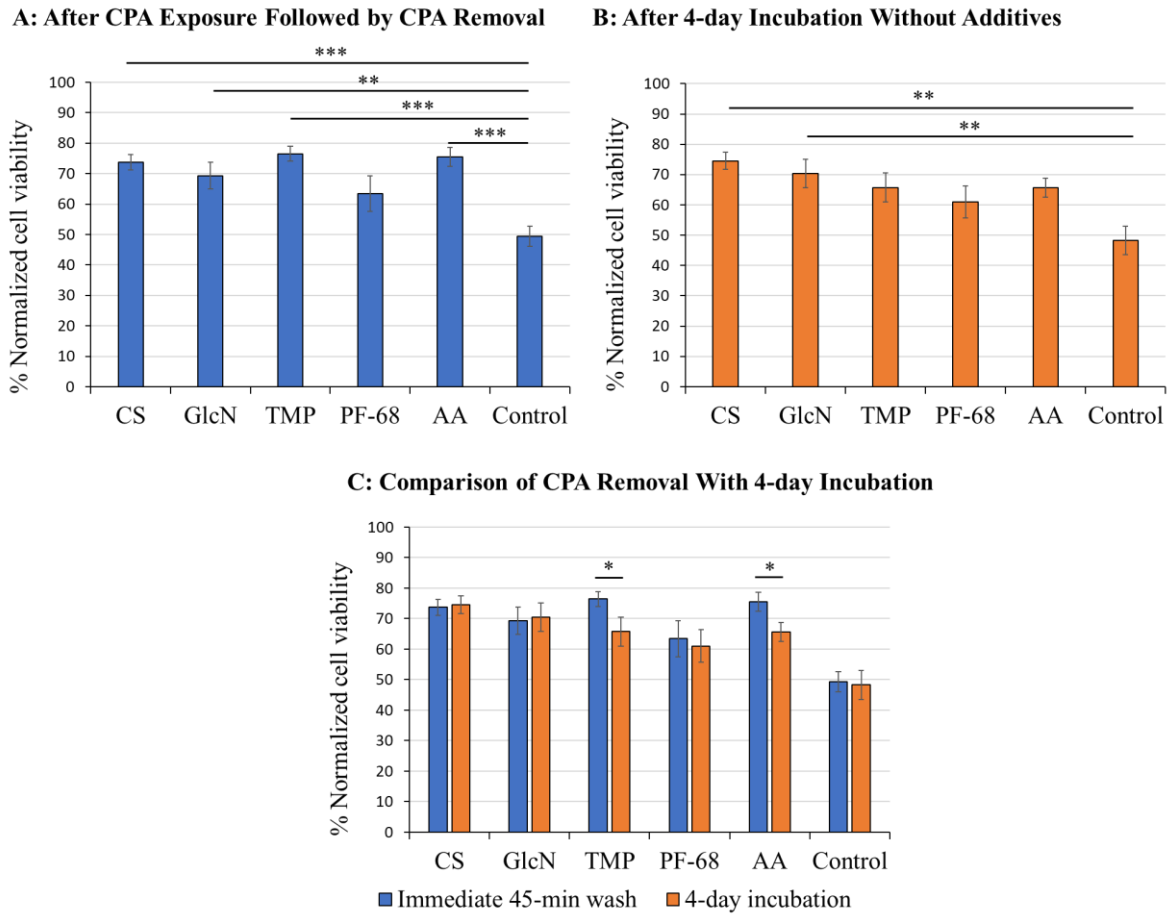

Figure 4.3 Chondrocyte viability in experimental groups exposed to CPAs with additives with results for the control group exposed to CPA without additives: Condyles from the two sources were mixed (n = 14). Condyles were exposed to the stepwise CPA protocol using five additives separately (CS: 0.1mg/ml; GlcN: 400µM; TMP: 400 µM; PF-68: 0.1% vol/vol; AA: 2000 µM) and a control group without additive. Condyles were then washed in DMEM alone for CPA removal and incubated in DMEM complete without additive.

(A): After CPA exposure followed by CPA removal, chondrocyte viability was significantly higher in TMP, AA, CS, and GlcN groups compared to the control group ($p_{CS\text{-}Control} < 0.001$, $p_{GlcN\text{-}Control} = 0.005$, $p_{TMP\text{-}Control} < 0.001$, $p_{AA\text{-}Control} < 0.001$);

(B): After 4-day incubation in DMEM complete, chondrocyte viability was significantly higher in CS and GlcN groups compared to the control group ($p_{CS\text{-}Control} = 0.001$, $p_{GlcN\text{-}Control} = 0.007$);

(C): After 4-day incubation in DMEM complete, chondrocyte viability in TMP and AA groups were significantly lower compared to immediately after CPA exposure followed by CPA removal ($p_{TMP} = 0.025$, $p_{AA} = 0.019$).

Experiment 2: Chondrocyte viability determination by tissue freshness and the effects of AA and TMP when added during CPA exposure, removal, and DMEM incubation.

After exposure to CPA cocktail solutions supplemented with 2000 μM AA or 400 μM TMP, chondrocyte viability was significantly higher in the AA +/− group from the Early Source when compared to those obtained from the Late Source (Fig. 4.4A). After 2-day and 4-day incubation of condyles in DMEM complete without additives, both AA +/− groups and TMP +/− groups showed significantly higher chondrocyte viability in condyles from the Early Source when compared to those from the Late Source (Fig. 4.4A). The inclusion of AA in the DMEM wash solution during CPA removal significantly improved chondrocyte viability in AA +/+ group condyles from the Late Source compared to AA +/− group condyles from the Late Source washed without AA (Fig. 4.4B). When TMP or AA was added only during CPA exposure, condyles in the TMP +/− group from the Early Source, or condyles in the AA +/− group from the Late Source, showed significantly higher chondrocyte viability after 2-day incubation than that after 4-day incubation (Fig. 4.4C). When AA was added during the CPA removal and DMEM incubation, condyles in AA +/+ group from both the Early Source and the Late Source showed significantly higher chondrocyte viability after 2-day incubation than that after 4-day incubation (Fig. 4.4C). When incubating condyles for

4 days, condyles from the Late Source incubated with AA or TMP showed a significantly higher chondrocyte viability than those incubated without AA or TMP respectively (Fig. 4.4C).

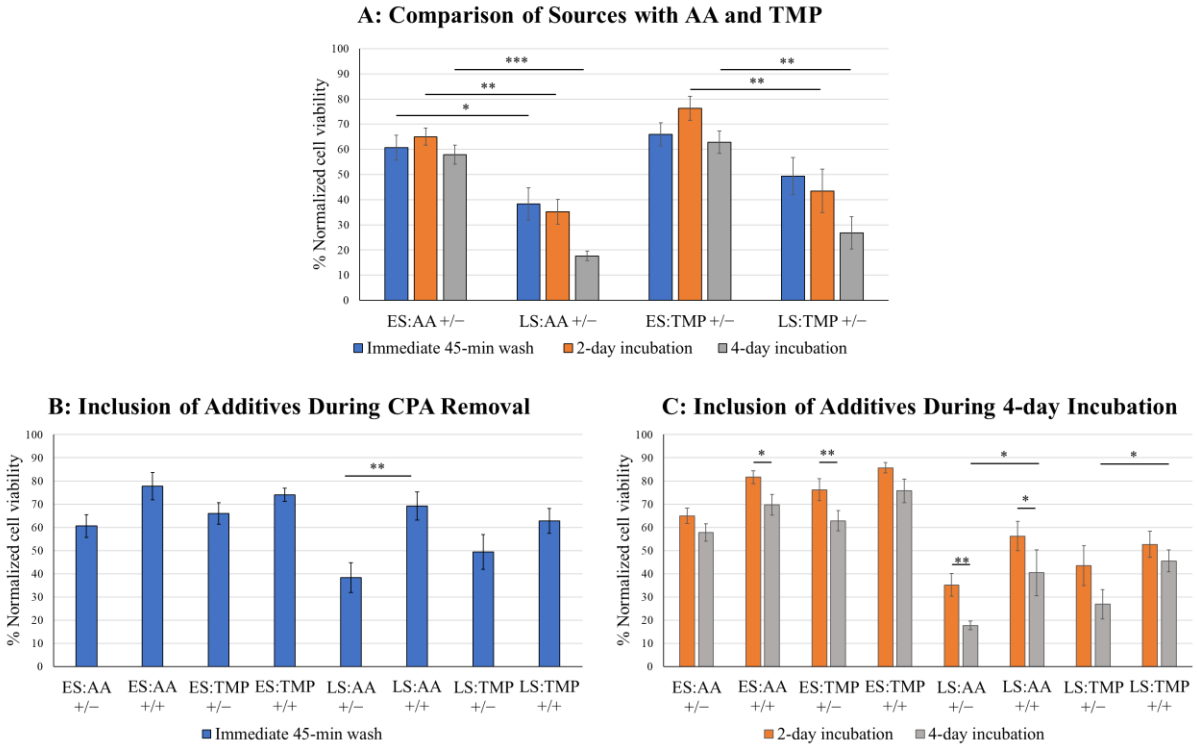

Figure 4.4 Chondrocyte viability determination by tissue freshness and the effects of AA and TMP when added during CPA exposure, removal, and DMEM incubation: Four groups (AA +/−, AA +/+, TMP +/−, and TMP +/+, n = 6) were set with condyles from the **Early Source** (ES) and the **Late Source** (LS). In group AA +/—, 2000 μM AA was added during CPA exposure only; in group AA +/+, 2000 μM AA was added during CPA exposure, CPA removal, and DMEM incubation. In group TMP +/−, 400 μM TMP was added during CPA exposure only; in group TMP +/+, 400 μM TMP was added during CPA exposure, CPA removal, and DMEM incubation.

(A): After CPA exposure followed by CPA removal, the AA +/− group showed a significantly higher chondrocyte viability in condyles obtained from the Early Source compared to those obtained from the Late Source ($p_{AA\text{-}45min}$ = 0.02). After 2 and 4-day incubation, chondrocyte

viability was significantly higher in the Early Source condyles treated with AA +/− or TMP +/− compared to the Late Source condyles ($p_{AA\text{-}2day} = 0.001$, $p_{AA\text{-}4day} < 0.001$, $p_{TMP\text{-}2day} = 0.008$, $p_{TMP\text{-}4day} = 0.001$);

(B): When AA was added during CPA removal, chondrocyte viability was significantly higher in the AA groups of the Late Source condyles ($p_{LS\text{-}AA} = 0.006$);

(C): During the condyle incubation with or without AA or TMP, chondrocyte viability was significantly higher in condyles incubated for 2 days when compared to those incubated for 4 days ($p_{ES:AA+/+} = 0.012$, $p_{ES:TMP+/-} = 0.004$, $p_{LS:AA+/-} = 0.007$, $p_{LS:AA+/+} = 0.038$); After the 4-day incubation, chondrocyte viability was significantly higher in condyles from the Late Source incubated with AA or TMP when compared to those incubated without AA or TMP ($p_{AA\text{-}4day} = 0.049$, $p_{TMP\text{-}4day} = 0.040$).

4.5 Discussion

The main goal of this study was to investigate the effect of five additives on chondrocyte viability after exposure to high CPA concentrations. We hypothesized that CPA toxicity is linked to oxidative stress, which is induced during the exposure of cells to the CPAs. We firstly investigated the effects of CS, GlcN, TMP, AA and PF-68 on chondrocyte viability in full porcine condyles during exposure to high concentrations of CPAs. Condyles exposed to the stepwise CPA cocktail solutions supplemented with additives (CS, GlcN, TMP, or AA) showed higher chondrocyte viability compared to condyles in the control group exposed to CPA solutions without additives (Fig. 4.3B). Our findings showed decreased chondrocyte damage after CPA exposure in the presence of additives which confirmed the beneficial effect of these additives (CS, GlcN, TMP, or

AA) during tissue exposure to high concentrations of CPAs. Cryopreservation has been proven to induce oxidative stress on the target cells both intracellularly and extracellularly during the freeze–thawing procedures[40,130,226]. Oxidative stress is one factor related to CPA toxicity that may aggravate cell sensitivity to high concentrations of CPA. The improvement in chondrocyte recovery of this study may be due to the antioxidative capacities of these compounds and this finding is consistent with previously reported work on the protective effects of antioxidants in cryopreservation[20,29,32,77,89,113,183]. However, unlike CS, GlcN, TMP, or AA, the use of PF-68 group did not statistically benefit chondrocyte viability. PF-68 is a non-ionic surfactant known to protect chondrocytes from shear stress on cell membranes[82]. In this study, PF-68 did not have a beneficial effect, possibly due to low permeation of PF-68 into the articular cartilage matrix. Another variable investigated was 4-day incubation post CPA exposure. The high cell recovery after the 4-day incubation in medium post exposure to CPA plus additives in treated groups showed that chondrocytes remained at a higher survival rate compared to the control non-treated group (*i.e.* no additives) (Fig. 4.3C). Interestingly, the chondrocyte viability was significantly lower after 4-day incubation in DMEM complete without additives in groups treated with TMP or AA (Fig. 4.3C) when compared to their own chondrocyte viability immediately after CPA removal. The underlying mechanism of this cell loss may be due to the therapeutic effect timeframe of these two antioxidants (TMP and AA) as the additives were not present in the 4-day incubation solution. Further research on the compounds' half-life elimination would help to understand their effects.

We investigated sample freshness that may be a factor in cell recovery after CPA exposure. For instance, the stifle joints received from the Early Source were harvested from pigs soon after the animal was slaughtered and transported directly to our lab within 4–6 hours of death. Alternatively,

joints received from the Late Source were harvested by meat plant employees and kept at 4 °C for 24 hours in the fridge before the stifle joints were transported to our lab. Although the chondrocyte viability from both sources indicated a high cell membrane integrity (85–99%) before CPA exposure, the ability of chondrocytes to tolerate oxidative stress might be different. Subsequent investigation (Fig. 4.4A) documented that chondrocytes in fresher condyles obtained from the Early Source tolerated CPA exposure better than those obtained from the Late Source, with a significantly higher chondrocyte viability after CPA exposure. CPAs may be falsely assumed to be toxic to the cells if cell membranes were breached or damaged due to time after death factors, or if enzyme function was impaired for other reasons[26,60]. We extended our work to the inclusion of additives during CPA removal and DMEM incubation using the two most promising additives—TMP and AA as per our current findings. Supplementation of media with additives during CPA removal and DMEM incubation improved chondrocyte recovery (Fig. 4.4B-C). A previous study using different concentrations of TMP demonstrated that TMP could inhibit interleukin-1β-induced iNOS expression and nitric oxide synthesis (NOS) in rabbit articular chondrocytes[99], while nitric oxide oxidation was one important reaction in the development of cartilage degradation during experimental osteoarthritis and chondrocyte apoptosis[92,120]. Possible mechanisms of TMP and AA include antioxidant effects that might aid cell robustness during CPA exposure. Moreover, Yang *et al.*[253] reported a protective effect of TMP on oxygen and glucose deprivation induced brain microvascular endothelial cell injury *via* the Rho/Rho-kinase signaling pathway. Wang *et al.*[238] found that TMP could protect against glucocorticoid-induced apoptosis by promoting autophagy in mesenchymal stem cells and improve bone mass in glucocorticoid-induced osteoporosis in rats. Johnson *et al.*[108] reported AA could reduce DNA damage in H_2O_2-treated human adipose-derived mesenchymal stem cells, and Alam *et al.*[8] discovered that AA could

prevent protein aggregation into oligomers and fibrils by inhibiting human insulin aggregation, and further protects against amyloid induced cytotoxicity. The higher chondrocyte viability in the AA and TMP groups indicates that these compounds are more likely to have a clinically significant effect and are good candidates for inclusion in cryopreservation protocols for cell preservation.

In addition, we investigated the effects of 2-day incubation vs 4-day incubation. The chondrocyte viability after incubation for 2 days was higher than that after incubation for 4 days (Fig. 4.4C). This is partially consistent with a study by Hahn *et al.*[89] that reported that TMP had a significant beneficial effect on chondrocyte viability after exposure to 1.6 M glycerol also after a 2-day incubation period. That study did not test the 4-day incubation period. There is a concern that chondrocyte apoptosis may be the cause of the 4-day cell recovery decline and further investigation may confirm this. From the clinical perspective, it is possible that transplantation within the 2-day time frame after warming from vitrification would provide the cells the optimal environment for recovery.

4.6 Conclusions

CS, GlcN, TMP, or AA had a significant beneficial effect on chondrocyte viability after exposure to high concentrations of CPA. Fresh tissue contributed to higher cell recovery after CPA exposure and should be regarded as one factor in future experiments. CPA removal and incubation of condyles with the preferred additives (TMP or AA) improved chondrocyte recovery. Chondrocytes from articular cartilage incubated for a 2-day period had higher chondrocyte viability compared to chondrocytes from articular cartilage incubated for a 4-day period. Overall, using additives was

beneficial for achieving higher chondrocyte viability after exposure to high CPA concentrations and this may be beneficial when developing cryopreservation protocols for articular cartilage in future research.

Chapter Five: Removing the surrounding vitrification solution is advantageous for vitrification of articular cartilage

Authors: Kezhou Wu[a,b], Leila Laouar[a], Janet A. W. Elliott[c,d], Nadr M. Jomha[a]*

Affiliations:

a. Division of Orthopedic Surgery, Department of Surgery, University of Alberta, Edmonton, AB, Canada

b. Department of Orthopedic Surgery, First affiliated hospital, Shantou University Medical College, Shantou, Guangdong, China

c. Department of Chemical and Materials Engineering, University of Alberta, Edmonton, AB, Canada

d. Department of Laboratory Medicine and Pathology, University of Alberta, Edmonton, AB, Canada

***Corresponding Author:** Nadr M. Jomha, address: 2D2.32 WMC, Division of Orthopedic Surgery, Department of Surgery, University of Alberta Hospital, Edmonton, Alberta, Canada T6G 2B7, Fax: +17804072819. Email address: njomha@ualberta.ca

5.1 Abstract

Background: Vitrifying articular cartilage for long-term storage will increase its availability for surgical repair of cartilage defects. For successful vitrification, a sufficient amount of cryoprotectant (CPA) needs to permeate into the cartilage tissue. After CPA permeation, cartilage tissue is usually kept in a high concentration CPA solution for vitrification below −130 °C. However, warming cartilage tissue from a vitrified glass is time-consuming and can cause cell damage if handled improperly, especially for larger cartilage samples (e.g., intact femoral condyle).

Hypothesis: We hypothesized that articular cartilage can be successfully vitrified and stored in liquid nitrogen once sufficient concentrations of CPA have permeated into the articular cartilage even if the surrounding vitrification solution has been removed before plunging into liquid nitrogen.

Study design: Controlled laboratory study.

Methods: Dimethyl sulfoxide, ethylene glycol, and propylene glycol were loaded using an optimized 7-hour stepwise protocol for appropriate CPA permeation into porcine cartilage tissue before vitrification. We compared two methods for storing cartilage tissue (10-mm diameter osteochondral dowels or full femoral condyles) at −196 °C after CPA permeation: (a) storage in a container surrounded by vitrification solution *vs* (b) storage in a vacuumed bag without a surrounding vitrification solution.

Results: Our results show no significant differences in chondrocyte survival in the 10-mm diameter porcine osteochondral dowels after vitrification with or without the surrounding CPA. Importantly, chondrocyte survival was significantly higher in porcine full femoral condyles after vitrification without the surrounding CPA compared with those with the surrounding CPA due to faster cooling/warming rates without the surrounding CPA solution being more important for the

large volume of tissue. Moreover, articular cartilage fractures were identified in those full femoral condyles vitrified with a surrounding vitrification solution.

Conclusion: An optimized 7-hr CPA permeation protocol was successful in vitrifying full femoral condyles of porcine articular cartilage grafts. Removing the surrounding vitrification solution is advantageous for the vitrification outcomes of articular cartilage of large sizes.

Clinical relevance: This is the first report on vitrification of articular cartilage grafts using full knee condyles. Our findings provide a novel method to store vitrified articular cartilage tissue and will aid in the development of vitrification protocols for intact human articular cartilage.

5.2 Introduction

Articular cartilage defects are a common injury treated in orthopaedic clinics around the world[35,98]; defects can develop into osteoarthritis without proper intervention or treatment, especially in young and active adults who often suffer from acute trauma to the knee[34,98]. Osteochondral allografting has proven to be an effective surgical procedure to treat articular cartilage defects[37,100,227]. Depending on the size of the articular cartilage defect, the procedure requires grafts that range from small to large pieces of osteochondral tissue. Fresh articular cartilage grafts can be stored up to 28 days and may not be delivered to patients in the operating room in time due to the long time frame of surgical preparation such as regulatory clearance for infectious disease testing, graft size matching, patient preparation, and arrangement of a surgical suite[84,121,242,243]. The short storage period of fresh articular cartilage grafts and the absence of chondrocyte survival and matrix distortion in frozen grafts[37,121] makes the long term preservation of large articular cartilage

grafts very important. Unfortunately, this has been a difficult challenge over the past fifty years. Successful cryopreservation of articular cartilage can increase the availability of articular cartilage allografts as an alternative transplantation source to treat large articular cartilage defects in clinical practice.

Cryopreservation by vitrification has been reported to preserve small articular cartilage grafts such as rabbit[218], porcine[30,248], and human[113] osteochondral grafts with a size from 3-mm to 10-mm diameter, and up to 12 cm^2. However, vitrification of full knee condyles has not yet been reported in the literature, and this is important because of the potential for surgical repair of large articular cartilage defects[3,113]. In current practice, a sufficient amount of CPA needs to be permeated into the articular cartilage for successful vitrification (see Fig. 5.1)[113]. CPA permeation is the essential step to avoid ice formation in the articular cartilage matrix during the cooling/warming processes of vitrification[30,110,113,178]. The development of CPA permeation protocols can be optimized using mathematical modelling. Nadia Shardt from our group developed an optimized 7-hr stepwise CPA permeation protocol for articular cartilage with 2-mm thickness[208], and the experimental results confirmed the efficiency of this protocol for 10-mm diameter porcine osteochondral dowels with a promising chondrocyte survival of approximately 75%[248]. Since our CPA permeation approach leads to a vitrifiable concentration of CPAs throughout the cartilage tissue and this has been successful in smaller osteochondral tissue fragments[208], it is of essential to document its effectiveness on a larger scale of articular cartilage tissue, e.g., full femoral condyles.

Sample packaging size is another critical factor in vitrification procedures. Vitrification of full femoral condyle articular cartilage is challenging due to its large volume. Following the CPA

permeation, articular cartilage is usually kept in a high concentration CPA solution[30,113,248] and plunged into liquid nitrogen at −196 °C for vitrification. The requirement of storing articular cartilage tissue in extra CPA solution for vitrification has not been investigated. Scaling up the vitrification process for increased tissue size faces the challenge of decreased cooling and warming rates. The long time required to warm articular cartilage from a large vitrified glass (e.g., intact femoral condyle surrounded by a correspondingly large amount of vitrification solution) from −196 °C to 37 °C may affect the chondrocyte survival due to devitrification[239]. In addition, another problem associated with vitrifying large samples is the non-uniform temperature throughout the sample during cooling and warming[196,216], which can cause tissue cracks or fractures[188]. Kroener and Luyet[134] reported observations of glycerol solution forming cracks during the vitrification process. Stolberg-Stolberg *et al.*[223] showed that fractures in cartilage allograft can increase the release of inflammatory makers that further impact the chondrocyte metabolic activity and viability *via* apoptosis. Tissue cracking caused by inhomogeneous thermal expansion of the glassy CPAs around the sample is an unsolved problem. Removing the surrounding CPAs from the tissue before storage in liquid nitrogen may be an appropriate approach to mitigate the cracking effect for the vitrification of large tissues.

Using additives to protect cells from exposure to CPAs is another approach to improve cryopreservation protocols[89]. Chondroitin sulphate was used as an additive for the vitrification of both human[113] and porcine[248] articular cartilage to protect chondrocytes from the toxic effects of high concentrations of CPA in our previous works (see Chapter Four). Additives such as chondroitin sulphate, ascorbic acid, or glucosamine were shown to have great potential to improve porcine chondrocyte survival after exposure to a high molarity CPA cocktail solution[247].

Herein, we present a study to compare two packaging methods (with a surrounding vitrification solution and without a surrounding vitrification solution) for storage of vitrified articular cartilage at −196 °C. We hypothesize that intact articular cartilage can be successfully vitrified once sufficient concentrations of CPA have permeated into the cartilage matrix and chondrocytes, even if the surrounding vitrification solution is removed before vitrification to −196 °C. In addition, we test the 7-hr CPA permeation protocol[208] on full femoral condyles to evaluate its effectiveness for vitrification of large size articular cartilage grafts. Furthermore, we evaluate the effects of two potential additives, chondroitin sulphate and ascorbic acid, for their protective abilities on chondrocytes in the vitrification of articular cartilage.

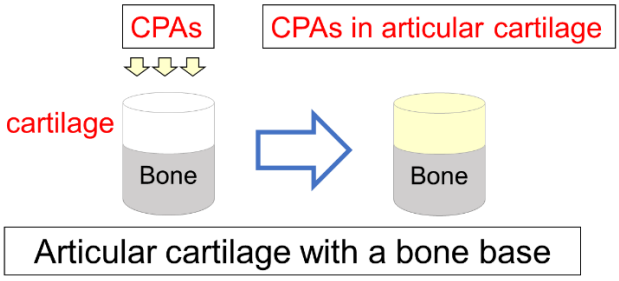

Figure 5.1 Cryoprotectant permeation into articular cartilage with a bone base before plunging into liquid nitrogen for vitrification

5.3 Materials and Methods

5.3.1 Preparation of articular cartilage

Healthy porcine stifle joints (n = 11) from sexually mature pigs (age 54 weeks) were collected within 6 hrs after slaughtering from a slaughterhouse. Porcine joints were immersed in phosphate buffered saline (PBS) and transported to the university lab in a cooler bag. Upon arrival in the lab, the joints were dissected and the femoral condyles were isolated from the tibia bone in a fume food designated for animal sample processing, followed by 15 min cleaning in 100 ml PBS + antibiotics (100 units/ml penicillin, 100 µg/ml streptomycin, 0.25 µg/ml amphotericin B (Gibco)) under a sterile biosafety cabin. After the cleaning, the femoral condyles were immersed in sterile DMEM complete medium (Dulbecco's Modified Eagle Medium Nutrient Mixture F12 (DMEM-F12) (Gibco) supplemented with 10% calf bovine serum, 1 mM sodium pyruvate, 100 units/ml penicillin, 100 µg/ml streptomycin and 0.25 µg/ml amphotericin B (Gibco)) and kept in the fridge at 4 °C until the vitrification experiments. When osteochondral dowels were required, they were cut from the tissue with a sharp cutting device with a 10-mm diameter opening.

5.3.2 Experimental variables

Fig. 5.2 shows the experimental variables for the vitrification experiments in red text. We evaluated two storage methods for articular cartilage vitrification (with surrounding solution, VS+; or without surrounding solution, VS−) using both 10-mm diameter osteochondral dowels (cartilage on a 10-mm thick bone base) and full femoral condyles (approximate length × width × height: 50×30×20 mm^3). In addition, we evaluated the inclusion of additives (chondroitin sulphate, CS or ascorbic acid, AA) to compare their effects on chondrocyte survival after vitrification.

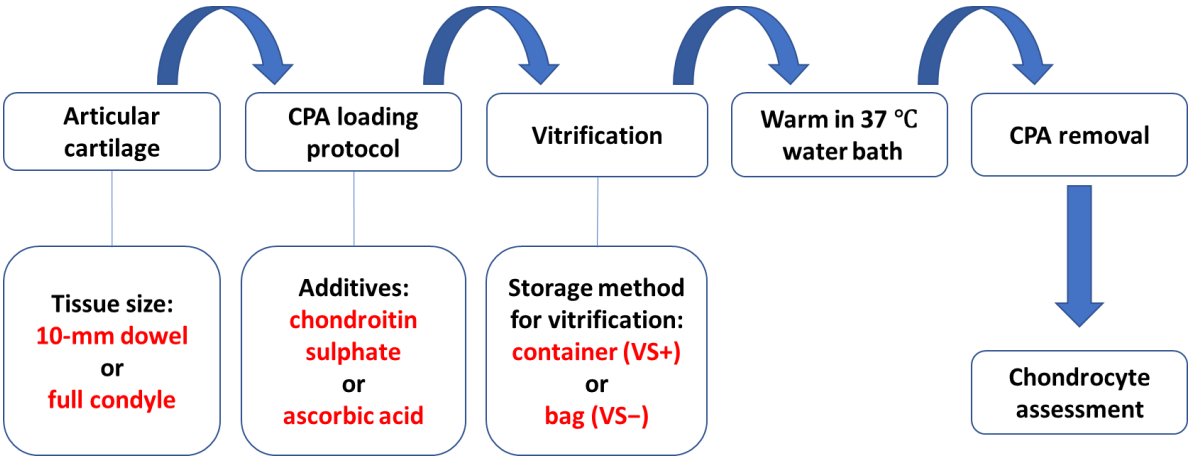

Figure 5.2 Experimental variables (in red text) for vitrification of articular cartilage

5.3.3 Vitrification flowchart

During the vitrification experiments, samples of either 10-mm diameter osteochondral dowels or full femoral condyles were exposed to the multi-CPA loading solution (by immersion in 50 ml for dowels or 200 ml for full femoral condyles) prepared with DMEM-F12 medium following the 7-hr three-step loading protocol developed previously[208,248], see Fig. 6.3 for the CPA concentrations, durations, and temperatures of each step. Once the CPA loading procedure was finished, the cartilage samples were transferred to the containers (15 ml Falcon tube with 5 ml vitrification solution for the dowels, 250 ml plastic cup with 100 ml vitrification solution for the femoral condyles, VS+ in Fig. 5.3, see Fig. 5.4A), or to the freezing bags (one sample per bag, for both dowels and femoral condyles, VS− in Fig. 5.3, see Fig. 5.4B) which were vacuumed to remove the air and sealed quickly with a packaging machine. Solution 2 (3M DMSO + 3M EG + 3M PG) prepared with DMEM-F12 was precooled to −10 °C and used as the vitrification solution for

packaging, VS+. All samples (pre-labelled with ID number and experiment date) were then plunged into the LN_2 dewar for storage.

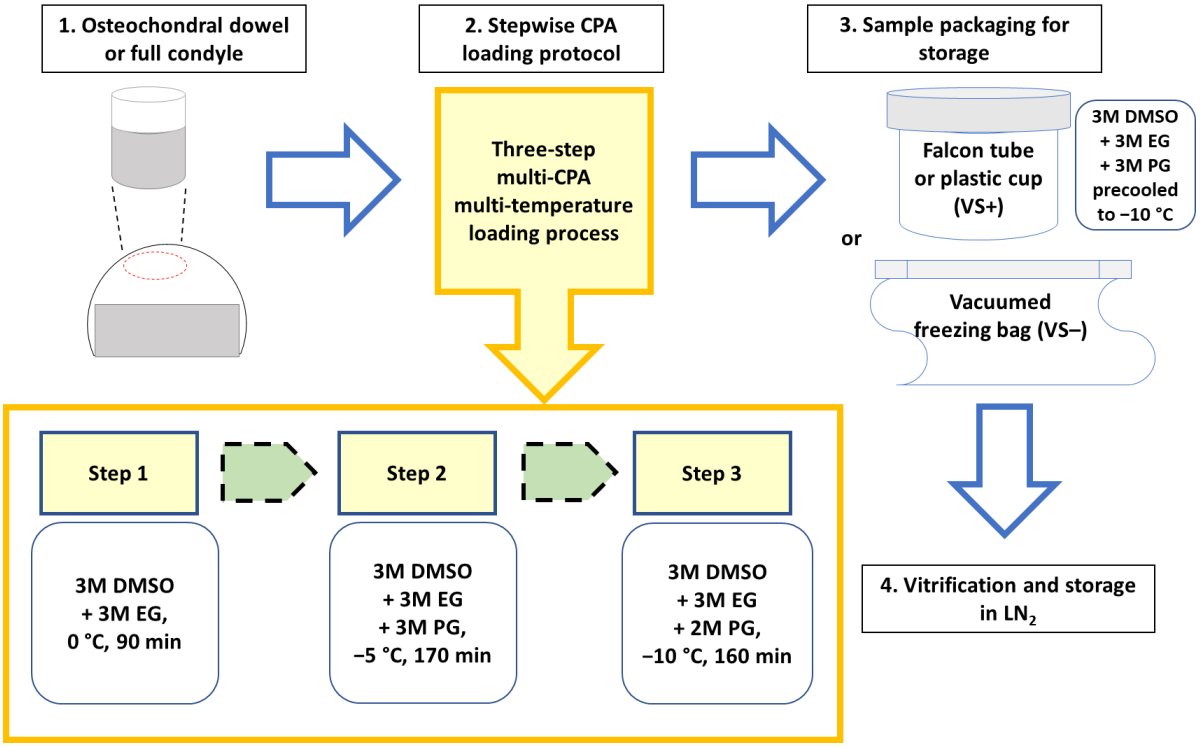

Figure 5.3 Flowchart for vitrification of articular cartilage using a three-step cryoprotectant loading protocol

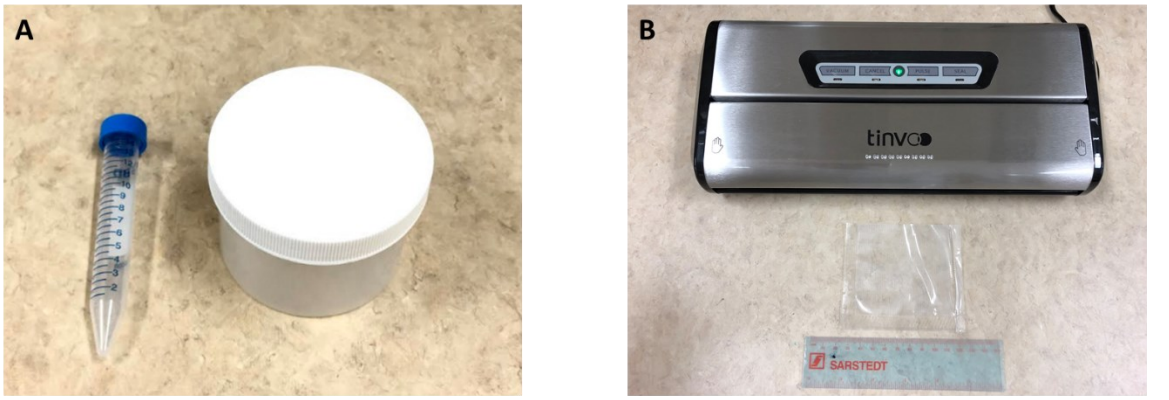

Figure 5.4 The two packaging methods for vitrification of articular cartilage A. A 15-ml Falcon tube for the osteochondral dowel and a 250-ml plastic container with a white lid for the condyle to be vitrified with surrounding CPAs; B. A freezing bag and the vacuumed machine for the osteochondral dowel and the condyle to be vitrified without surrounding CPAs.

5.3.4 Assessment of articular cartilage

5.3.4.1 Chondrocyte viability via cell membrane integrity stain

Chondrocyte viability was quantified *via* cell membrane integrity using fluorescent microscopy similar to our previous work[248] (see Chapter Three). After tissue warming and CPA removal, a vibratome (vibratome-1000 plus, the Vibratome Company, St. Louis, MO) was used for sectioning cartilage slices. The vibratome basin was filled with 500 ml 1X PBS (4 °C) to avoid cartilage dehydration during sectioning. The osteochondral dowel was placed in a metal sample holder and cartilage slices with a thickness of 100 µm were sectioned in a transverse plane, then transferred to one labelled well of a 24-well plate filled with 2.0 ml X-Vivo 10 (Lonza) and kept on crushed ice with distilled water before sample staining. For imaging, a mixture of two fluorescent dyes:

6.25 µM Syto 13 (Molecular Probes) and 9 µM Propidium Iodide (PI, Sigma) were used to label membrane-intact (live cell, green color) and membrane-damaged (dead cell, red color) chondrocytes. Cartilage slices were placed on labelled microscope slides and excess X-Vivo on the slices was removed with Kimwipe. Each slice was overlaid with approximately 50 µl stain mixture and covered with a coverslip. Cartilage slices were incubated in the dark for 10–15 min to allow dye permeation into chondrocytes. Cartilage slices were imaged using a Nikon digital camera (model: DS-Fi2) under a Nikon inverted fluorescent microscope (model: ECLIPSE Ti-5). Dual filters with the following spectra peak maxima: excitation/emission: 488 nm/503 nm and 535 nm/617 nm were used to image all the slices. The cell viability for each cartilage slice was determined by counting the numbers of the green-stained (viable) cells and red-stained (non-viable) cells, using custom made software Viability 3.2 (Locksley McGann, University of Alberta)[111]. An inclusion criteria of positive control cell viability from fresh cartilage slices of greater than 85% was used to screen healthy cartilage for the study.

Normalized cell viability of the experimental samples was determined according to the following formula:

$$\text{Normalized cell viability (\%)} = \frac{\frac{\#\text{ of green cells after vitrification}}{\#\text{ of green cells }+\#\text{ of red cells after vitrification}}}{\frac{\#\text{ of green cells before CPA loading}}{\#\text{ of green cells }+\#\text{ of red cells before CPA loading}}} \times 100\% \qquad (1)$$

5.3.4.2 Chondrocyte metabolic activity assessed with alamarBlue

Chondrocyte metabolic activity was determined by alamarBlue as documented in our previous work[248] (see Chapter Three). AlamarBlue is a fluorescence indicator based on the reduction reaction of metabolically active cells to convert the blue-colored resazurin (non-fluorescent) into red-colored resorufin (highly fluorescent). Briefly, after tissue warming and CPA removal, cartilage from each experimental group was removed from the osteochondral dowel bone base and

weighed and washed in 5 ml sterile PBS supplemented with antibiotics for 15 minutes. Positive controls consisted of articular cartilage that was neither exposed to CPAs nor vitrified; negative controls were articular cartilage plunged into liquid nitrogen without CPAs. Cartilage samples were then incubated in an alamarBlue (Invitrogen, Burlington, Canada) assay solution containing 5 ml X-VIVO 10 (a serum-free medium (Lonza, California, USA)) supplemented with 0.1 mM ascorbic acid, 100 nM dexamesasone, and 10 ng/ml transforming growth factor beta 1, and mixed with 500 µl alamarBlue in a 6-well plate and incubated at 37 °C for fluorescence readings every 24 hr for 4 days using Cytofluor 2.0 software. The fluorescence parameters were set to emission wavelengths of 580/50 nm, excitation wavelengths of 485/20 nm, and a gain of 45. Fluorescence was measured for each sample per experimental group at 24 hr, 48 hr, 72 hr, and 96 hr. Readings of blank samples (alamarBlue assay solution without cartilage samples) were subtracted from readings of the experimental samples to yield a value in relative fluorescent units (RFU) divided by weight in grams of articular cartilage. The RFU readings of chondrocytes after vitrification were normalized to the fresh positive controls and presented as a percentage in the figures.

5.3.4.3 Cooling and warming temperature profile of full femoral condyles

To compare the cooling and warming rates of articular cartilage stored with different methods, a dual thermometer with two thermocouple detectors was used to determine the temperature as a function of time of full femoral condyles (N = 3 condyles per group, in a container or in a bag) as they were cooled from −10 °C to −196 °C then warmed to 37 °C. Two 2-mm deep holes were drilled on the weight bearing area of the condyle cartilage surface to place the thermal detectors for temperature measurement (see Fig. 6.6). The temperatures of articular cartilage at different

time points (0 min, 1 min, 3 min, 5 min, 10 min, 15 min, 20 min, 30 min) were recorded and plotted to observe the cooling and warming rates of articular cartilage.

5.3.5 Statistical analysis

The numerical data are presented as mean ± standard deviation (SD) of the results. The equality of variances for experimental variables was determined by Levene's test before multiple comparisons. Analysis of variance (ANOVA) with post hoc tests (Tukey test) or nonparametric tests (Mann–Whitney U test) was performed for multiple comparisons on sample cell viability or metabolic activity based on the sample configuration for different experimental conditions. The numerical data were analysed using SPSS 20.0 software for statistical significance and figures were plotted with GraphPad prism 8.0 software. The p values are reported in the results or figure legends, statistical significance in the figures was indicated with asterisks respectively: * indicates $p < 0.05$, ** indicates $p < 0.01$.

5.4 Results

5.4.1 Comparison of chondrocyte viability of osteochondral dowels using two packaging methods

Fig. 5.5A-D shows representative fluorescent images of cartilage slices from osteochondral dowels among the four experimental groups after vitrification. As shown in Fig. 5.5E, for the CS group, the normalized chondrocyte viability of osteochondral dowels stored with vitrification solution in a Falcon tube was 74.4 ± 8.9 % (mean ± SD); while the chondrocyte viability was 70.4 ± 6.3 % in

the osteochondral dowels stored without vitrification solution in a bag. For the AA group, the normalized chondrocyte viability of osteochondral dowels stored with vitrification solution in a tube was 67.4 ± 12.1 %; and the chondrocyte viability in the osteochondral dowels stored without vitrification solution in a bag was 69.8 ± 8.4 %. There were no statistical significances between the storage with or without vitrification solution and the usage of CS or AA as additives during the vitrification procedure ($p > 0.05$).

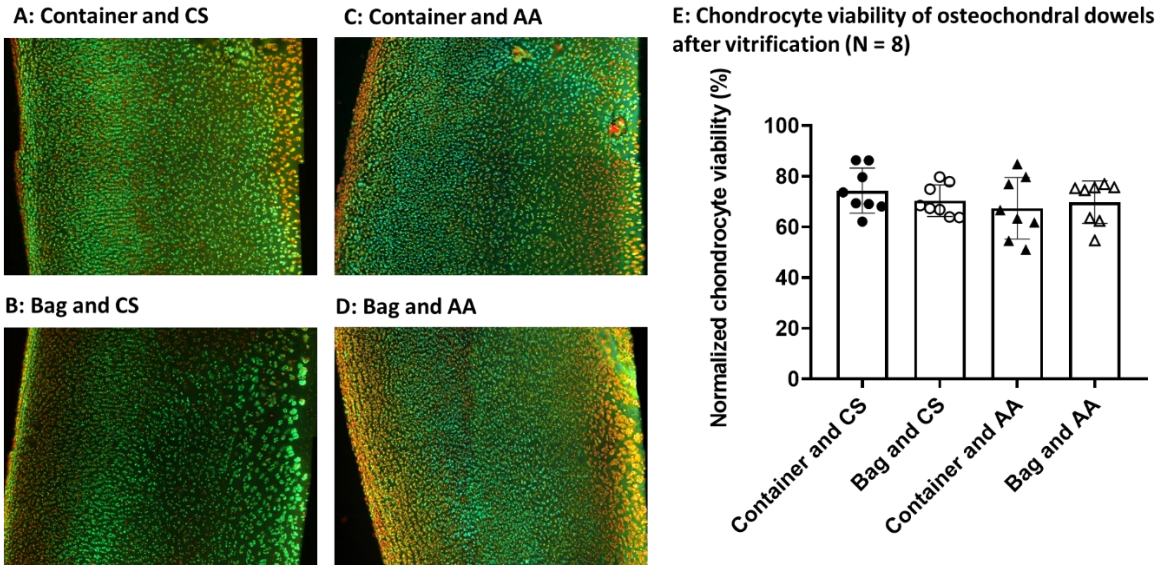

Figure 5.5 Chondrocyte viability of osteochondral dowels after vitrification using two storage methods with (in a Falcon tube) or without (in a bag) a surrounding vitrification solution A. A representative image from an osteochondral dowel in the CS group after vitrification with surrounding cryoprotectants in a container; B. A representative image from an osteochondral dowel in the CS group after vitrification with surrounding cryoprotectants in a bag; C. A representative image from an osteochondral dowel in the AA group after vitrification with surrounding cryoprotectants in a container; D. A representative image of an osteochondral dowel in the AA group after vitrification with surrounding cryoprotectants in a bag; E. Quantification of

chondrocyte viability of osteochondral dowels after vitrification between two storage methods in two additive groups.

5.4.2 Comparison of chondrocyte viability of full femoral condyles using two packaging methods

Fig. 5.6A-D shows representative fluorescent images of cartilage slices from full femoral condyles among the four experimental groups after vitrification. As shown in Fig. 5.6E, for the CS group, the normalized chondrocyte viability of full femoral condyles stored without vitrification solution in a bag (69.8 ± 9.0 %) was significantly higher than the chondrocyte viability of the full femoral condyles stored with vitrification solution in a plastic container (35.6 ± 14.4 %) ($p = 0.03$). For the AA group the normalized chondrocyte viability of full femoral condyles stored without vitrification solution in a bag (67.3 ± 22.7 %) was significantly higher than the chondrocyte viability of the full femoral condyles stored with vitrification solution in a plastic container (7.9 ± 9.6 %) ($p = 0.01$).

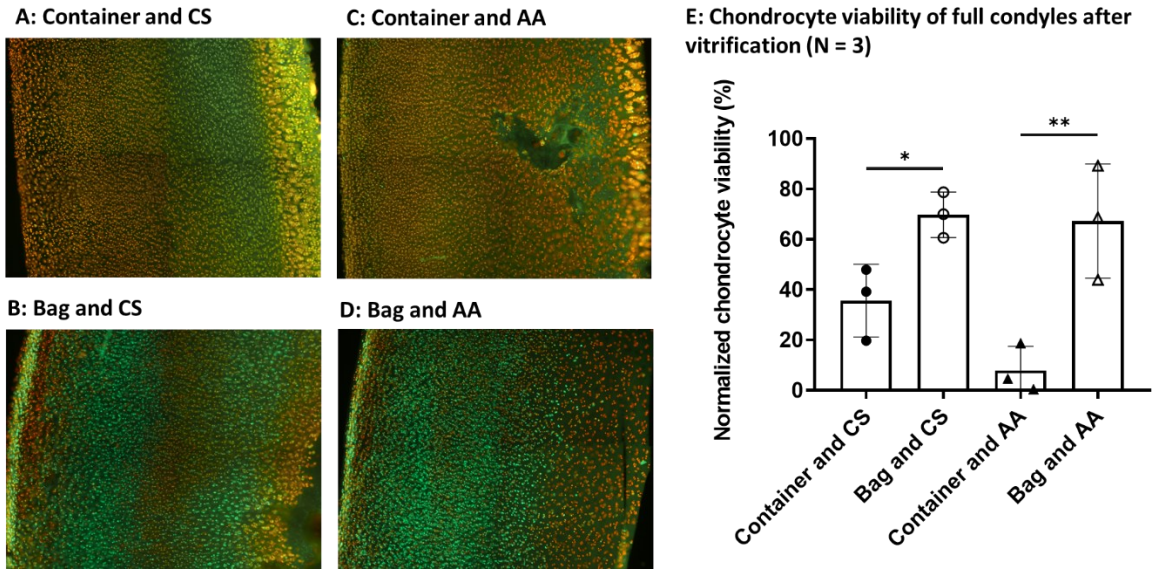

Figure 5.6 Chondrocyte viability of full femoral condyles after vitrification using two storage methods with (in a container) or without (in a bag) a surrounding vitrification solution A. A representative image from a full condyle in the CS group after vitrification with surrounding cryoprotectants in a container; B. A representative image from a full condyle in the CS group after vitrification with surrounding cryoprotectants in a bag; C. A representative image from a full condyle in the AA group after vitrification with surrounding cryoprotectants in a container; D. A representative image from a full condyle in the AA group after vitrification with surrounding cryoprotectants in a bag; E. Quantification of chondrocyte viability of full femoral condyles after vitrification between two storage methods in the two additive groups.

5.4.3 Comparison of chondrocyte metabolic activity of full femoral condyles using two packaging methods

Fig. 5.7A shows representative images of chondrocyte metabolic activity of cartilage post vitrification of full femoral condyles among the four experimental groups from Day 0 to Day 4.

After cartilage treatment with CS or AA and vitrification in a bag without vitrification solution, the viable chondrocytes showed an active metabolic function at Day 4 similar to the positive control group. However, chondrocytes from full femoral condyles vitrified in a container showed no cellular activity in both groups treated with either CS or AA, similar to the negative control group. In addition, a similar normalized chondrocyte metabolic activity was seen in groups treated with CS or AA when using the same storage method (either stored in a container or stored in a bag) during the vitrification procedure (see Fig. 5.7B).

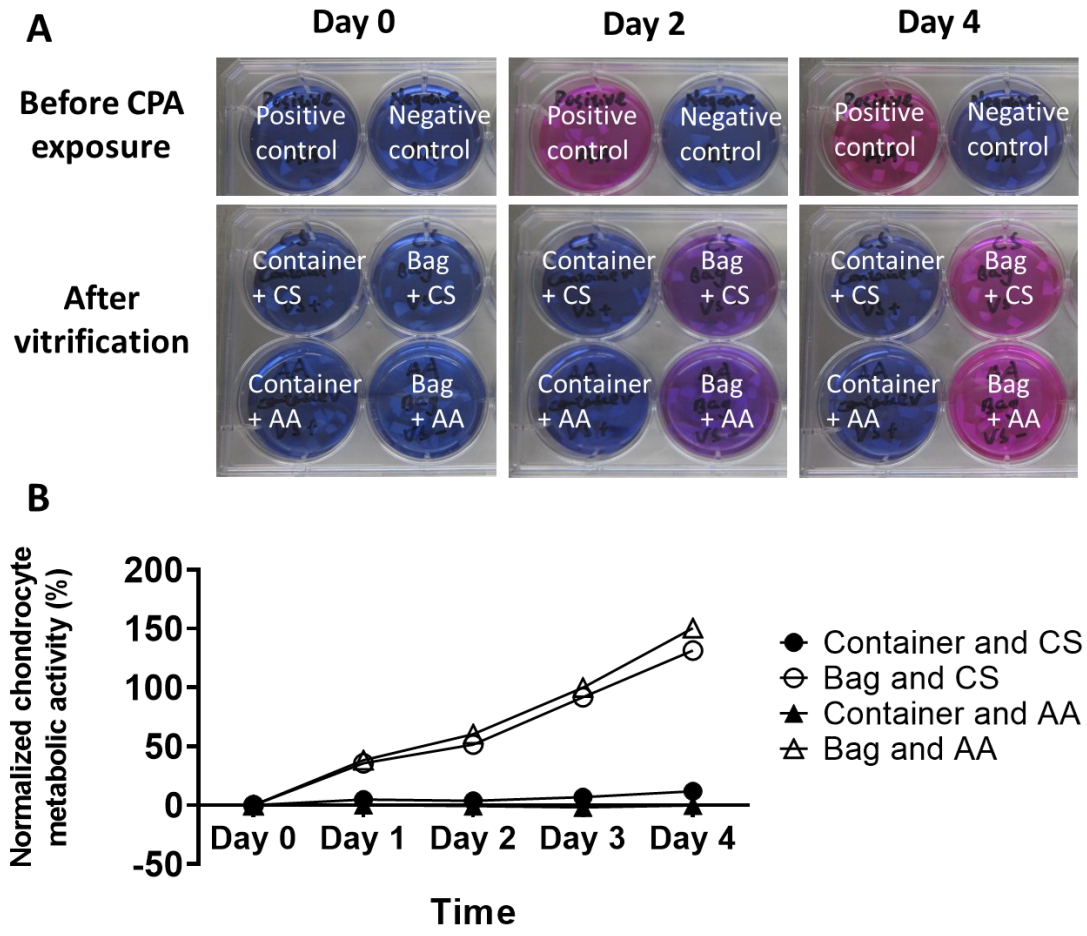

Figure 5.7 Chondrocyte metabolic activity of full femoral condyles after vitrification A. Representative alamarBlue images of chondrocyte metabolic activity in full femoral condyles after

vitrification with (in a container) or without (in a bag) a surrounding vitrification solution; B. Normalized chondrocyte metabolic activity of the four experimental groups after vitrification followed by the 4-day alamarBlue assessment (N = 2 replicates per group).

5.4.4 Temperature profile of full femoral condyles during the vitrification and warming processes

Fig. 5.8A shows a representative image of a full condyle with two positions on the cartilage surface for temperature measurement. Fig. 5.8B shows the temperatures during cooling and warming of full femoral condyles vitrified with (in a container) or without (in a bag) a surrounding vitrification solution during plunge into liquid nitrogen (−196 °C) followed by warming to 37 °C in a water bath. The temperature of full femoral condyles stored in a bag reached below −150 °C between 2–3 min after plunge into liquid nitrogen, while full femoral condyles stored in a container took more than 15 min to reach below −150 °C. During the warming process, the full femoral condyles stored in a bag reached above 0 °C within 1 min, compared to full femoral condyles stored in a container that took more than 7 min to reach 0 °C.

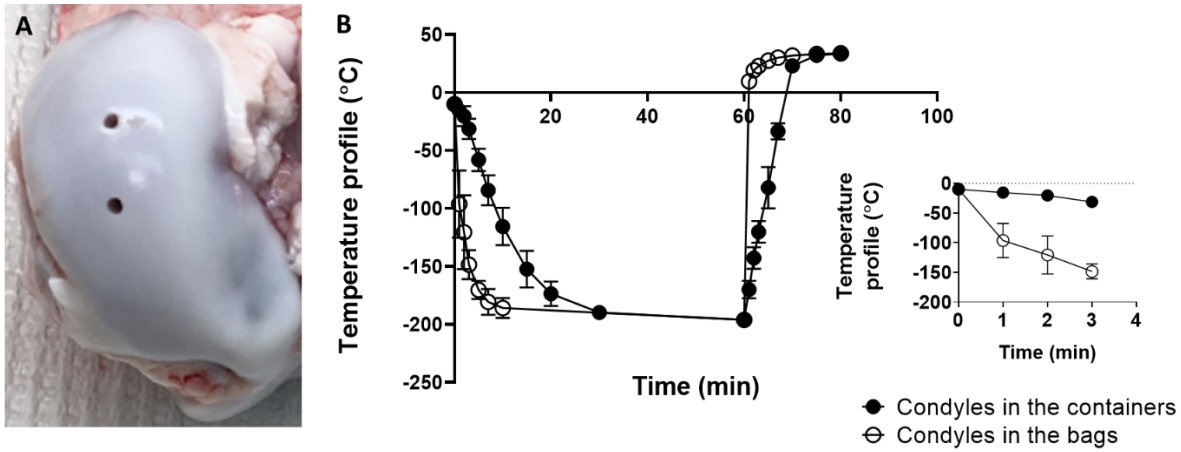

Figure 5.8 Temperature profile of porcine femoral condyles. A. Two points on the porcine condyle cartilage surface for temperature measurement; B. The temperatures of full femoral condyles (N = 3) when vitrified with (in a container) or without (in a bag) a surrounding vitrification solution during plunge into liquid nitrogen followed by warming back to 37 °C in water bath.

5.4.5 Gross morphology of porcine femoral condyles after vitrification

Figure 5.9 shows the morphologies of full femoral condyles after vitrification and warming. The full femoral condyles were either stored with surrounding CPAs in a plastic cup (Fig. 5.9A) or stored without surrounding CPAs in a vacuumed bag (Fig. 5.9B). After warming and CPA removal, condyles stored with vitrification solution in the containers (either treated with CS, Fig. 5.9C or AA, Fig. 5.9E) demonstrated more visible fractures in the cartilage surface (indicated by blue arrows) compared to those condyles stored without vitrification solution in vacuumed bags (either treated with CS, Fig. 5.9D or AA, Fig. 5.9F).

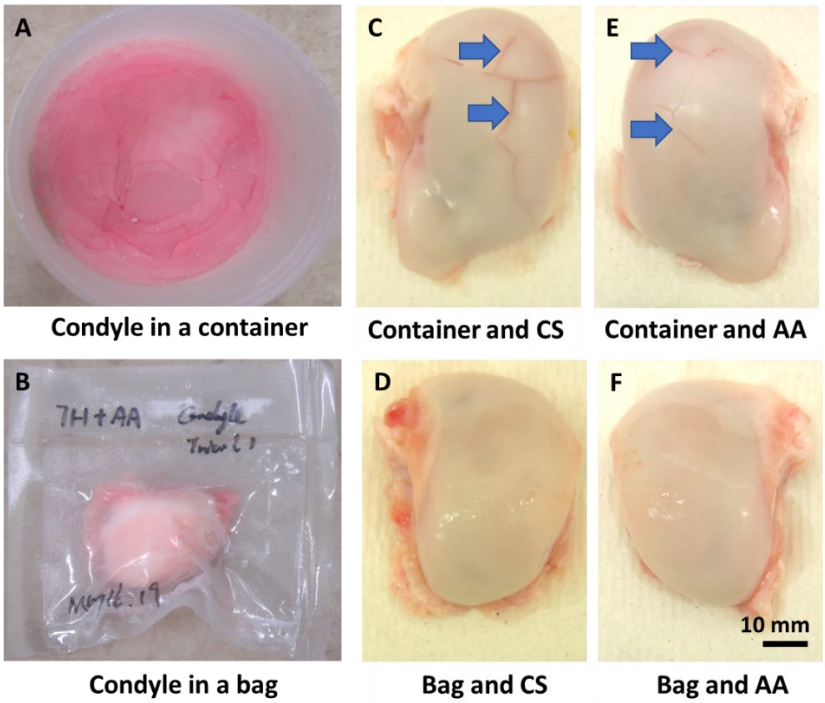

Figure 5.9 Gross morphology of porcine femoral condyles after vitrification and storage with (in a container) or without (in a bag) a surrounding vitrification solution. A. A condyle vitrified with surrounding cryoprotectants in a plastic container; B. A condyle vitrified without surrounding cryoprotectants in a sealed vacuumed freezing bag; C. Gross appearance of a post-vitrified condyle from the container and CS group (Blue arrows: cartilage fracture); D. Gross appearance of a post-vitrified condyle from the vacuumed freezing bag and CS group; E. Gross appearance of a post-vitrified condyle from the container and AA group (Blue arrows: cartilage fracture); F. Gross appearance of a post-vitrified condyle from the vacuumed freezing bag and AA group.

5.5 Discussion

Cryopreservation by vitrification is a promising technology to preserve cells and tissue for long term without ice crystal formation, and it can be achieved by two approaches[69]; the first approach is an equilibrium approach which involves permeating high concentrations of CPA into the cells and matrix, and the second approach is a nonequilibrium approach which involves cooling the sample fast enough to outrun ice formation and kinetically avoid ice crystal formation. Both approaches require permeating large amounts of CPAs into the tissue. CPA permeation is a main factor that determines whether the vitrification of articular cartilage tissue will be successful. Shardt *et al.*[208] proposed an optimized 7-hr CPA permeation protocol based on an engineering model incorporating predictions of CPA concentration, freezing point, and tissue vitrifiability. In the current study, we found that after applying the optimized 7-hr CPA permeation protocol, the chondrocyte viability after vitrification in small osteochondral dowels (10-mm diameter on a bone base) showed approximately 70% chondrocyte viability after vitrification for both storage in a Falcon plastic tube surrounded with CPAs and storage in a vacuumed bag without CPAs (Fig. 5.5D). Next, we found a similar chondrocyte viability (~65–70%) in the full femoral condyles for which the surrounding CPAs were removed from the containers before plunging into liquid nitrogen (Fig. 5.5D and 5.6D). These results indicate that the 7-hr CPA permeation strategy[208] is applicable to the vitrification of full condyle articular cartilage tissue.

Importantly, we found no statistically significant differences in the chondrocyte viability of 10-mm diameter osteochondral dowels between the storage in a Falcon plastic tube with surrounding CPAs and storage in a vacuumed bag without surrounding CPAs (Fig. 5.5D). This result indicated that even if the surrounding CPAs are removed from around the osteochondral tissue during

cooling to −196 °C, the permeated CPAs in the articular cartilage is sufficient to protect the chondrocytes from freezing injuries. Thus, we addressed the gaps in the literature to show that a surrounding CPA solution is not required for vitrification of articular cartilage. We proposed that after a high concentration of CPAs had been permeated throughout the articular cartilage, the concentration of CPAs in the chondrocytes and extracellular matrix was high enough to transform the tissue into a solid without ice formation when the articular cartilage is cooled sufficiently rapidly to cryogenic temperatures. Successful vitrification of articular cartilage can be achieved in the absence of a surrounding CPA solution, which is contrary to the current cryopreservation practices, in which articular cartilage is immersed in a certain amount of CPA solution for vitrification before cooling below −130 °C[30,113,185,218].

Tissue fractures can be induced by the non-uniform thermal gradients during solution freezing and this can affect the outcomes of vitrification for articular cartilage. More cartilage factures were noted on the surface of full femoral condyles after vitrification with a surrounding CPA solution (Fig. 5.9). We found that the cracking phenomenon was not significant in the 10-mm diameter osteochondral dowels; this is probably due to the small volumes of osteochondral tissue. However, cracking becomes a challenge when scaling to a large tissue size, such as full femoral condyles. Fig. 5.8 shows the temperature profiles within the articular cartilage during the different methods of vitrification and warming. The cooling and warming rates of full femoral condyles stored in vacuumed bags without surrounding CPAs were faster than those condyles stored in plastic containers with surrounding CPAs. Having a solution surrounding the cartilage tissue is disadvantageous not only because it induced thermal cracking to the cartilage, but also because it slows down the cooling and warming of the cartilage that may lead to tissue devitrification and

chondrocyte death. From the above findings, we concluded that removing the CPAs can 1) improve the cooling and warming of articular cartilage (Fig. 5.8); and 2) reduce the thermal-mechanical stress in the large volume that results in cracks propagating through the articular cartilage (Fig. 5.9), and this help to retain a high chondrocyte viability (Fig. 5.5) and functionality (Fig. 5.6).

There are other approaches to reduce thermal stress in the literature. Pegg *et al.*[188] proposed an approach to avoid thermal stress in arteries by controlling the cooling and warming rates. However, this approach required careful calculation of the thermal properties of the vitrification solution and the targeted sample. Rabin *et al.*[195,196,222] further developed a mathematical model to calculate the thermal-mechanical stress during the freezing of biological samples, e.g. rabbit liver, kidney and brain. More investigation is required to quantify and understand the thermal-mechanical effects in articular cartilage when it undergoes vitrification/warming processes. Our current approach is simple and successful in preventing cartilage fractures caused by the surrounding CPAs and is effective in improving the vitrification outcomes of articular cartilage.

Lastly, the inclusion of ascorbic acid was able to maintain a similar high chondrocyte survival compared to the inclusion of chondroitin sulphate during the CPA permeation and vitrification processes (see Fig. 5.5 and Fig. 5.6). The use of ascorbic acid in the vitrification of articular cartilage is a promising alternative to chondroitin sulphate for future investigations.

5.6 Conclusions

This is the first study demonstrating the vitrification of porcine full femoral condyles, indicating the possibility to scale up the vitrification of articular cartilage from small osteochondral dowels to full size osteochondral condyles. After tissue vitrification and subsequent warming, our results showed similar chondrocyte viability of post-vitrified 10-mm diameter osteochondral dowels when stored with or without a surrounding vitrification solution, which confirmed that articular cartilage can be vitrified with sufficient CPA permeation and appropriate storage method. In addition, higher chondrocyte viability and metabolic activity can be maintained in full femoral condyles when stored without a surrounding vitrification solution when compared to those with a surrounding vitrification solution. This difference is due to faster cooling/warming rates and less thermal-mechanical stress on the large volume of articular cartilage tissue. This study provides guidance for the development of articular cartilage packaging processes for vitrification and will benefit tissue banking of intact human articular cartilage.

Chapter Six: General Discussion and Conclusions

6.1 General discussion

Articular cartilage is a few-millimeters-thick tissue covering the ends of bones in articulating joints and provides a vital function in joint mobility. However, the avascular and aneural structure of AC has very limited self-repair capacity after injury[33]. AC allograft transplantation is an established procedure for treatment of AC defects[23,37,244], but this procedure is greatly limited by the availability of fresh AC grafts which can be alleviated by successfully long-term cryopreservation.

Preserving viable tissue is becoming a popular approach to alleviate the shortage of tissue grafts for clinical transplantation. Cryopreservation of AC grafts is one way to increase the availability of AC grafts to assist clinical repair of AC defects[3,113]. AC is a connective tissue that consists primarily of chondrocytes and is an ideal tissue for developing cryopreservation protocols when compared to other tissues that contain multiple cell types; but the chondrocytes are distributed within a dense cartilage matrix approximately 2–4 mm thick[101] that requires a relatively longer period (e.g. hours) for CPAs to fully permeate into the ECM and chondrocytes[113,209]. This unique structure makes it challenging to successfully cryopreserve intact AC, particularly for intact human AC.

On account of the advances in cryopreservation technology, many approaches have been developed to improve the outcomes of cryopreserved AC[30,113,185,218]. One typical feature of previous research from some groups[30,178,218] is that they usually investigated one part of the AC

vitrification, while other groups[113,185,208] worked on developing new approaches or combining available approaches for use in AC vitrification.

The success of AC vitrification relies on a multi-disciplinary group that involves professionals from at least four fields[3], which include orthopedic surgeons who know the clinical requirements and biological basis of articular cartilage, cryobiologists who understand the principal of cryopreservation and protocol designs, engineers who are good at mathematical modelling and simulation, and laboratory researchers who can perform experiments for validation. However, such a team setting is not easy to be established without tremendous and continuous input and cooperation. The strength of this thesis is the integration of several strategies into one approach for vitrification of AC.

Particulated AC cubes have been used to repair AC defects in clinical practice[93,233,255]; however, there is no report of cryopreserving particulated AC . Chapter Two presented the first study of vitrifying particulated AC in both porcine and human species with promising results that met the clinical requirement of 70% chondrocyte viability[121]. This chapter demonstrated a detailed approach for the development of appropriate vitrification protocols for small particulated AC cubes. The content of this chapter provided the generation of CPA permeation protocols (the engineering modelling was performed by Nadia Shardt)[208], the stepwise procedure of processing AC tissue into small particulated size, followed by CPA permeation, vitrification and storage in cryovials at −196 °C, all of which can be reproduced in other laboratories or tissue banks. The experimental results obtained from this chapter validated the effectiveness of the engineered CPA permeation protocols, showing the potential of engineering models that can be used to guide and

generate vitrification protocols for a specific size of AC grafts, e.g. 1 mm^3. In addition, Chapter Two documented the storage of 6 months for the vitrified particulated AC cubes in LN_2 without deterioration in chondrocyte viability and functionality. The extended storage period of 6 months is critical to providing orthopedic surgeons a flexible timeline to make appropriate surgical arrangements for patients with AC defects who require a surgical reconstruction.

Although the *in vitro* results from Chapter Two provided evidence for both porcine and human tissue that the post-vitrified particulated AC cubes can be used as an alternative source of AC grafts, further animal transplantation studies and clinical trials in human patients are necessary to ensure the safety and effectiveness when applying cryopreserved particulated AC in clinical transplantation to repair AC defects.

Osteochondral grafts consisting of intact AC on a bone base are the most popular AC grafts that are being used in clinical transplantation to repair AC defects[23,38,46]. Vitrification of osteochondral grafts has been studied for years with progress noted in rabbit[218], porcine[30,248] and human[113] species. Due to the dense structure of the AC matrix, the process of CPA diffusion throughout the AC matrix to reach a high and vitrifiable concentration is time consuming[113,209]. The first report of successful vitrification of intact human osteochondral grafts required 9.5 hr for a four-step CPA permeation procedure[113], which is complicated and not very practical for use in tissue banks. Shortening the CPA permeation protocol while maintaining a high chondrocyte survival is a challenging but realistic scientific question that needed to be answered. Chapter Three[248] compared two shorter-duration three-step CPA permeation protocols (an optimized 7-hr protocol, and an ad hoc 5-hr protocol) to the four-step permeation protocol for their effectiveness in vitrification of

porcine osteochondral grafts. The experimental results of this chapter concluded that the optimized 7-hr three-step CPA permeation protocol generated by Nadia Shardt's engineering modelling achieved similar chondrocyte survival when compared to the 9.5-hr four-step CPA permeation protocol. The shortening by 2.5 hr gained by using the 7-hr protocol makes the procedure achievable within an 8-hr working shift for staff working in tissue banks.

In addition to the validation of the optimized 7-hr protocol, Chapter Three demonstrated the relationship between vitrification outcomes and tissue size, and container size when using different CPA permeation protocols. In Chapter Three, two sizes of osteochondral grafts (10 mm diameter and 6.9 mm diameter dowels) were selected for investigation. Generally, the smaller the tissue, the shorter the time that was required for the CPA permeation in the tissue. The ad hoc 5-hr three-step CPA permeation protocol was capable to vitrify the small 6.9 mm diameter osteochondral grafts, possibly due to the CPA permeation being sufficient for such a small size of AC. This protocol was unsuccessful when applied to the 10 mm diameter osteochondral grafts. When vitrifying the bigger grafts, e.g. 10 mm diameter, CPA permeation was critical and required a longer time period, as shown by the better vitrification outcomes using the optimized 7-hr protocol or the 9.5-hr protocol.

The osteochondral grafts were stored in a container before plunging into liquid nitrogen, the size of the container can affect the heat transfer to the tissue. Larger containers result in slower cooling and warming rates of the osteochondral grafts which may further result in failure of vitrification. Although the cooling and warming rates were not measured in this study, the chondrocyte viability

results provided evidence to support the conclusion that a smaller and appropriate container size may benefit vitrification outcomes of osteochondral grafts.

CPA toxicity is another major issue when vitrifying AC due to the long exposure of chondrocytes to the high concentrations of CPA mixture[9,63,65,116]. Chapter Four[247] demonstrated the protective effects of additives on chondrocyte survival when AC was exposed to high concentrations of CPA during permeation that was required for cryopreservation. Previous studies have demonstrated the potential of using additives during cell cryopreservation with encouraging improvements[77,89,234]. Hahn *et al.*[89] investigated the protective effects of CS, TMP, AA, and GlcN on human AC chondrocytes when exposed to 1.6 M glycerol for 90 min at room temperature and concluded that these additives were beneficial to improving chondrocyte survival by reducing the CPA toxicity. Inspired by this study, Chapter Four evaluated the effects of five additives (CS, TMP, AA, GlcN, and PF-68) using a stepwise CPA permeation procedure with multi-CPA mixtures that reflected a more realistic cryopreservation protocol. Chapter Four confirmed the potential of adding additives, including CS, TMP, AA, and GlcN, to the multi-CPA mixtures to reduce the CPA toxicity on porcine chondrocytes with improved chondrocyte survival. These findings provided additional evidence that inclusion of additives can aid in the design of cryopreservation protocols for AC. Optimization of additive usage such as combination of additives or modification of additive concentrations can be investigated in further research.

Femoral condyle grafts are a flexible tissue graft option for repairing large AC defects. Successful long-term preservation of femoral condyles will greatly increase the number of AC allografts available to the practice of orthopedic surgery. However, vitrification of femoral condyles is more

challenging due to the complexity of graft size, CPA permeation, storage and tissue fracture. With the optimization on CPA permeation, container selection, and additive usage, Chapter Five demonstrated the first report of femoral condyle vitrification using an integrated vitrification approach.

To address the CPA permeation into a relatively large piece of AC, Chapter Five applied the optimized 7-hr three-step CPA permeation protocol[208]. The optimized 7-hr protocol has been shown to be effective in vitrification of 10 mm diameter osteochondral grafts[248]. And because AC is a thin layer with a similar thickness no matter the size of the tissue piece (2.4 mm in average of adult human hyaline AC[101]) that covers the articulating bone ends (the bony end is a natural barrier that prevents CPA permeation[209,257]), it is reasonable to expect that the time required for CPA to permeate into the entire AC layer of a large femoral condyle is a similar time to that taken to permeate smaller pieces. Once CPA permeation reaches a sufficiently high concentration in the AC matrix, the entire AC layer of the femoral condyle can be vitrified when cooled appropriately fast below the glass transition temperatures. The chondrocyte viability after vitrification in the AC of porcine femoral condyles confirmed that the optimized 7-hr protocol provided sufficient CPA permeation throughout the femoral condyle AC matrix.

Solution fractures during cooling below the glass transition temperatures can be harmful to the vitrified tissue[134,188,216], for instance, resulting in AC fractures. Cooling and warming large femoral condyle grafts took more time if the grafts were surrounded with a glassy CPA, putting the tissue at risk of devitrification[241,249]. Pegg *et al.*[188] used a slowed cooling and warming protocol to minimize the fracturing effects when the rabbit artery reached close to the glass transition

temperatures. Rabin *et al.*[59,195,196,222]developed a thermo-mechanical model to calculate the thermal stress and the expansion characteristics of a freezing system. To minimize the solution cracking effects, Chapter Five documented a novel packaging method to store AC tissue at −196 °C by removing the surrounding vitrification solution around the AC grafts immediately prior to immersion in liquid nitrogen. The results from this chapter showed that the vitrification solution surrounding the AC grafts was unnecessary for vitrification and it can even be harmful to the vitrification outcomes. This study enhanced the understanding of AC vitrification and provided new insights to improve the packaging process during AC vitrification.

6.2 Conclusions

Using cryopreserved AC grafts is a potential approach to repair AC defects. This thesis investigates several aspects of CPA permeation, heat transfer, tissue storage, and additives for the development of cryopreservation protocols for AC, and the experimental findings provide valuable knowledge to aid in long-term storage of healthy porcine and human AC at cryogenic temperatures *via* vitrification. These studies address the gaps in current practices of AC vitrification at different scales, which include small particulate cartilage grafts, medium osteochondral grafts and large femoral condyle grafts. The integration of advancing approaches is shown to be beneficial for the design of protocols and experimental outcomes of AC vitrification. The strategies applied in this work demonstrate that vitrification of AC is achievable with improved chondrocyte survival, metabolic activity, and cellular functionality. The encouraging results obtained from these studies provide a solid base for further investigation and optimization of AC vitrification. This thesis

supports the design and development of practical vitrification protocols of AC that can be translated into clinical practice in the future.

References

1. Abazari A, Elliott JAW, Law GK, McGann LE, Jomha NM. A biomechanical triphasic approach to the transport of nondilute solutions in articular cartilage. *Biophys J*. 2009;97(12):3054-3064. doi:10.1016/j.bpj.2009.08.058.
2. Abazari A, Elliott JAW, McGann LE, Thompson RB. MR spectroscopy measurement of the diffusion of dimethyl sulfoxide in articular cartilage and comparison to theoretical predictions. *Osteoarthr Cartil*. 2012;20(9):1004-1010.
3. Abazari A, Jomha NM, Elliott JAW, McGann LE. Cryopreservation of articular cartilage. *Cryobiology*. 2013;66(3):201-209. doi:10.1016/j.cryobiol.2013.03.001.
4. Abazari A, Jomha NM, Law GK, Elliott JAW, McGann LE. Erratum to "Permeation of several cryoprotectants in porcine articular cartilage" [Cryobiology 58 (2009) 110-114]. *Cryobiology*. 2009;59(3):369. doi:10.1016/j.cryobiol.2009.09.002.
5. Abazari A, Thompson RB, Elliott JAW, McGann LE. Transport phenomena in articular cartilage cryopreservation as predicted by the modified triphasic model and the effect of natural inhomogeneities. *Biophys J*. 2012;102(6).
6. Aboagla EM-E, Terada T. Trehalose-enhanced fluidity of the goat sperm membrane and its protection during freezing. *Biol Reprod*. 2003;69(4):1245-1250. doi:10.1095/biolreprod.103.017889.
7. Agung M, Ochi M, Yanada S, et al. Mobilization of bone marrow-derived mesenchymal stem cells into the injured tissues after intraarticular injection and their contribution to tissue regeneration. *Knee Surgery, Sport Traumatol Arthrosc*. 2006;14(12):1307-1314. doi:10.1007/s00167-006-0124-8.
8. Alam P, Beg AZ, Siddiqi MK, et al. Ascorbic acid inhibits human insulin aggregation and

protects against amyloid induced cytotoxicity. *Arch Biochem Biophys*. 2017;621:54-62.

9. Almansoori KA, Prasad V, Forbes JF, et al. Cryoprotective agent toxicity interactions in human articular chondrocytes. *Cryobiology*. 2012;64(3):185-191. doi:10.1016/j.cryobiol.2012.01.006.

10. Anchordoguy TJ, Rudolph AS, Carpenter JF, Crowe JH. Modes of interaction of cryoprotectants with membrane phospholipids during freezing. *Cryobiology*. 1987;24(4):324-331.

11. Anderson JW, Nicolosi RJ, Borzelleca JF. Glucosamine effects in humans: a review of effects on glucose metabolism, side effects, safety considerations and efficacy. *Food Chem Toxicol*. 2005;43(2):187-201. doi:10.1016/J.FCT.2004.11.006.

12. Anger JT, Gilbert BR, Goldstein M. Cryopreservation of sperm: indications, methods and results. *J Urol*. 2003;170(4):1079-1084. doi:10.1097/01.ju.0000084820.98430.b8.

13. Arakawa T, Carpenter JF, Kita YA, Crowet JH, T Arakawa, JF Carpenter, YA Kita JC. The basis for toxicity of certain cryoprotectants: a hypothesis. *Cryobiology*. 1990;27(4):401-415. doi:10.1016/0011-2240(90)90017-X.

14. Arrigoni O, De Tullio MC. Ascorbic acid: much more than just an antioxidant. *Biochim Biophys Acta (BBA)-General Subj*. 2002;1569(1):1-9.

15. Aye M, Di Giorgio C, De Mo M, Botta A, Perrin J CB. Assessment of the genotoxicity of three cryoprotectants used for human oocyte vitrification: Dimethyl sulfoxide, ethylene glycol and propylene glycol. *Food Chem Toxicol*. 2010;48(7):1905-1912. doi:10.1016/J.FCT.2010.04.032.

16. Bae JH. Oxidative stress in ovariectomy menopause and role of chondroitin sulfate. *Arch Pharm Res*. 2004;27(8):867-872.

17. Balasubramanian SK, Coger RN. Heat and mass transfer during the cryopreservation of a bioartificial liver device: a computational model. *ASAIO J*. 1992;51(3):184-193.

18. Barbero A, Ploegert S, Heberer M, Martin I. Plasticity of clonal populations of dedifferentiated adult human articular chondrocytes. *Arthritis Rheum*. 2003;48(5):1315-1325. doi:10.1002/art.10950.

19. Bartlett W, Gooding CR, Carrington RWJ, Skinner JA, Briggs TWR, Bentley G. Autologous chondrocyte implantation at the knee using a bilayer collagen membrane with bone graft. A preliminary report. *J Bone Joint Surg Br*. 2005;87(3):330-332.

20. Bathgate R. Antioxidant mechanisms and their benefit on post-thaw boar sperm quality. *Reprod Domest Anim*. 2011;46:23-25. doi:10.1111/j.1439-0531.2011.01826.x.

21. Baust JG, Gao D, Baust JM. Cryopreservation. *Organogenesis*. 2009;5(3):90-96. doi:10.4161/org.5.3.10021.

22. Baxter SJ, Lathe GH. Biochemical effects on kidney of exposure to high concentrations of dimethyl sulphoxide. *Biochem Pharmacol*. 1971;20(6):1079-1091. doi:10.1016/0006-2952(71)90337-6.

23. Beer AJ, Tauro TM, Redondo ML, Christian DR, Cole BJ, Frank RM. Use of allografts in orthopaedic surgery: safety, procurement, storage, and outcomes. *Orthop J Sport Med*. 2019;7(12):2325967119891435. doi:10.1177/2325967119891435.

24. Bennett JE, Bry WI, Collins GM, Halasz NA. The effects of oxygen free radicals on the preserved kidney. *Cryobiology*. 1987;24:264-269.

25. Benson JD, Kearsley AJ, Higgins AZ. Mathematical optimization of procedures for cryoprotectant equilibration using a toxicity cost function. *Cryobiology*. 2012;64(3):144-151. doi:10.1016/j.cryobiol.2012.01.001.

26. Best BP. Cryoprotectant toxicity: facts, issues, and questions. *Rejuvenation Res*. 2015;18(5):422-436. doi:10.1089/rej.2014.1656.

27. Bischof J. Nanowarming: a new concept in tissue and organ preservation. *Cryobiology*. 2015;71(1):167. doi:10.1016/J.CRYOBIOL.2015.05.017.

28. Bos-Mikich A, Marques L, Rodrigues JL, Lothhammer N, Frantz N. The use of a metal container for vitrification of mouse ovaries, as a clinical grade model for human ovarian tissue cryopreservation, after different times and temperatures of transport. *J Assist Reprod Genet*. 2012;29(11):1267-1271. doi:10.1007/s10815-012-9867-y.

29. Branco CS, Garcez ME, Pasqualotto FF, Erdtman B, Salvador M. Resveratrol and ascorbic acid prevent DNA damage induced by cryopreservation in human semen. *Cryobiology*. 2009;60:235-237. doi:10.1016/j.cryobiol.2009.10.012.

30. Brockbank KGM, Chen ZZ, Song YC. Vitrification of porcine articular cartilage. *Cryobiology*. 2010;60(2):217-221. doi:10.1016/j.cryobiol.2009.12.003.

31. Brockbank KGM, Rahn E, Wright GJ, Chen Z, Yao H. Impact of hypothermia upon chondrocyte viability and cartilage matrix permeability after 1 month of refrigerated storage. *Transfus Med Hemother*. 2011;38:387-392. doi:10.1159/000334595.

32. Bucak MN, Tuncer PB, Sarıözkan S, et al. Effects of antioxidants on post-thawed bovine sperm and oxidative stress parameters: Antioxidants protect DNA integrity against cryodamage. *Cryobiology*. 2010;61:248-253. doi:10.1016/j.cryobiol.2010.09.001.

33. Buckwalter JA. Articular cartilage: injuries and potential for healing. *J Orthop Sport Phys Ther*. 1998;28(4):192-202. doi:10.2519/jospt.1998.28.4.192.

34. Buckwalter JA, Mankin HJ. Articular cartilage: degeneration and osteoarthritis, repair, regeneration, and transplantation. *Instr Course Lect*. 1998;47:487-504.

35. Buckwalter JA, Mankin HJ. Articular cartilage repair and transplantation. *Arthritis Rheum*. 1998;41(8):1331-1342. doi:10.1002/1529-0131(199808)41:8<1331::AID-ART2>3.0.CO;2-J.

36. Budiani-Saberi DA, Delmonico FL. Organ trafficking and transplant tourism: a commentary on the global realities. *Am J Transplant*. 2008;8(5):925-929.

37. Bugbee WD, Pallante-Kichura AL, Görtz S, Amiel D, Sah R. Osteochondral allograft transplantation in cartilage repair: graft storage paradigm, translational models, and clinical applications. *J Orthop Res*. 2016;34(1):31-38. doi:10.1002/jor.22998.

38. Cavendish PA, Everhart JS, Peters NJ, Sommerfeldt MF, Flanigan DC. Osteochondral allograft transplantation for knee cartilage and osteochondral defects: a review of indications, technique, rehabilitation, and outcomes. *JBJS Rev*. 2019;7(6):e7. doi:10.2106/JBJS.RVW.18.00123.

39. Cetinkaya G, Arat S. Cryopreservation of cartilage cell and tissue for biobanking. *Cryobiology*. 2011;63(3):292-297. doi:10.1016/j.cryobiol.2011.09.143.

40. Chen G, Ren L, Zhang J, Reed BM, Zhang D, Shen X. Cryopreservation affects ROS-induced oxidative stress and antioxidant response in Arabidopsis seedlings. *Cryobiology*. 2015;70(1):38-47.

41. Chen H, Sun J, Hoemann CD, et al. Drilling and microfracture lead to different bone structure and necrosis during bone-marrow stimulation for cartilage repair. *J Orthop Res*. 2009;27(11):1432-1438. doi:10.1002/jor.20905.

42. Chen SU, Lien YR, Chao Kh, Lu HF, Ho HN YY. Cryopreservation of mature human oocytes by vitrification with ethylene glycol in straws. *Fertil Steril*. 2000;74(4):804-808. doi:10.1016/S0015-0282(00)01516-8.

43. Chen Y. Scratch wound healing assay. *BIO-PROTOCOL*. 2012;2(5). doi:10.21769/BioProtoc.100.

44. Chi HJ, Koo JJ, Kim MY, Joo JY, Chang SS, Chung KS. Cryopreservation of human embryos using ethylene glycol in controlled slow freezing. *Hum Reprod*. 2002;17(8):2146-2151.

45. Clark AG, Rohrbaugh AL, Otterness I, Kraus VB. The effects of ascorbic acid on cartilage metabolism in guinea pig articular cartilage explants. *Matrix Biol*. 2002;21(2):175-184.

46. Cotter EJ, Hannon CP, Christian DR, et al. Clinical outcomes of multifocal osteochondral allograft transplantation of the knee: an analysis of overlapping grafts and multifocal lesions. *Am J Sports Med*. 2018;46(12):2884-2893. doi:10.1177/0363546518793405.

47. Crawford DC, Heveran CM, Cannon WD, Foo LF, Potter HG. An autologous cartilage tissue implant neocart for treatment of grade III chondral injury to the distal femur: Prospective clinical safety trial at 2 years. *Am J Sports Med*. 2009;37(7):1334-1343. doi:10.1177/0363546509333011.

48. Crowe JH, Hoekstra FA, Crowe LM, Anchordoguy TJ, Drobnis E. Lipid phase transitions measured in intact cells with Fourier transform infrared spectroscopy. *Cryobiology*. 1989;26(1):76-84. http://www.ncbi.nlm.nih.gov/pubmed/2924595. Accessed November 28, 2017.

49. Curran RC, Gibson T. The uptake of labelled sulphate by human cartilage cells and its use as a test for viability. *Proc R Soc London Ser B, Biol Sci*. 1956;144(917):572-576.

50. Daly J, Zuchowicz N, Nuñez Lendo CI, et al. Successful cryopreservation of coral larvae using vitrification and laser warming. *Sci Rep*. 2018;8(1):15714. doi:10.1038/s41598-018-34035-0.

51. Damien M, Luciano AA, Peluso JJ. Propanediol alters intracellular pH and developmental potential of mouse zygotes independently of volume change. *Hum Reprod*. 1990;5(2):212-216.

52. David Pegg E, Wusteman MC, Wang L. Cryopreservation of articular cartilage. Part 1: Conventional cryopreservation methods. *Cryobiology*. 2006;52:335-346. doi:10.1016/j.cryobiol.2006.01.005.

53. Davidson AF, Glasscock C, Mcclanahan DR, Benson JD, Higgins AZ. Toxicity minimized cryoprotectant addition and removal procedures for adherent endothelial cells. He X, ed. *PLoS One*. 2015;10(11):e0142828. doi:10.1371/journal.pone.0142828.

54. Design I for PP. DIPPR Project 801 - Full Version. 2016.

55. Doebbler GF. Cryoprotective compounds: Review and discussion of structure and function. *Cryobiology*. 1966;3(1):2-11. doi:10.1016/S0011-2240(66)80144-X.

56. Doebbler GF, Sakaida RR, Cowley CW, Rinfret AP. Cryogenic preservation of whole blood for transfusion in vitro study of a process using rapid freezing, thawing and protection by polyvinylpyrrolidone. *Transfusion*. 1962;6(2):104-111.

57. Dowthwaite GP, Bishop JC, Redman SN, et al. The surface of articular cartilage contains a progenitor cell populations. *J Cell Sci*. 2004;117(6):889-897. doi:10.1242/jcs.00912.

58. Ehrlich LE, Fahy GM, Wowk BG, Malen JA, Rabin Y. Thermal analyses of a human kidney and a rabbit kidney during cryopreservation by vitrification. *J Biomech Eng*. 2017;140(1):011005. doi:10.1115/1.4037406.

59. Eisenberg DP, Bischof JC, Rabin Y. Thermomechanical stress in cryopreservation via vitrification with nanoparticle heating as a stress-moderating effect. *J Biomech Eng*. 2016;138(1). doi:10.1115/1.4032053.

60. Elliott GD, Wang S, Fuller BJ. Cryoprotectants: a review of the actions and applications of cryoprotective solutes that modulate cell recovery from ultra-low temperatures. *Cryobiology*. 2017;76:74-91. doi:10.1016/j.cryobiol.2017.04.004.

61. Elliott JAW, Prickett RC, Elmoazzen HY, Porter KR, McGann LE. A multisolute osmotic virial equation for solutions of interest in biology. *J Phys Chem B*. 2007;111:1775-1785.

62. Elmoazzen HY, Elliott JAW, Mcgann LE. Osmotic transport across cell membranes in nondilute solutions: a new nondilute solute transport equation. *Biophys J*. 2009;96(7):2559-2571. doi:10.1016/j.bpj.2008.12.3929.

63. Elmoazzen HY, Poovadan A, Law GK, Elliott JAW, McGann LE, Jomha NM. Dimethyl sulfoxide toxicity kinetics in intact articular cartilage. *Cell Tissue Bank*. 2007;8(2):125. doi:10.1007/s10561-006-9023-y.

64. Etheridge ML, Xu Y, Rott L, Choi J, Glasmacher B, Bischof JC. RF heating of magnetic nanoparticles improves the thawing of cryopreserved biomaterials. *Technology*. 2014;02(03):229-242. doi:10.1142/s2339547814500204.

65. Fahmy MD, Almansoori KA, Laouar L, et al. Dose-injury relationships for cryoprotective agent injury to human chondrocytes. *Cryobiology*. 2014;68(1):50-56. doi:10.1016/j.cryobiol.2013.11.006.

66. Fahy GM, Wowk B, Wu J PS. Improved vitrification solutions based on the predictability of vitrification solution toxicity. *Cryobiology*. 2004;48(1):22-35. doi:10.1016/J.CRYOBIOL.2003.11.004.

67. Fahy GM. Prevention of toxicity from high concentrations of cryoprotective agents. In: *Organ Preservation*. Springer; 1982:367-369. doi:10.1007/978-94-011-6267-8_53.

68. Fahy GM, Lilley TH, Linsdell H, Douglas MSJ, Meryman HT. Cryoprotectant toxicity

and cryoprotectant toxicity reduction: in search of molecular mechanisms. *Cryobiology*. 1990;27(3):247-268. doi:10.1016/0011-2240(90)90025-Y.

69. Fahy GM, MacFarlane DR, Angell CA, Meryman HT. Vitrification as an approach to cryopreservation. *Cryobiology*. 1984;21(4):407-426.

70. Fahy GM, Wowk B. Principles of cryopreservation by vitrification. In: *Methods in Molecular Biology (Clifton, N.J.)*. Vol 1257. ; 2015:21-82. doi:10.1007/978-1-4939-2193-5_2.

71. Fang Y, Chu L, Li L, et al. Tetramethylpyrazine protects bone marrow-derived mesenchymal stem cells against hydrogen peroxide-induced apoptosis through PI3K/Akt and ERK1/2 pathways. *Biol Pharm Bull*. 2017;40(12):2146-2152. doi:10.1248/bpb.b17-00524.

72. Farr J, Tabet SK, Margerrison E, Cole BJ. Clinical, radiographic, and histological outcomes after cartilage repair with particulated juvenile articular cartilage. *Am J Sports Med*. 2014;42(6):1417-1425. doi:10.1177/0363546514528671.

73. Farrant J. Mechanism of cell damage during freezing and thawing and its prevention. *Nature*. 1965;205(4978):1284-1287. doi:10.1038/2051284a0.

74. Farrant J, Walter CA, Lee H, McGann LE. Use of two-step cooling procedures to examine factors influencing cell survival following freezing and thawing. *Cryobiology*. 1977;14(3):273-286. http://www.ncbi.nlm.nih.gov/pubmed/891223.

75. Fioravanti A, Collodel G. In vitro effects of chondroitin sulfate. *Adv Pharmacol*. 2006;53:449-465. doi:10.1016/S1054-3589(05)53022-9.

76. Flik KR, Verma N, Cole BJ, Bach BR. Articular cartilage structure, biology, and function. In: *Cartilage Repair Strategies*. Humana Press; 2007:1-12. doi:10.1007/978-1-59745-343-

1_1.

77. Fujita R, Hui T, Chelly M, Demetriou AA. The Effect of Antioxidants and a Caspase Inhibitor on Cryopreserved Rat Hepatocytes. *Cell Transplant*. 2005;14:391-396.

78. Gao D, Critser JK. Mechanisms of cryoinjury in living cells. *ILAR J*. 2000;41(4):187-196. doi:10.1093/ilar.41.4.187.

79. Gao L, Goebel LKH, Orth P, Cucchiarini M, Madry H. Subchondral drilling for articular cartilage repair: A systematic review of translational research. *DMM Dis Model Mech*. 2018;11(6). doi:10.1242/dmm.034280.

80. Gao X, Zhao X, Zhu Y, et al. Tetramethylpyrazine protects palmitate-induced oxidative damage and mitochondrial dysfunction in C2C12 myotubes. *Life Sci*. 2011;88(17-18):803-809. doi:10.1016/j.lfs.2011.02.025.

81. Gardner TB, Manning HL, Beelen AP, Cimis RJ, Cates JMM, Lewis LD. Ethylene glycol toxicity associated with ischemia, perforation, and colonic oxalate crystal deposition. *J Clin Gastroenterol*. 2004;38(5):435-439.

82. Gigout A, Buschmann MD, Jolicoeur M. The fate of Pluronic F-68 in chondrocytes and CHO cells. *Biotechnol Bioeng*. 2008;100(5):975-987. doi:10.1002/bit.21840.

83. Goodfriend B, Essilfie AA, Jones IA, Thomas Vangsness C. Fresh osteochondral grafting in the United States: the current status of tissue banking processing. *Cell Tissue Bank*. 2019;20(3):331-337. doi:10.1007/s10561-019-09768-5.

84. Görtz S, Bugbee WD. Fresh osteochondral allografts: graft processing and clinical applications. *J Knee Surg*. 2006;19(3):231-240. https://europepmc.org/abstract/med/16893164. Accessed November 11, 2019.

85. Gosden R. Cryopreservation: a cold look at technology for fertility preservation. *Fertil*

Steril. 2011;96(2):264-268. doi:10.1016/j.fertnstert.2011.06.029.

86. Gross AE, Agnidis Z, Hutchison CR. Osteochondral defects of the talus treated with fresh osteochondral allograft transplantation. *Foot Ankle Int*. 2001;22(5):385-391. doi:10.1177/107110070102200505.

87. Gross AE, McKee NH, Pritzker KPH, Langer F. Reconstruction of skeletal deficits at the knee a comprehensive osteochondral transplant program. *Clin Orthop Relat Res*. 1983;174:96-106.

88. Guo L, Wang A, Sun Y, Xu C. Evaluation of antioxidant and immunity function of tetramethylpyrazine phosphate tablets in vivo. *Molecules*. 2012;17(5):5412-5421. doi:10.3390/molecules17055412.

89. Hahn J, Laouar L, Elliott JAW, Korbutt GS, Jomha NM. The effect of additive compounds on glycerol-induced damage to human chondrocytes. *Cryobiology*. 2017;75:68-74. doi:10.1016/j.cryobiol.2017.02.002.

90. Hammerstedt RH, Graham JK. Cryopreservation of poultry sperm: the enigma of glycerol. *Cryobiology*. 1992;29(1):26-38.

91. Hangody L, Feczkó P, Bartha L, Bodó G, Kish G. Mosaicplasty for the treatment of articular defects of the knee and ankle. *Clin Orthop Relat Res*. 2001;(391 Suppl):S328-36.

92. Hashimoto S, Takahashi K, Amiel D, Coutts RD, Lotz M. Chondrocyte apoptosis and nitric oxide production during experimentally induced osteoarthritis. *Arthritis Rheumatol*. 1998;41(7):1266-1274.

93. Hatic SO, Berlet GC. Particulated juvenile articular cartilage graft (DeNovo NT Graft) for treatment of osteochondral lesions of the talus. *Foot Ankle Spec*. 2010;3(6):361-364. doi:10.1177/1938640010388602.

94. Hattori S, Oxford C, Reddi AH. Identification of superficial zone articular chondrocyte stem/progenitor cells. *Biochem Biophys Res Commun*. 2007;358(1):99-103. doi:10.1016/j.bbrc.2007.04.142.

95. Hendrickson DA, Nixon AJ, Grande DA, et al. Chondrocyte-fibrin matrix transplants for resurfacing extensive articular cartilage defects. *J Orthop Res*. 1994;12(4):485-497. doi:10.1002/jor.1100120405.

96. Hess R, Bartels MJ, Pottenger LH. Ethylene glycol: an estimate of tolerable levels of exposure based on a review of animal and human data. *Arch Toxicol*. 2004;78(12):671-680.

97. Heyner S. The survival of embryonic mammalian cartilage after freezing to--79 degrees C. *J Exp Zool*. 1960;144:165-176.

98. Hjelle K, Solheim E, Strand T, Muri R, Brittberg M. Articular cartilage defects in 1,000 knee arthroscopies. *Arthrosc J Arthrosc Relat Surg*. 2002;18(7):730-734. doi:10.1053/JARS.2002.32839.

99. Huang J, He Y, Lai G. Tetramethylpyrazine inhibits interleukin-1β-induced iNOS expression and NO synthesis in rabbit articular chondrocytes [J]. *J Third Mil Med Univ*. 2012;16:15.

100. Hunziker EB. Articular cartilage repair: basic science and clinical progress. a review of the current status and prospects. *Osteoarthr Cartil*. 2002;10(6):432-463.

101. Hunziker EB, Quinn TM, Häuselmann HJ. Quantitative structural organization of normal adult human articular cartilage. *Osteoarthr Cartil*. 2002;10(7):564-572. doi:10.1053/joca.2002.0814.

102. Huskisson E. Glucosamine and chondroitin for osteoarthritis. *J Int Med Res*.

2008;36(6):1161-1179. doi:10.1177/147323000803600602.

103. Ishimori H, Takahashi Y, Kanagawa H. Factors affecting survival of mouse blastocysts vitrified by a mixture of ethylene glycol and dimethyl sulfoxide. *Theriogenology*. 1992;38(6):1175-1185.

104. Jakob RP, Franz T, Gautier E, Mainil-Varlet P. Autologous osteochondral grafting in the knee: indication, results, and reflections. *Clin Orthop Relat Res*. 2002;(401):170-184. doi:10.1097/00003086-200208000-00020.

105. Jang TH, Park SC, Yang JH, et al. Cryopreservation and its clinical applications. *Integr Med Res*. 2017.

106. Janjic D, Andereggen E, Deng S, et al. Improved insulin secretion of cryopreserved human islets by antioxidant treatment. *Pancreas*. 1996;13(2):166-172.

107. Jiang Y, Tuan RS. Origin and function of cartilage stem/progenitor cells in osteoarthritis. *Nat Rev Rheumatol*. 2015;11(4):206-212. doi:10.1038/nrrheum.2014.200.

108. Johnson AA, Naaldijk Y, Hohaus C, Meisel HJ. Protective effects of alpha phenyl-tert-butyl nitrone and ascorbic acid in human adipose derived mesenchymal stem cells from differently aged donors. *Aging (Albany NY)*. 2017;9(2):340.

109. Johnson K, Zhu S, Tremblay MS, et al. A stem cell-based approach to cartilage repair. *Science (80-)*. 2012;336(6082):717-721. doi:10.1126/science.1215157.

110. Jomha NM, Anoop PC, Bagnall K, McGann LE. Effects of increasing concentrations of dimethyl sulfoxide during cryopreservation of porcine articular cartilage. *Cell Preserv Technol*. 2002;1(2):111-120. doi:10.1089/153834402320882610.

111. Jomha NM, Anoop PC, Elliott JA, Bagnall K, McGann LE. Validation and reproducibility of computerised cell-viability analysis of tissue slices. *BMC Musculoskelet Disord*.

2003;4(1):5. doi:10.1186/1471-2474-4-5.

112. Jomha NM, Anoop PC, McGann LE. Intramatrix events during cryopreservation of porcine articular cartilage using rapid cooling. *J Orthop Res*. 2004;22:152-157. doi:10.1016/S0736-0266(03)00158-X.

113. Jomha NM, Elliott JAW, Law GK, et al. Vitrification of intact human articular cartilage. *Biomaterials*. 2012;33(26):6061-6068. doi:10.1016/j.biomaterials.2012.05.007.

114. Jomha NM, Lavoie G, Muldrew K, Schachar NS, McGann LE. Cryopreservation of intact human articular cartilage. *J Orthop Res*. 2002;20(6):1253-1255.

115. Jomha NM, Law GK, Abazari A, Rekieh K, Elliott JAW, McGann LE. Permeation of several cryoprotectant agents into porcine articular cartilage. *Cryobiology*. 2009;58(1):110-114. doi:10.1016/j.cryobiol.2008.11.004.

116. Jomha NM, Weiss ADH, Forbes JF, Law GK, Elliott JAW, McGann LE. Cryoprotectant agent toxicity in porcine articular chondrocytes. *Cryobiology*. 2010;61(3):297-302.

117. Jones CW, Willers C, Keogh A, et al. Matrix-induced autologous chondrocyte implantation in sheep: objective assessments including confocal arthroscopy. *J Orthop Res*. 2008;26(3):292-303. doi:10.1002/jor.20502.

118. Jones KJ, Mosich GM, Williams RJ. Fresh precut osteochondral allograft core transplantation for the treatment of femoral cartilage defects. *Arthrosc Tech*. 2018;7(8):e791-e795. doi:10.1016/j.eats.2018.03.016.

119. Jones KJ, Sheppard WL, Arshi A, Hinckel BB, Sherman SL. Articular cartilage lesion characteristic reporting is highly variable in clinical outcomes studies of the knee. *Cartilage*. 2019;10(3):299-304. doi:10.1177/1947603518756464.

120. Ju X, Deng M, Ao Y, et al. The protective effect of tetramethylpyrazine on cartilage

explants and chondrocytes. *J Ethnopharmacol*. 2010;132(2):414-420. doi:10.1016/J.JEP.2010.08.020.

121. Judas F, Rosa S, Teixeira L, C Lopes A, Mendes F. Chondrocyte viability in fresh and frozen large human osteochondral allografts: effect of cryoprotective agents. *Transplant Proc*. 2007;39(8):2531-2534. doi:10.1016/J.TRANSPROCEED.2007.07.028.

122. Kao T-K, Chang C-Y, Ou Y-C, et al. Tetramethylpyrazine reduces cellular inflammatory response following permanent focal cerebral ischemia in rats. *Exp Neurol*. 2013;247:188-201. doi:10.1016/j.expneurol.2013.04.010.

123. Karlsson C, Lindahl A. Articular cartilage stem cell signalling. *Arthritis Res Ther*. 2009;11(4):121. doi:10.1186/ar2753.

124. Karow AM. Cryoprotectants-a new class of drugs. *J Pharm Pharmacol*. 1969;21(4):209-223. doi:10.1111/j.2042-7158.1969.tb08235.x.

125. Kasai M, Mukaida T. Cryopreservation of animal and human embryos by vitrification. *Reprod Biomed Online*. 2004;9(2):164-170.

126. Katkov I, Bolyukh VF, Snyder EY, Agarwal S. Krioblast^{TM}, a system for kinetic vitrification by hyperfast cooling: applications for reproductive & stem cells. *Fertility_and_Sterility*. 2013;100:3.

127. Kawabe N, Yoshinao M. Cryopreservation of cartilage. *Int Orthop*. 1990;14(3):231-235.

128. Kempson GE. Relationship between the tensile properties of articular cartilage from the human knee and age. *Ann Rheum Dis*. 1982;41:508-511.

129. Kim YM, Uhm SJ, Gupta MK, et al. Successful vitrification of bovine blastocysts on paper container. *Theriogenology*. 2012;78(5):1085-1093. doi:10.1016/J.THERIOGENOLOGY.2012.05.004.

130. Klinc P, Rath D. Reduction of oxidative stress in bovine spermatozoa during flow cytometric sorting. *Reprod Domest Anim*. 2007;42(1):63-67. doi:10.1111/j.1439-0531.2006.00730.x.

131. Koelling S, Miosge N. Stem cell therapy for cartilage regeneration in osteoarthritis. *Expert Opin Biol Ther*. 2009;9(11):1399-1405. doi:10.1517/14712590903246370.

132. Kon E, Buda R, Filardo G, et al. Platelet-rich plasma: intra-articular knee injections produced favorable results on degenerative cartilage lesions. *Knee Surgery, Sport Traumatol Arthrosc*. 2010;18(4):472-479. doi:10.1007/s00167-009-0940-8.

133. Krill M, Early N, Everhart JS, Flanigan DC. Autologous chondrocyte implantation (ACI) for knee cartilage defects. *JBJS Rev*. 2018;6(2):e5. doi:10.2106/JBJS.RVW.17.00078.

134. Kroener C, Luyet B. Formation of cracks during the vitrification of glycerol solutions and disappearance of the cracks during rewarming. *Biodynamica*. 1966;10(198):47-52.

135. Labens R, Daniel C, Hall S, Xia XR, Schwarz T. Effect of intra-articular administration of superparamagnetic iron oxide nanoparticles (SPIONs) for MRI assessment of the cartilage barrier in a large animal model. *PLoS One*. 2017;12(12):e0190216. doi:10.1371/journal.pone.0190216.

136. Lai D, Ding J, Smith GW, Smith GD, Takayama S. Slow and steady cell shrinkage reduces osmotic stress in bovine and murine oocyte and zygote vitrification. *Hum Reprod*. 2015;30(1):37-45. doi:10.1093/humrep/deu284.

137. Lai WM, Hou JS, Mow VC. A triphasic theory for the swelling and deformation behaviors of articular cartilage. *J Biomech Eng*. 1991;113(3). doi:10.1115/1.2894880.

138. LaPrade RF, Botker J, Herzog M, Agel J. Refrigerated osteoarticular allografts to treat articular cartilage defects of the femoral condyles. *J Bone Jt Surgery-American Vol*.

2009;91(4):805-811. doi:10.2106/JBJS.H.00703.

139. Lawson A, Mukherjee I, Sambanis A. Mathematical modeling of cryoprotectant addition and removal for the cryopreservation of engineered or natural tissues. *Cryobiology*. 2012;64(1):1-11.

140. Lemmon, E.W., Huber, M.L., McLinden MO. NIST standard reference database 23: reference fluid thermodynamic and transport properties-REFPROP. 2007.

141. Levine DW, Mondano L, Halpin M. FDA regulatory pathways for knee cartilage repair products. *Sports Med Arthrosc*. 2008;16(4):202-207. doi:10.1097/JSA.0b013e31818cdb97.

142. Liang Y, Idrees E, Szojka ARA, et al. Chondrogenic differentiation of synovial fluid mesenchymal stem cells on human meniscus-derived decellularized matrix requires exogenous growth factors. *Acta Biomater*. 2018;80:131-143. doi:10.1016/J.ACTBIO.2018.09.038.

143. Liu C-F, Lin C-H, Chen C-F, Huang T-C, Lin S-C. Antioxidative effects of tetramethylpyrazine on acute ethanol-induced lipid peroxidation. *Am J Chin Med*. 2005;33(06):981-988. doi:10.1142/S0192415X05003570.

144. Loeser RF. Aging and osteoarthritis: the role of chondrocyte senescence and aging changes in the cartilage matrix. *Osteoarthr Cartil*. 2009;17(8):971-979.

145. Losina E, Paltiel AD, Weinstein AM, et al. Lifetime Medical Costs of Knee Osteoarthritis Management in the United States: Impact of Extending Indications for Total Knee Arthroplasty. *Arthritis Care Res (Hoboken)*. 2015;67(2):203-215. doi:10.1002/acr.22412.

146. Loutradi KE, Kolibianakis EM, Venetis CA, et al. Cryopreservation of human embryos by vitrification or slow freezing: a systematic review and meta-analysis. *Fertil Steril*.

2008;90(1):186-193. doi:10.1016/j.fertnstert.2007.06.010.

147. Lovelock JE. The protective action of neutral solutes against haemolysis by freezing and thawing. *Biochem J*. 1954;56(2):265-270. doi:10.1042/bj0560265.

148. Lovelock JE, Polge C. The immobilization of spermatozoa by freezing and thawing and the protective action of glycerol. *Biochem J*. 1954;58(4):618-622. doi:10.1042/bj0580618.

149. Luyet BJ, Gehenio PM. The mechanism of injury and death by low temperature. A review. *Biodynamica*. 1940;3(60):33-99.

150. Macfadyen MA, Daniel Z, Kelly S, et al. The commercial pig as a model of spontaneously-occurring osteoarthritis. *BMC Musculoskelet Disord*. 2019;20(1). doi:10.1186/s12891-019-2452-0.

151. Malinin TI, Wagner JL, Pita JC, Lo H. Hypothermic storage and cryopreservation of cartilage: an experimental study. *Clin Orthop Relat Res*. 1985;(197):15-26. http://www.ncbi.nlm.nih.gov/pubmed/4017330. Accessed March 15, 2020.

152. Manuchehrabadi N, Gao Z, Zhang J, et al. Improved tissue cryopreservation using inductive heating of magnetic nanoparticles. *Sci Transl Med*. 2017;9(379):eaah4586. doi:10.1126/scitranslmed.aah4586.

153. Manuchehrabadi N, Shi M, Roy P, et al. Ultrarapid inductive rewarming of vitrified biomaterials with thin metal forms. *Ann Biomed Eng*. June 2018. doi:10.1007/s10439-018-2063-1.

154. Marks R. Articular cartilage regeneration: an update of possible treatment approaches. *Int J Orthop*. 2017;4(4):770-778. doi:10.17554/IJO.V4I4.2010.

155. Mazur P. Cryobiology: the freezing of biological systems. *Science (80-)*. 1970;168(3934):939-949. doi:10.1126/science.168.3934.939.

156. Mazur P. Freezing of living cells: mechanisms and implications. *Am J Physiol Physiol*. 1984;247(3):C125-C142. doi:10.1152/ajpcell.1984.247.3.c125.

157. Mazur P. The role of intracellular freezing in the death of cells cooled at supraoptimal rates. *Cryobiology*. 1977;14(3):251-272. doi:10.1016/0011-2240(77)90175-4.

158. Mazur P, Leibo SP, Chu EHY. A two-factor hypothesis of freezing injury: evidence from chinese hamster tissue-culture cells. *Exp Cell Res*. 1972;71(2):345-355. doi:10.1016/0014-4827(72)90303-5.

159. McCormick F, Yanke A, Provencher MT, Cole BJ. Minced articular cartilage - basic science, surgical technique, and clinical application. *Sports Med Arthrosc*. 2008;16(4):217-220. doi:10.1097/JSA.0b013e31818e0e4a.

160. McCoy B, Miniaci A. Osteochondral autograft transplantation/mosaicplasty. *J Knee Surg*. 2012;25(2):99-108. doi:10.1055/s-0032-1322508.

161. McGann LE, Stevenson M, Muldrew K, Schachar N. Kinetics of osmotic water movement in chondrocytes isolated from articular cartilage and applications to cryopreservation. *J Orthop Res*. 1988;6(1):109-115. doi:10.1002/jor.1100060114.

162. Meryman HT. Cryopreservation of living cells: principles and practice. *Transfusion*. 2007;47(5):935-945. doi:10.1111/j.1537-2995.2007.01212.x.

163. Meryman HT. Cryoprotective agents. *Cryobiology*. 1971;8(2):173-183. doi:10.1016/0011-2240(71)90024-1.

164. Minas T, Ogura T, Bryant T. Autologous chondrocyte implantation. *JBJS Essent Surg Tech*. 2016;6(2). doi:10.2106/JBJS.ST.16.00018.

165. Mukherjee IN, Li Y, Song YC, Long RC, Sambanis A. Cryoprotectant transport through articular cartilage for long-term storage: experimental and modeling studies. *Osteoarthr*

Cartil. 2008;16(11):1379-1386. doi:10.1016/j.joca.2008.03.027.

166. Muldrew K. The osmotic rupture hypothesis and its application to the cryopreservation of articular cartilage. 1995. https://www.elibrary.ru/item.asp?id=5683664. Accessed March 17, 2020.

167. Muldrew K, Hurtig M, Novak K, Schachar N, McGann LE. Localization of freezing injury in articular cartilage. *Cryobiology*. 1994;31(1):31-38. doi:10.1006/cryo.1994.1004.

168. Muldrew K, McGann LE. The osmotic rupture hypothesis of intracellular freezing injury. *Biophys J*. 1994;66(2 Pt 1):532-541. doi:10.1016/S0006-3495(94)80806-9.

169. Muldrew K, Novak K, Yang H, Zernicke R, Schachar NS, McGann LE. Cryobiology of articular cartilage: ice morphology and recovery of chondrocytes. *Cryobiology*. 2000;40(2):102-109. doi:10.1006/CRYO.2000.2236.

170. Muldrew K, Sykes B, Schachar N, McGann L. Permeation kinetics of dimethyl sulfoxide in articular cartilage. *CryoLetters*. 1996;17:331-340.

171. Nash T. The chemical constitution of compounds which protect erythrocytes against freezing damage. *J Gen Physiol*. 1962;46(1):167-175. doi:10.1085/JGP.46.1.167.

172. Nawaz SZ, Bentley G, Briggs TWR, et al. Autologous chondrocyte implantation in the knee: mid-term to long-term results. *J Bone Jt Surg - Am Vol*. 2014;96(10):824-830. doi:10.2106/JBJS.L.01695.

173. Nikolaou V., Giannoudis P. History of osteochondral allograft transplantation. *Injury*. 2017;48(7):1283-1286. doi:10.1016/j.injury.2017.05.005.

174. Nixon AJ, Sparks HD, Begum L, et al. Matrix-Induced autologous chondrocyte implantation (MACI) using a cell-seeded collagen membrane improves cartilage healing in the equine model. *J Bone Jt Surg - Am Vol*. 2017;99(23):1987-1998.

doi:10.2106/JBJS.16.00603.

175. Noh MJ, Copeland RO, Yi Y, et al. Pre-clinical studies of retrovirally transduced human chondrocytes expressing transforming growth factor-beta-1 (TG-C). *Cytotherapy*. 2010;12(3):384-393. doi:10.3109/14653240903470639.

176. Odink J, Sprokholt R. The influence of DMSO and cooling conditions on the cryopreservation of human platelets in Platelet Preservation and Transfusion. In: *Blood Transfusion Symposium*. ; 1964.

177. Oldenhof H, Gojowsky M, Wang S, et al. Osmotic stress and membrane phase changes during freezing of stallion sperm: mode of action of cryoprotective agents. *Biol Reprod*. 2013;8868(3):1-11. doi:10.1095/biolreprod.112.104661.

178. Onari I, Hayashi M, Ozaki N, Tsuchiya H. Vitreous preservation of articular cartilage from cryoinjury in rabbits. *Cryobiology*. 2012;65(2):98-103. doi:10.1016/j.cryobiol.2012.05.006.

179. Outerbridge, RE. The etiology of chondromalacia patellae. *J Bone Joint Surg Br*. 1961;43-B:752-757. doi:10.1302/0301-620x.43b4.752.

180. Page B, Page M, Noel C. A new fluorometric assay for cytotoxicity measurements in-vitro. *Int J Oncol*. 1993;3(3):473-476.

181. Pan J, Ren S, Sekar PK, et al. Investigation of electromagnetic resonance rewarming enhanced by magnetic nanoparticles for cryopreservation. *Langmuir*. 2019;35(23):7560-7570. doi:10.1021/acs.langmuir.8b03060.

182. Patterson D, Dieterich J, Bartelstein M, et al. Mid-term results of particulated juvenile articular cartilage allograft transplantation to the knee. *Arthrosc J Arthrosc Relat Surg*. 2017;33(6):e31-e32. doi:10.1016/j.arthro.2017.04.095.

183. Paudel K, Kumar S, Meur S, Kumaresan A. Ascorbic acid, catalase and chlorpromazine reduce cryopreservation-induced damages to crossbred bull spermatozoa. *Reprod Domest Anim*. 2010;45(2):256-262. doi:10.1111/j.1439-0531.2008.01278.x.

184. Pearle AD, Warren RF, Rodeo SA. Basic science of articular cartilage and osteoarthritis. *Clin Sports Med*. 2005;24(1):1-12. doi:10.1016/j.csm.2004.08.007.

185. Pegg, D.E., Wang, L., Vaughan D. Cryopreservation of articular cartilage. Part 3: The liquidus-tracking method. *Cryobiology*. 2006;52(3):360-368. http://www.ncbi.nlm.nih.gov/pubmed/16527263. Accessed November 27, 2017.

186. Pegg DE. Principles of cryopreservation. *Cryopreserv Free Protoc*. 2007:39-57.

187. Pegg DE, Wang L, Vaughan D, Hunt CJ. Cryopreservation of articular cartilage. Part 2: Mechanisms of cryoinjury. *Cryobiology*. 2006;52(3):347-359. doi:10.1016/j.cryobiol.2006.01.007.

188. Pegg DE, Wusteman MC, Boylan S. Fractures in cryopreserved elastic arteries. *Cryobiology*. 1997;34(2):183-192. doi:10.1006/CRYO.1996.1997.

189. Peterson L, Vasiliadis HS, Brittberg M, Lindahl A. Autologous chondrocyte implantation: A long-term follow-up. *Am J Sports Med*. 2010;38(6):1117-1124. doi:10.1177/0363546509357915.

190. Polge C, Smith AU, Parkes AS. Revival of spermatozoa after vitrification and dehydration at low temperatures. *Nature*. 1949;164(4172):666.

191. Porter BB, Lance EM. Limb and joint transplantation. A review of research and clinical experience. *Clin Orthop Relat Res*. 1974;(104):249-274.

192. Prasad TK, Anderson MD, Martin BA, Stewart CR. Evidence for chilling-induced oxidative stress in maize seedlings and a regulatory role for hydrogen peroxide. *Plant*

Cell. 1994;6(1):65-74. doi:10.1105/tpc.6.1.65.

193. Prickett RC, Elliott JAW, McGann LE. Application of the multisolute osmotic virial equation to solutions containing electrolytes. *J Phys Chem B*. 2011;115(49):14531-14543. doi:10.1021/jp206011m.

194. Prickett RC, Elliott JAW, McGann LE. Application of the osmotic virial equation in cryobiology. *Cryobiology*. 2010;60:30-42. doi:10.1016/j.cryobiol.2009.07.011.

195. Rabin Y, Steif PS, Taylor MJ, Julian TB, Wolmark N. An experimental study of the mechanical response of frozen biological tissues at cryogenic temperatures. *Cryobiology*. 1996;33(4):472-482. doi:10.1006/cryo.1996.0048.

196. Rabin Y, Wolmark N, Taylor MJ. Thermal expansion measurements of frozen biological tissues at cryogenic temperatures. *J Biomech Eng*. 1998;120(2):259-266. doi:10.1115/1.2798310.

197. Racz B, Reglodi D, Fodor B, et al. Hyperosmotic stress-induced apoptotic signaling pathways in chondrocytes. *Bone*. 2007;40(6):1536-1543. doi:10.1016/j.bone.2007.02.011.

198. Rall WF, Fahy GM. Ice-free cryopreservation of mouse embryos at −196 °C by vitrification. *Nature*. 1985;313(6003):573-575. doi:10.1038/313573a0.

199. Rall WF, Meyer TK. Zona fracture damage and its avoidance during the cryopreservation of mammalian embryos. *Theriogenology*. 1989;31(3):683-692. doi:10.1016/0093-691X(89)90251-3.

200. Riboh JC, Cole BJ, Farr J. Particulated articular cartilage for symptomatic chondral defects of the knee. *Curr Rev Musculoskelet Med*. 2015;8(4):429-435. doi:10.1007/s12178-015-9300-0.

201. Riff AJ, Davey A, Cole BJ. Emerging technologies in cartilage restoration. In: *Joint*

Preservation of the Knee: A Clinical Casebook. Springer International Publishing; 2019:295-319. doi:10.1007/978-3-030-01491-9_18.

202. Rowe AW. Biochemical aspects of cryoprotective agents in freezing and thawing. *Cryobiology*. 1966;3(1):12-18. http://www.ncbi.nlm.nih.gov/pubmed/5967970. Accessed November 28, 2017.

203. Rubinsky B. Thermal stresses during solidification processes. *J Heat Transfer*. 1982;104(1):196-199. doi:10.1115/1.3245051.

204. Schachar N, McAllister D, Stevenson M, Novak K, McGann L. Metabolic and biochemical status of articular cartilage following cryopreservation and transplantation: a rabbit model. *J Orthop Res*. 1992;10(5):603-609. doi:10.1002/jor.1100100502.

205. Schachar NS, McGann LE. Investigations of low-temperature storage of articular cartilage for transplantation. *Clin Orthop Relat Res*. 1986;(208):146-150. http://www.ncbi.nlm.nih.gov/pubmed/3720115. Accessed November 3, 2018.

206. Schinhan M, Gruber M, Vavken P, et al. Critical-size defect induces unicompartmental osteoarthritis in a stable ovine knee. *J Orthop Res*. 2012;30(2):214-220. doi:10.1002/jor.21521.

207. Schneiderman R, Keret D, Maroudas A. Effects of mechanical and osmotic pressure on the rate of glycosaminoglycan synthesis in the human adult femoral head cartilage: an in vitro study. *J Orthop Res*. 1986;4(4):393-408. doi:10.1002/jor.1100040402.

208. Shardt N, Chen Z, Yuan SC, Wu K, Laouar L, Jomha NM, Elliott JAW. Using engineering models to shorten cryoprotectant loading time for the vitrification of articular cartilage. *Cryobiology*. 2020; 92: 180-188. doi:doi.org/10.1016/j.cryobiol.2020.01.008.

209. Shardt N, Al-Abbasi KK, Yu H, Jomha NM, McGann LE, Elliott JAW. Cryoprotectant

kinetic analysis of a human articular cartilage vitrification protocol. *Cryobiology*. 2016;73(1):80-92. doi:10.1016/J.CRYOBIOL.2016.05.007.

210. Sharif B, Kopec JA, Wong H, Anis AH. Distribution and Drivers of Average direct cost of osteoarthritis in Canada from 2003 to 2010. *Arthritis Care Res (Hoboken)*. 2017;69(2):243-251. doi:10.1002/acr.22933.

211. Sharma R, Law GK, Rekieh K, et al. A novel method to measure cryoprotectant permeation into intact articular cartilage. *Cryobiology*. 2007;54(2):196-203. doi:10.1016/J.CRYOBIOL.2007.01.006.

212. Shortkroff S, Barone L, Hsu HP, et al. Healing of chondral and osteochondral defects in a canine model: the role of cultured chondrocytes in regeneration of articular cartilage. *Biomaterials*. 1996;17(2):147-154.

213. Shum D, Radu C, Kim E, et al. A high density assay format for the detection of novel cytotoxic agents in large chemical libraries. *J Enzyme Inhib Med Chem*. 2008;23(6):931-945. doi:10.1080/14756360701810082.

214. Siclari A, Mascaro G, Gentili C, Kaps C, Cancedda R, Boux E. Cartilage repair in the knee with subchondral drilling augmented with a platelet-rich plasma-immersed polymer-based implant. *Knee Surgery, Sport Traumatol Arthrosc*. 2014;22(6):1225-1234. doi:10.1007/s00167-013-2484-1.

215. Smith AU. Survival of frozen chondrocytes isolated from cartilage of adult mammals. *Nature*. 1965;205(4973):782-784. doi:10.1038/205782a0.

216. Solanki PK, Bischof JC, Rabin Y. Thermo-mechanical stress analysis of cryopreservation in cryobags and the potential benefit of nanowarming. *Sci Transl Med*. 2017;76:129-139. doi:10.1126/scitranslmed.aah458610.1016/j.cryobiol.2017.02.001.

217. Sommerfeldt MF, Magnussen RA, Hewett TE, Kaeding CC, Flanigan DC. Microfracture of articular cartilage. *JBJS Rev*. 2016;4(6):1. doi:10.2106/JBJS.RVW.15.00005.

218. Song YC, Lightfoot FG, Chen Z, Taylor MJ, Brockbank KGM. Vitreous preservation of rabbit articular cartilage. *Cell Preserv Technol*. 2004;2(1):67-74. doi:10.1089/153834404322708772.

219. Sophia Fox AJ, Bedi A, Rodeo SA. The basic science of articular cartilage: structure, composition, and function. *Sport Heal A Multidiscip Approach*. 2009;1(6):461-468. doi:10.1177/1941738109350438.

220. Spindler R, Wolkers WF, Glasmacher B. Effect of Me2SO on membrane phase behavior and protein denaturation of human pulmonary endothelial cells studied by in situ FTIR spectroscopy. *J Biomech Eng*. 2009;131(7):074517. doi:10.1115/1.3156802.

221. Steadman JR, Miller BS, Karas SG, Schlegel TF, Briggs KK, Hawkins RJ. The microfracture technique in the treatment of full-thickness chondral lesions of the knee in National Football League players. *J Knee Surg*. 2003;16(2):83-86.

222. Steif PS, Noday DA, Rabin Y. Can thermal expansion differences between cryopreserved tissue and cryoprotective agents alone cause cracking? *Cryo Letters*. 2009;30(6):414-421. http://www.ncbi.nlm.nih.gov/pubmed/20309497. Accessed August 16, 2019.

223. Stolberg-Stolberg JA, Furman BD, William Garrigues N, et al. Effects of cartilage impact with and without fracture on chondrocyte viability and the release of inflammatory markers. *J Orthop Res*. 2013;31(8):1283-1292. doi:10.1002/jor.22348.

224. Storey BT, Noiles EE, Thompson KA. Comparison of glycerol, other polyols, trehalose, and raffinose to provide a defined cryoprotectant medium for mouse sperm cryopreservation. *Cryobiology*. 1998;37:46-58.

225. Tas ßdemir U, Büyükleblebici S, Tuncer PB, et al. Effects of various cryoprotectants on bull sperm quality, DNA integrity and oxidative stress parameters. *Cryobiology*. 2013;66(1):38-42.

226. Tatone C, Di Emidio G, Vento M, Ciriminna R, Artini PG. Cryopreservation and oxidative stress in reproductive cells. *Gynecol Endocrinol*. 2010;26(8):563-567. doi:10.3109/09513591003686395.

227. Temple H. Allograft reconstruction of the knee—methods and outcomes. *J Knee Surg*. 2019;32(04):315-321. doi:10.1055/s-0038-1672123.

228. Temple MM, Bae WC, Chen MQ, et al. Age- and site-associated biomechanical weakening of human articular cartilage of the femoral condyle. *Osteoarthr Cartil*. 2007;15(9):1042-1052. doi:10.1016/j.joca.2007.03.005.

229. Tiku ML, Narla H, Jain M, Yalamanchili P. Glucosamine prevents in vitro collagen degradation in chondrocytes by inhibiting advanced lipoxidation reactions and protein oxidation. *Arthritis Res Ther*. 2007;9. doi:10.1186/ar2274.

230. Ting AY, Mullen SF, Zelinski MB. Vitrification of ovarian tissue for fertility preservation. In: *Pediatric and Adolescent Oncofertility*. Springer; 2017:79-97.

231. Toh WS, Foldager CB, Pei M, Hui JHP. Advances in mesenchymal stem cell-based strategies for cartilage repair and regeneration. *Stem Cell Rev Reports*. 2014;10(5):686-696. doi:10.1007/s12015-014-9526-z.

232. Tomford WW, Fredericks GR, Mankin HJ. Studies on cryopreservation of articular cartilage chondrocytes. *J Bone Jt Surg*. 1984;66(2):253-259. doi:10.2106/00004623-198466020-00012.

233. Tompkins M, Adkisson HD, Bonner KF. DeNovo NT allograft. *Oper Tech Sports Med*.

2013;21(2):82-89. doi:10.1053/j.otsm.2013.03.005.

234. Tuncer PB, Bucak MN, Sariözkan S, et al. The effect of raffinose and methionine on frozen/thawed Angora buck (Capra hircus ancryrensis) semen quality, lipid peroxidation and antioxidant enzyme activities. *Cryobiology*. 2010;61(1):89-93. doi:10.1016/j.cryobiol.2010.05.005.

235. Walczak-Jedrzejowska R, Wolski JK, Slowikowska-Hilczer J. The role of oxidative stress and antioxidants in male fertility. *Cent Eur J Urol*. 2013;66(1):60-67. doi:10.5173/ceju.2013.01.art19.

236. Wang J, Zhao G, Zhang Z, Xu X, He X. Magnetic induction heating of superparamagnetic nanoparticles during rewarming augments the recovery of hUCM-MSCs cryopreserved by vitrification. *Acta Biomater*. 2016;33:264-274. doi:10.1016/j.actbio.2016.01.026.

237. Wang L, Pegg DE, Lorrison J, Vaughan D, Rooney P, L Wang, DE Pegg, J Lorrison, D Vaughan PR. Further work on the cryopreservation of articular cartilage with particular reference to the liquidus tracking (LT) method. *Cryobiology*. 2007;55(2):138-147.

238. Wang L, Zhang H-Y, Gao B, et al. Tetramethylpyrazine protects against glucocorticoid-induced apoptosis by promoting autophagy in mesenchymal stem cells and improves bone mass in glucocorticoid-induced osteoporosis rats. *Stem Cells Dev*. 2017.

239. Weiss ADH, Fraser Forbes J, Scheuerman A, et al. Statistical prediction of the vitrifiability and glass stability of multi-component cryoprotective agent solutions. *Cryobiology*. 2010;61(1):123-127. doi:10.1016/J.CRYOBIOL.2010.05.008.

240. Wells T, Davidson C, Mörgelin M, Bird JLE, Bayliss MT, Dudhia J. Age-related changes in the composition, the molecular stoichiometry and the stability of proteoglycan aggregates extracted from human articular cartilage. *Biochem J*. 2003;370(1):69-79.

doi:10.1042/BJ20020968.

241. Williams R. Four modes of nucleation in viscous solutions. *Cryobiology*. 1989;26(6):568.

242. Williams RJ, Dreese JC, Chen CT. Chondrocyte survival and material properties of hypothermically stored cartilage: an evaluation of tissue used for osteochondral allograft transplantation. *Am J Sports Med*. 2004;32(1):132-139. doi:10.1177/0095399703258733.

243. Williams SK, Amiel D, Ball ST, et al. Prolonged storage effects on the articular cartilage of fresh human osteochondral allografts. *J Bone Jt Surg - Ser A*. 2003;85(11):2111-2120. doi:10.2106/00004623-200311000-00008.

244. WilliamsIII RJ, Ranawat AS, Potter HG, Carter T, Warren RF. Fresh stored allografts for the treatment of osteochondral defects of the knee. *J Bone Jt Surg*. 2007;89(4):718-726. doi:10.2106/JBJS.F.00625.

245. Wowk B. Thermodynamic aspects of vitrification. *Cryobiology*. 2010;60(1):11-22.

246. Wright GJ, Brockbank KGM, Rahn E, Halwani DO, Chen Z, Yao H. Impact of storage solution formulation during refrigerated storage upon chondrocyte viability and cartilage matrix. *Cells Tissues Organs*. 2014;199(1):51-58. doi:10.1159/000363134.

247. Wu K, Laouar L, Dong R, Elliott JAW, Jomha NM. Evaluation of five additives to mitigate toxicity of cryoprotective agents on porcine chondrocytes. *Cryobiology*. 2019;88:98-105. doi:10.1016/J.CRYOBIOL.2019.02.004.

248. Wu K, Shardt N, Laouar L, Chen Z, Prasad V, Elliott JAW, Jomha NM. Comparison of three multi-cryoprotectant loading protocols for vitrification of porcine articular cartilage. *Cryobiology*. 2020; 92: 151-160. doi:10.1016/j.cryobiol.2020.01.001.

249. Wusteman M, Robinson M, Pegg D. Vitrification of large tissues with dielectric warming: biological problems and some approaches to their solution. *Cryobiology*. 2004;48(2):179-

189. doi:10.1016/j.cryobiol.2004.01.002.

250. Wydra FB, York PJ, Vidal AF. Allografts: osteochondral, shell, and paste. *Clin Sports Med*. 2017;36(3):509-523. doi:10.1016/j.csm.2017.02.007.

251. Xing R, Liu S, Guo Z, et al. The antioxidant activity of glucosamine hydrochloride in vitro. *Bioorg Med Chem*. 2006;14(6):1706-1709. doi:10.1016/j.bmc.2005.10.018.

252. Xu Y, Sun HJ, Lv Y, Zou JC, Lin BL, Hua TC. Effects of freezing rates and cryoprotectant on thermal expansion of articular cartilage during freezing process. *Cryo Letters*. 2013;34(4):313-323.

253. Yang G, Qian C, Wang N, et al. Tetramethylpyrazine protects against oxygen-glucose deprivation-induced brain microvascular endothelial cells injury via Rho/Rho-kinase signaling pathway. *Cell Mol Neurobiol*. 2017;37(4):619-633.

254. Yang HY, Lee KB. Arthroscopic microfracture for osteochondral lesions of the talus: second-look arthroscopic and magnetic resonance analysis of cartilage repair tissue outcomes. *J Bone Joint Surg Am*. 2020;102(1):10-20. doi:10.2106/JBJS.19.00208.

255. Yanke AB, Tilton AK, Wetters NG, Merkow DB, Cole BJ. DeNovo NT particulated juvenile cartilage implant. *Sports Med Arthrosc*. 2015;23(3):125-129. doi:10.1097/JSA.0000000000000077.

256. Ye W, Zhu S, Liao C, et al. Advanced oxidation protein products induce apoptosis of human chondrocyte through reactive oxygen species-mediated mitochondrial dysfunction and endoplasmic reticulum stress pathways. *Fundam Clin Pharmacol*. 2017;31(1):64-74. doi:10.1111/fcp.12229.

257. Yu H, Al-Abbasi KK, Elliott JAW, McGann LE, Jomha NM. Clinical efflux of cryoprotective agents from vitrified human articular cartilage. *Cryobiology*.

2013;66(2):121-125. doi:10.1016/j.cryobiol.2012.12.005.

258. Zachari MA, Chondrou PS, Pouliliou SE, et al. Evaluation of the alamarblue assay for adherent cell irradiation experiments. *Dose-Response*. 2014;12(2):246-258. doi:10.2203/dose-response.13-024.Koukourakis.

259. Zar T, Graeber C, Perazella MA. Reviews: recognition, treatment, and prevention of propylene glycol toxicity. In: *Seminars in Dialysis*. Vol 20. Wiley Online Library; 2007:217-219.

260. Zheng SK, Xia Y, Bidthanapally A, Badar F, Ilsar I, Duvoisin N. Damages to the extracellular matrix in articular cartilage due to cryopreservation by microscopic magnetic resonance imaging and biochemistry. *Magn Reson Imaging*. 2009;27(5):648-655. doi:10.1016/j.mri.2008.10.003.

261. Zhou C-J, Wang D-H, Niu X-X, et al. High survival of mouse oocytes using an optimized vitrification protocol. *Sci Rep*. 2016;6(1):19465. doi:10.1038/srep19465.

262. Zhu SE, Kasai M, Otoge H, Sakurai T, Machida T. Cryopreservation of expanded mouse blastocysts by vitrification in ethylene glycol-based solutions. *J Reprod Fertil*. 1993;98(1):139-145. doi:10.1530/JRF.0.0980139.

263. Zielinski MW, McGann LE, Nychka JA, Elliott JAW. Comparison of non-ideal solution theories for multi-solute solutions in cryobiology and tabulation of required coefficients. *Cryobiology*. 2014;69(2):305-317. doi:10.1016/J.CRYOBIOL.2014.08.005.